Electronic Supplementary Material (ESI) for RSC Advances.

SUPPORTING INFORMATION

Palladium nanoparticles stabilised by cinchona-based alkaloids in glycerol: efficient catalysts for surface assisted processes

A. Reina, C. Pradel, E. Martin, E. Teuma and M. Gómez

Table of contents

General Experimental Part

Unless otherwise stated, all chemical reagents were obtained from commercial suppliers and used without further purification. All manipulations were performed using standard Schlenk techniques under argon atmosphere. Glycerol was dried under vacuum at 80 °C for 18h prior to use. NMR spectra were recorded on a Bruker Advance 300 spectrometer at 293 K (300 MHz for ^{1}H NMR, 75.5 MHz for ^{13}C NMR and 50.6 MHz for ^{15}N NMR). GC analyses were carried out on a GC Perkin Elmer Clarus 500 with ionization flame detector, using a SGE BPX5 column composed by 5% phenylmethylsiloxane and a Perkin Elmer Clarus MS560 mass detector. The determination of enantiomeric excesses was carried out by GC analyses on a HP 6890 Series GC instrument with a FS-cyclodex beta I/P chiral column. TEM images of particles in the solid state and dispersed in glycerol were obtained from transmission electron microscopes JEOL JEM 1400 running at 120 kV and HR-TEM from JEOL JEM 2100F running at 200 kV equipped with X PGT (detection of light elements, resolution 135 eV). The nanoparticles size, distribution and average diameter were determined from TEM images with Image-J software associated to a Microsoft Excel macro developed by Christian Pradel. XPS experiments were performed in a PHI 5500 Multi-technique System (from Physical Electronics) with a monochromatic X-ray source (Al Kα line of 1486.6 eV energy, 350 W), placed perpendicular to the analyser axis and calibrated using the $3d_{5/2}$ line of Ag with a full width at half maximum (FWHM) of 0.8 eV. The analysed area was a circle of 0.8 mm diameter. The selected resolution for the survey spectra was 187.85 eV of Pass Energy and 0.8 eV/step, while a Pass Energy of 23.5 eV and 0.1 eV/step was used for the high-resolution spectra of the main orbitals of the different elements. In order to avoid possible contamination in the analysis chamber, samples remained long times (> 12 h) in a pre-chamber under high vacuum (*ca.* 10^{-7} mbar). As a result of it, little but perceptible optical changes were noticed in samples, and low and high-resolution analyses could be performed working on ultra-high vacuum (under 10^{-8} mbar) without evaporation of the liquid phase. IR spectra were recorded in the range of 4000-400 cm^{-1} on a Varian 640-IR FTIR Spectrometer. The powder X-ray diffraction patterns were collected on a XPert (Theta-Theta mode) Panalytical diffractometer with α(Cu Kα1, Kα2)=1.54060, 1.54443 Å. High-pressure reactions were carried out in a Top Industrie Autoclave suitable from 0-50 bar and from 15-150 °C. Elemental and ICP-AES analyses were carried out at the “Service d’Analyse” of Laboratoire de Chimie de Coordination (Toulouse) using a Perkin Elmer 2400 series II analyser and an iCAP 6300 ICP Spectrometer.

Table S1. TEM images of **PdxL** nanoparticles stabilised by alkaloids (cinchonidine and quinidine) in glycerol, using different palladium precursors (**x** = **I**, $Pd(OAc)_2$; **x** = **II**, $[PdCl_2(cod)]$; **x** = **III**, $[Pd_2(dba)_3]$)

Stabiliser (right)/ **Pd precursor** (bottom)	Cinchonidine (**a**)	Quinidine (**d**)
$Pd(OAc)_2$ (**I**)	Not well-dispersed nanoparticles, tending to be aggregated: 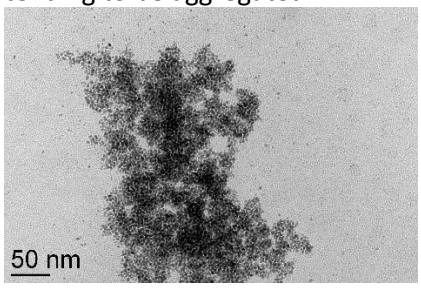 After centrifugation and redispersion in glycerol, well-dispersed nanoparticles, not homogeneous in size: 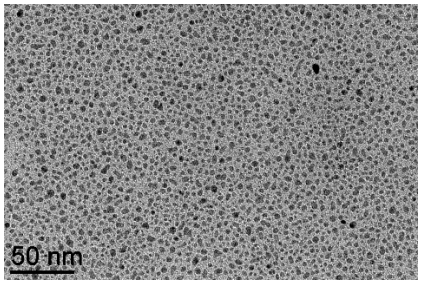 d_{mean} = 2.1 ± 0.6 nm (1759 particles)	Well-dispersed nanoparticles, quite homogeneous in size: 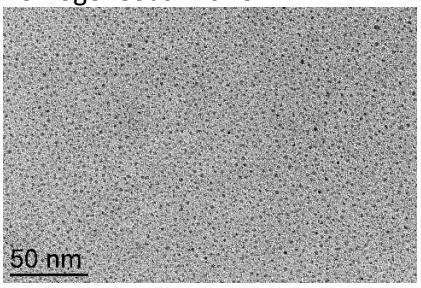 d_{mean} = 1.4 ± 0.3 nm (954 particles)
$[PdCl_2(cod)]$ (**II**)	Not well-dispersed nanoparticles, tending to be aggregated: 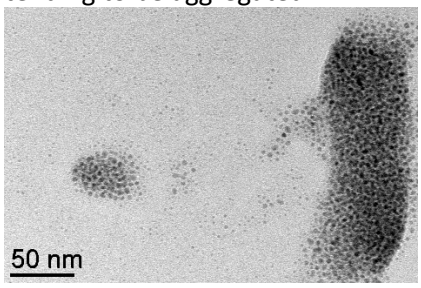 	Well-dispersed nanoparticles, quite homogeneous in size: 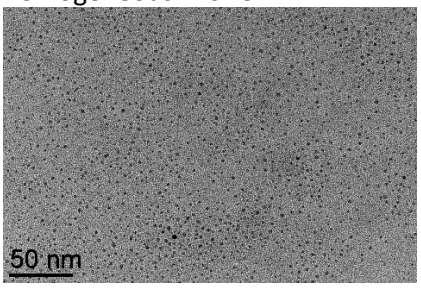 d_{mean} = 1.6 ± 0.3 nm (642 particles)
$[Pd_2(dba)_3]$ (**III**)	Well-dispersed nanoparticles (d_{mean} = 1.5 ± 0.3 nm (1524 particles)), together with agglomerates 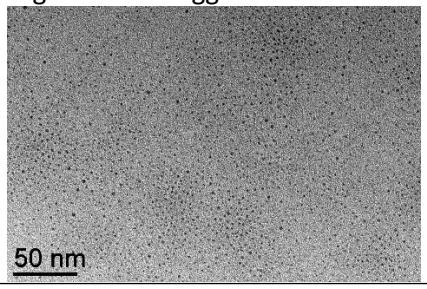 	No colloidal dispersion, only precipitate

	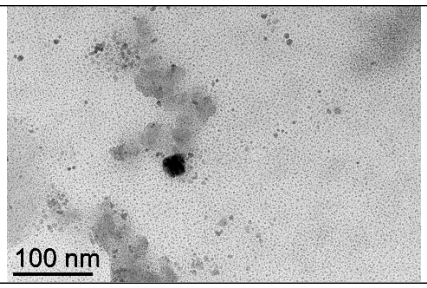 100 nm	

Table S2. Hydrogenation of compounds containing C=C or C≡C bonds and nitroarenes catalysed by **PdIa**.[a]

Entry	Substrate	Product	Pd mol% (pH_2)	Conv. (yield) (%)[b]
1	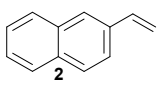 **2**	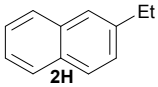 **2H**	0.1[c] (1)	>99 (96)
2	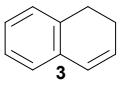 **3**	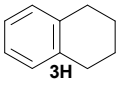 **3H**	0.1[c] (1)	86 (80)
3	 **4**	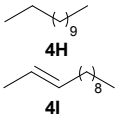 **4H** **4I**	1 (1)	83 (9/1)[d]
4	 **4**	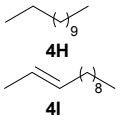 **4H** **4I**	1 (3)	99 (93)[e] (94/6)
5	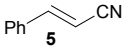 **5**	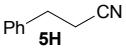 **5H**	1 (1)	95 (92)
6	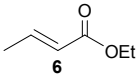 **6**	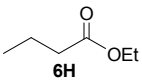 **6H**	1 (1)	99 (96)
7	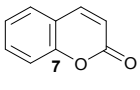 **7**	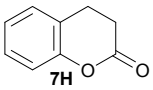 **7H**	1 (10)	53 (50)
8	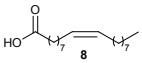 **8**	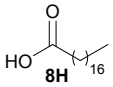 **8H**	1 (1)	>99 (94)
9	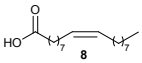 **8**	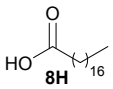 **8H**	0.1[c] (1)	47 (44)[f]
10	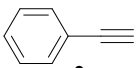 **9**	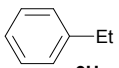 **9H**	1 (1)	>99 (96)
11	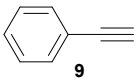 **9**	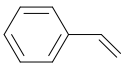 **9HE**	0.5[g] (1)	80 (84)[h]
12	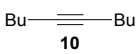 **10**	 **10H**	1 (3)	98 (70)[i,k]
13	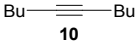 **10**	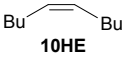 **10HE**	0.5[g] (1)	97 (93)[i]

14	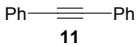 **11**	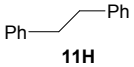 **11H**	0.5[g] (1)	97 (91)
15	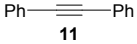 **11**	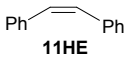 **11HE**	0.1[c] (1)	47 (43)
16	**12**	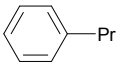 **12H**	1 (3)	>99 (95)
17	**12**	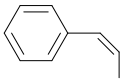 **12HE**	0.5[g] (1)	48 (42)[j]
18	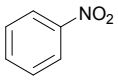 **13**	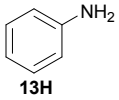 **13H**	1 (3)	76 (73)
19	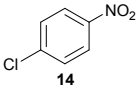 **14**	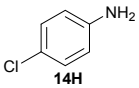 **14H**	1 (3)	80 (76)
20	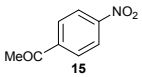 **15**	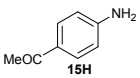 **15H**	1 (3)	97 (95)
21	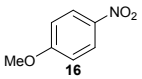 **16**	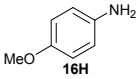 **16H**	1 (3)	61 (58)

[a] Results from duplicated experiments. Reaction conditions: 1 mmol of substrate (**2-16**) and 1 mL of the catalytic glycerol solution of **PdIa** (10^{-2} molL^{-1}, 0.01 mmol of total Pd). [b] Determined by GC and GC-MS using decane as internal standard. [c] 10 mmol of substrate for 1 mL of catalytic solution (0.01 mmol of total Pd). [d] In brackets, **4H**/**4I** ratio. [e] For 12h. [f] At 30 °C for 24h. [g] 5 mmol of substrate for 1 mL of catalytic solution (0.01 mmol of total Pd). [h] 16% of **9H** was detected. [i] Determined by GC and GC-MS using cyclooctane as internal standard. [j] At 35 °C for 6h. [k] 25% of **10HE** was detected.

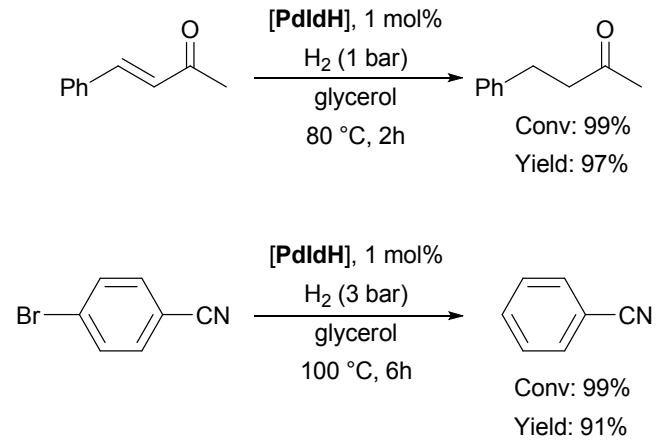

Scheme S1. Hydrogenation (top) and hydrodebromination (bottom) catalysed by **PdIdH**. Conversions and yields were determined by GC and GC-MS using decane as internal standard.

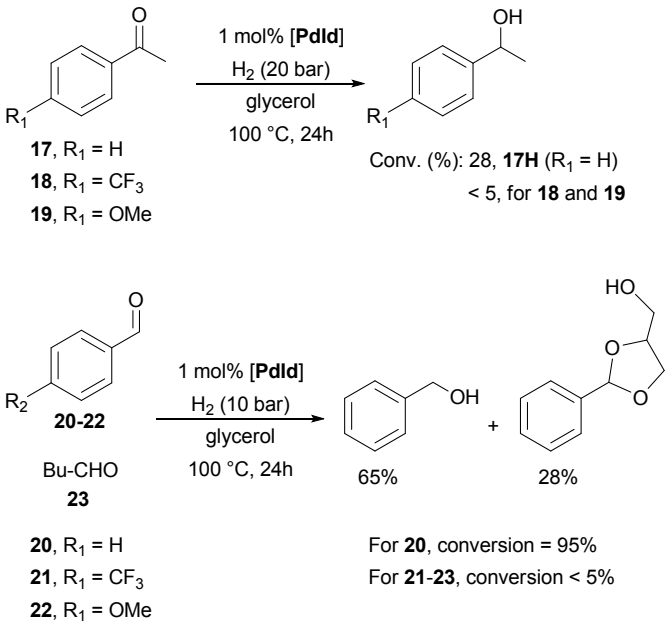

Scheme S2. Hydrogenation of ketones (top) and aldehydes (bottom) catalysed by **PdId**. Conversions and yields were determined by GC and GC-MS using decane as internal standard.

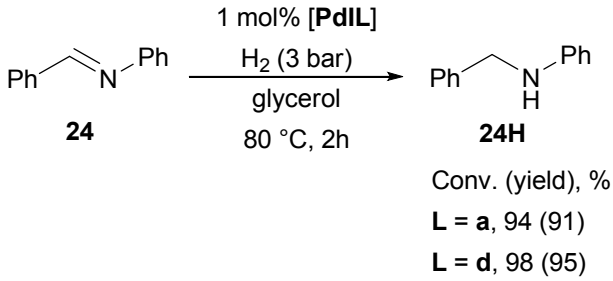

Scheme S3. Pd-catalysed hydrogenation of *N*-benzylideneaniline (**24**) by **PdIa** and **PdId**. Conversions and yields were determined by GC and GC-MS using decane as internal standard.

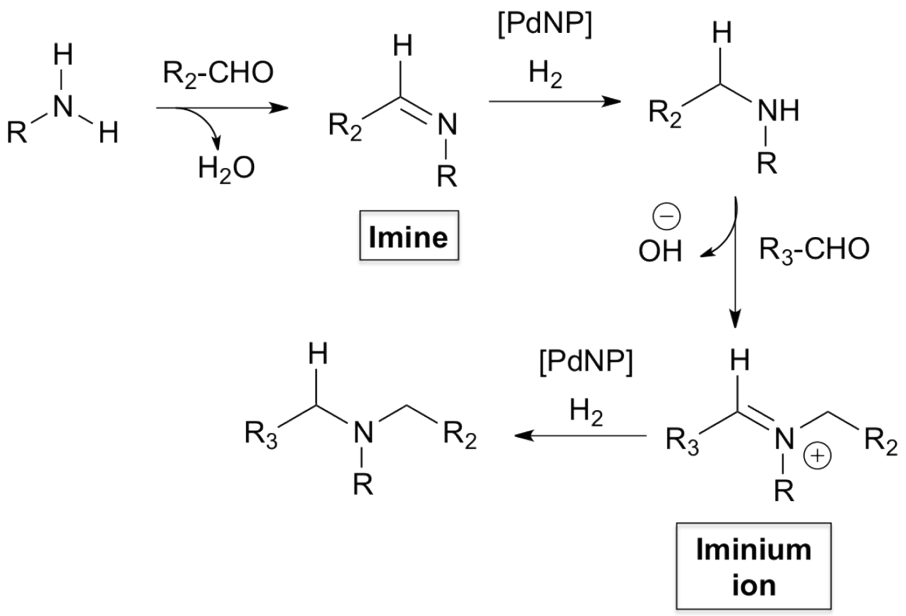

Scheme S4. Pathwy of Pd-catalysed synthesis of secondary and tertiary amines from aldehyde and amine reagents under hydrogen pressure, showing the formation of imine and iminium ion intermediates.

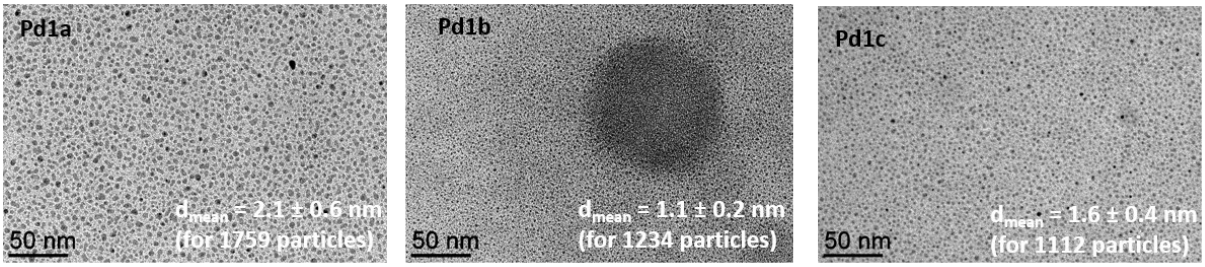

Figure S1. TEM images in glycerol corresponding to **PdIa**, **PdIb** and **PdIc** after centrifugation (isolation of PdNPs at the solid state) and redispersion in glycerol.

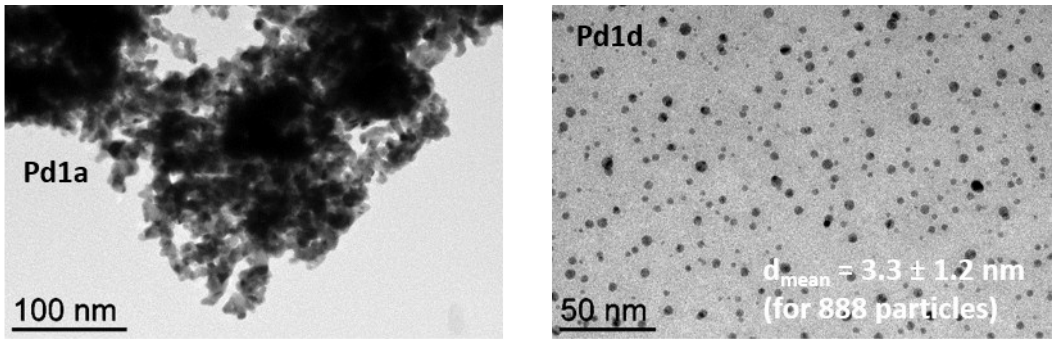

Figure S2. TEM images for **PdIa** and **PdId** after centrifugation and redispersion in ethanol (analyses at solid state).

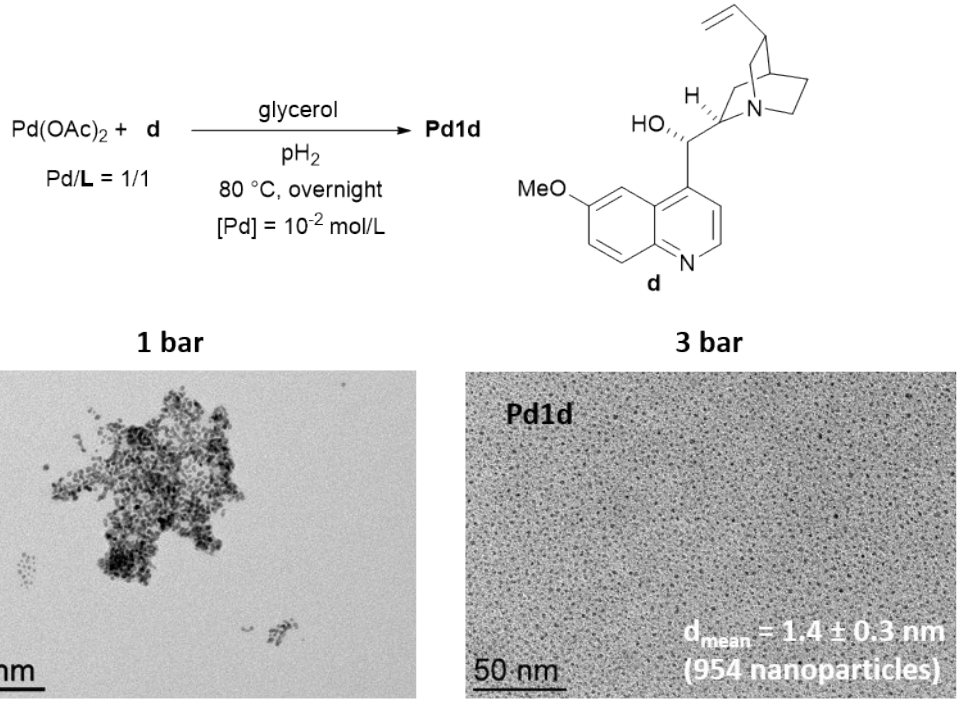

Figure S3. TEM images for **PdId** working at different dihydrogen pressures.

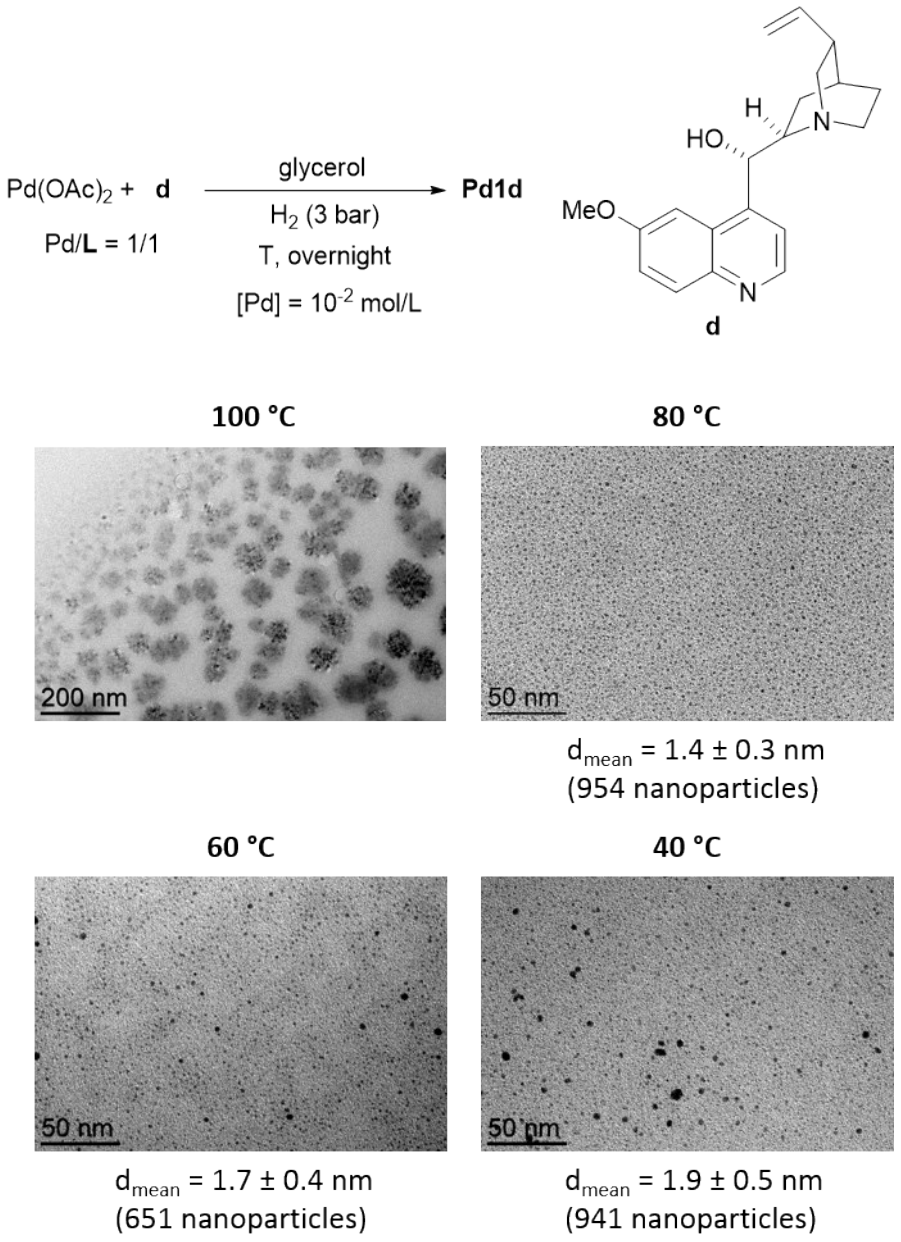

Figure S4. TEM images for **Pd1d** working at different temperatures.

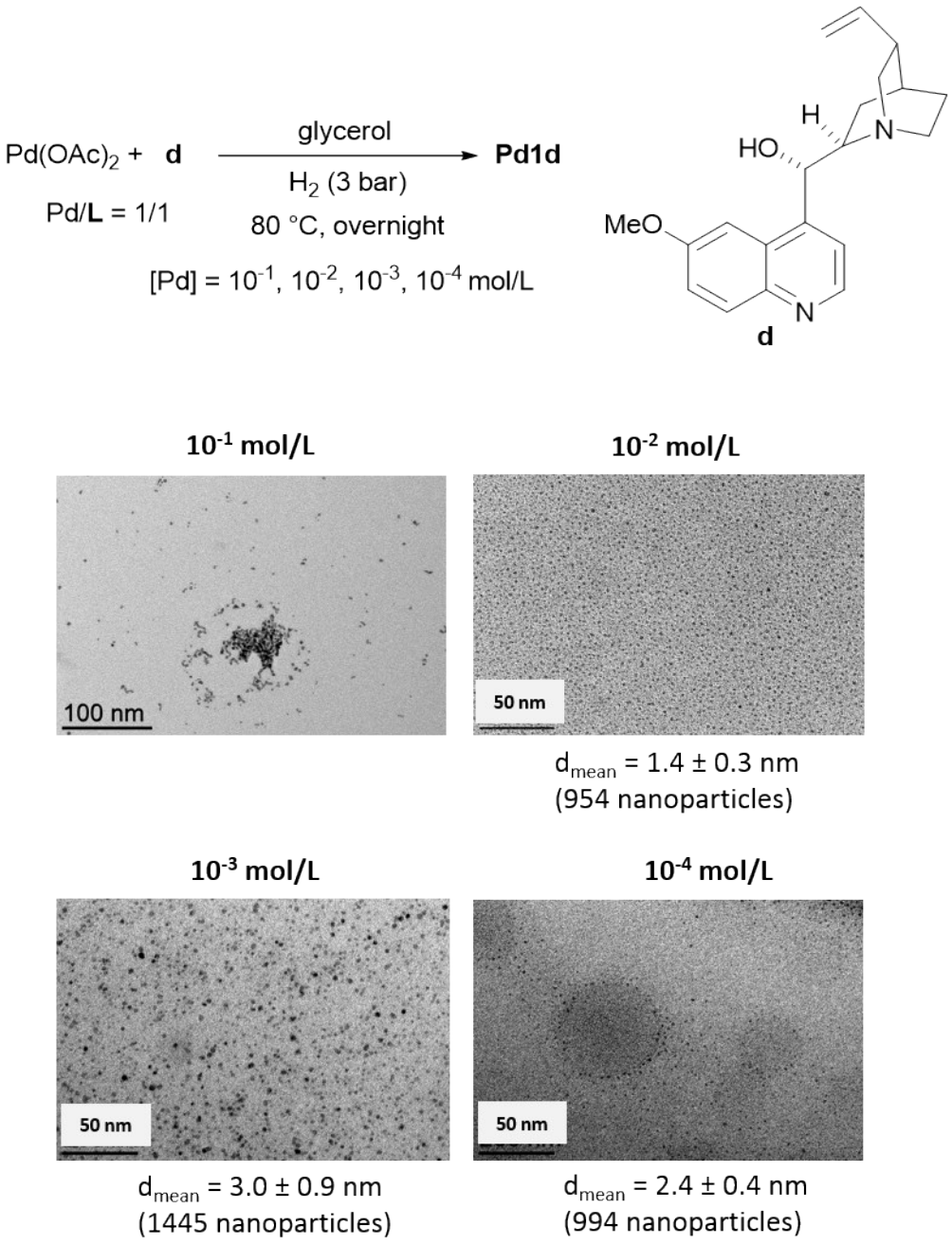

Figure S5. TEM images for **PdId** working at different metal concentrations.

(a)

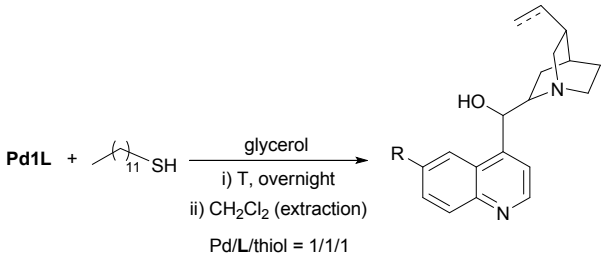

R = H: 90% yield, **a**/**aH** = 1.3/1

R = OMe: 87% yield, **d**/**dH** = 2/1

(b)

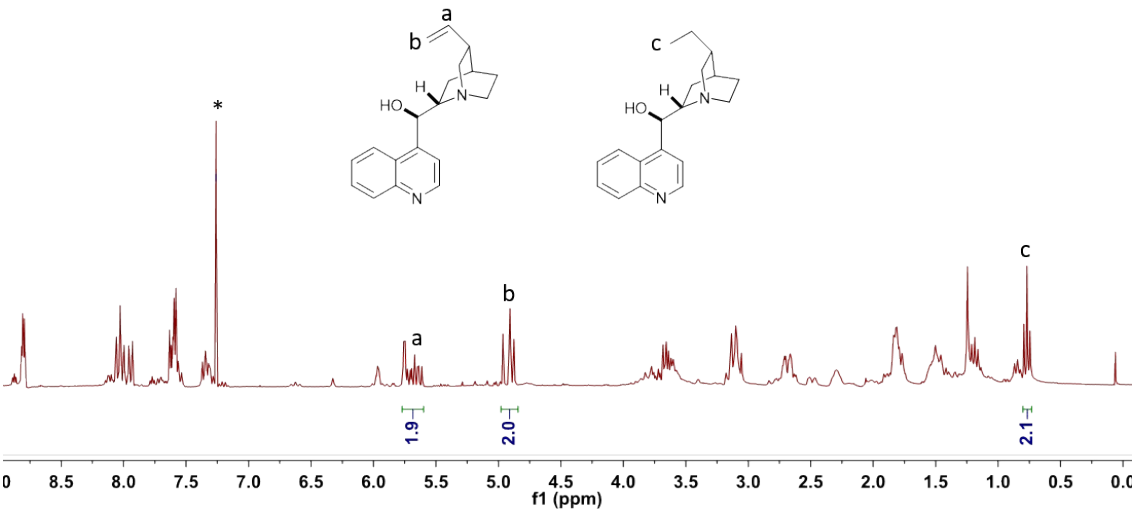

(c)

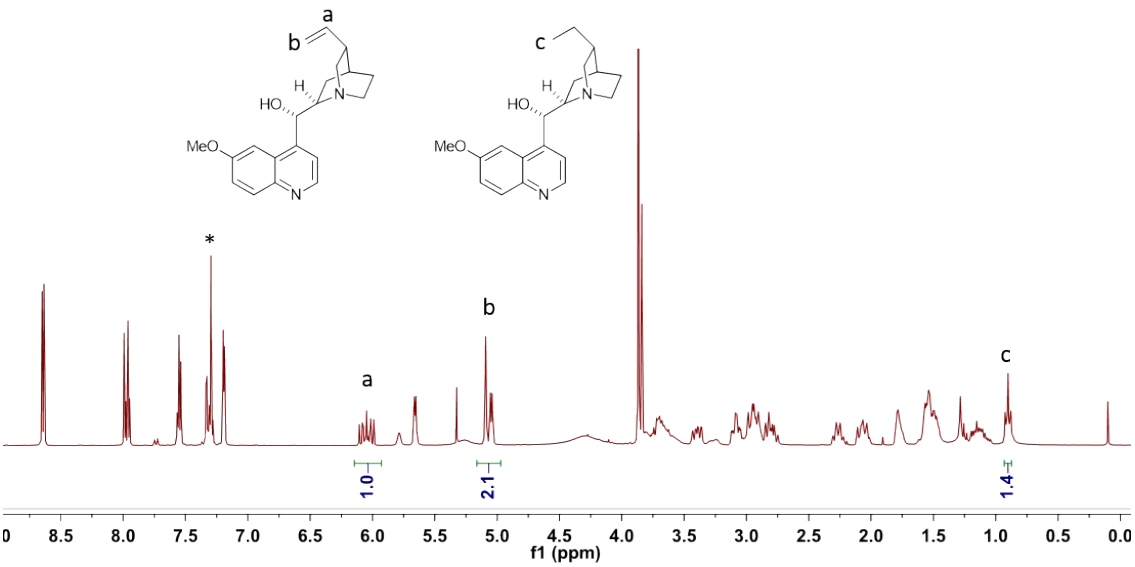

Figure S6. Exchange ligand reaction between **Pd1L** (L = **a**, **d**) and dodecanethiol (a). ^{1}H NMR spectra (300 MHz, $CDCl_3$, 298 K) corresponding to the extracted organic product from the reaction involving **PdIa** (b) and **PdId** (c). * Denotes $CHCl_3$.

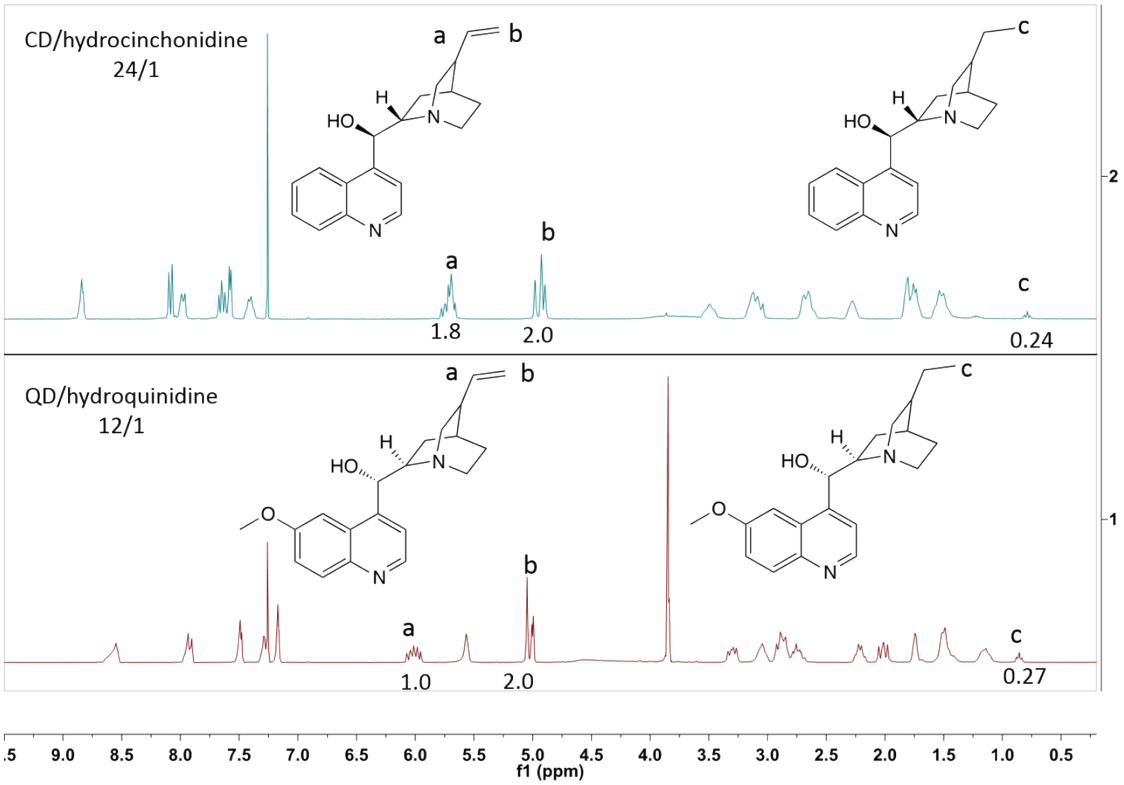

Figure S7. ^{1}H NMR spectra (300 MHz, $CDCl_3$, 298 K) for commercially available cinchonidine (top) and quinidine (bottom).

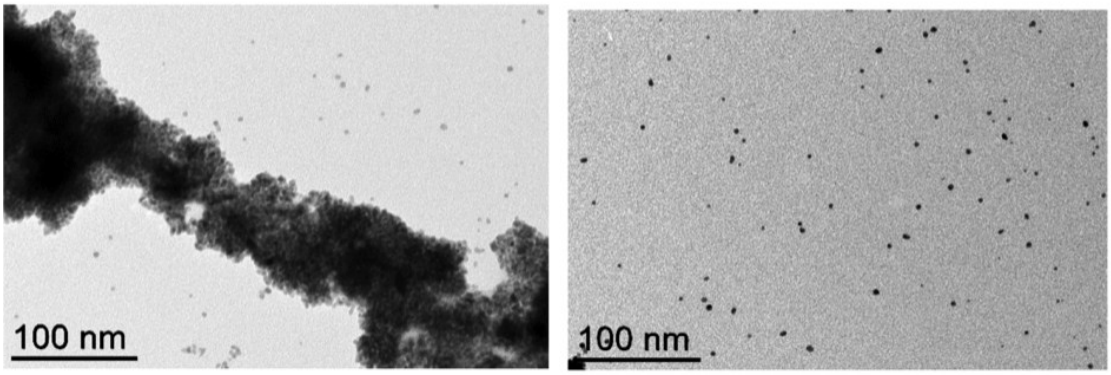

Figure S8. TEM images in glycerol of PdNPs stabilised by **dH** (**PdIdH**).

(a)

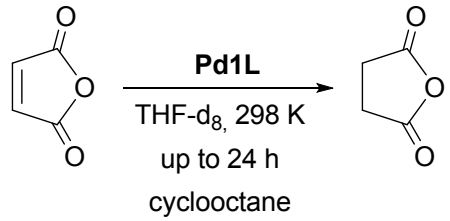
Pd1L
THF-d8, 298 K
up to 24 h
cyclooctane

(b)

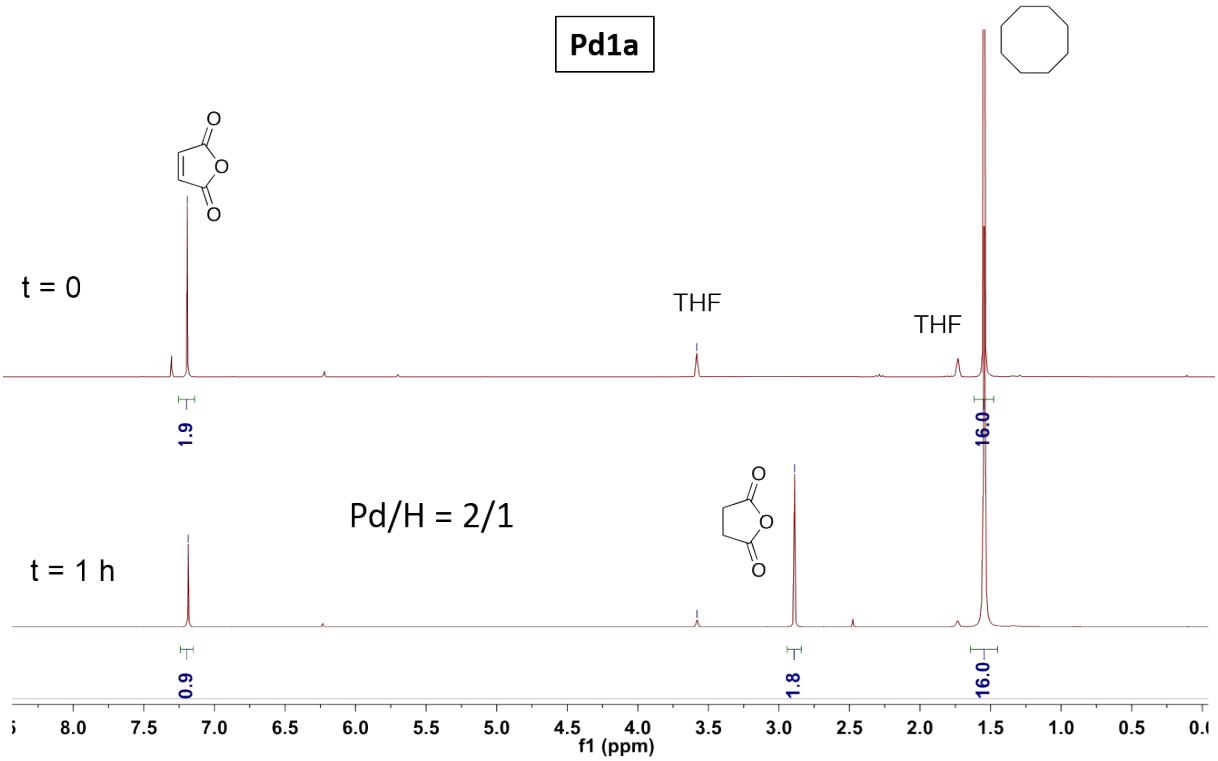
Pd1a
t = 0
THF
THF
1.9
16.0
Pd/H = 2/1
t = 1 h
0.9
1.8
16.0
8.0
7.5
7.0
6.5
6.0
5.5
5.0
4.5
4.0
3.5
3.0
2.5
2.0
1.5
1.0
0.5
f1 (ppm)

(c)

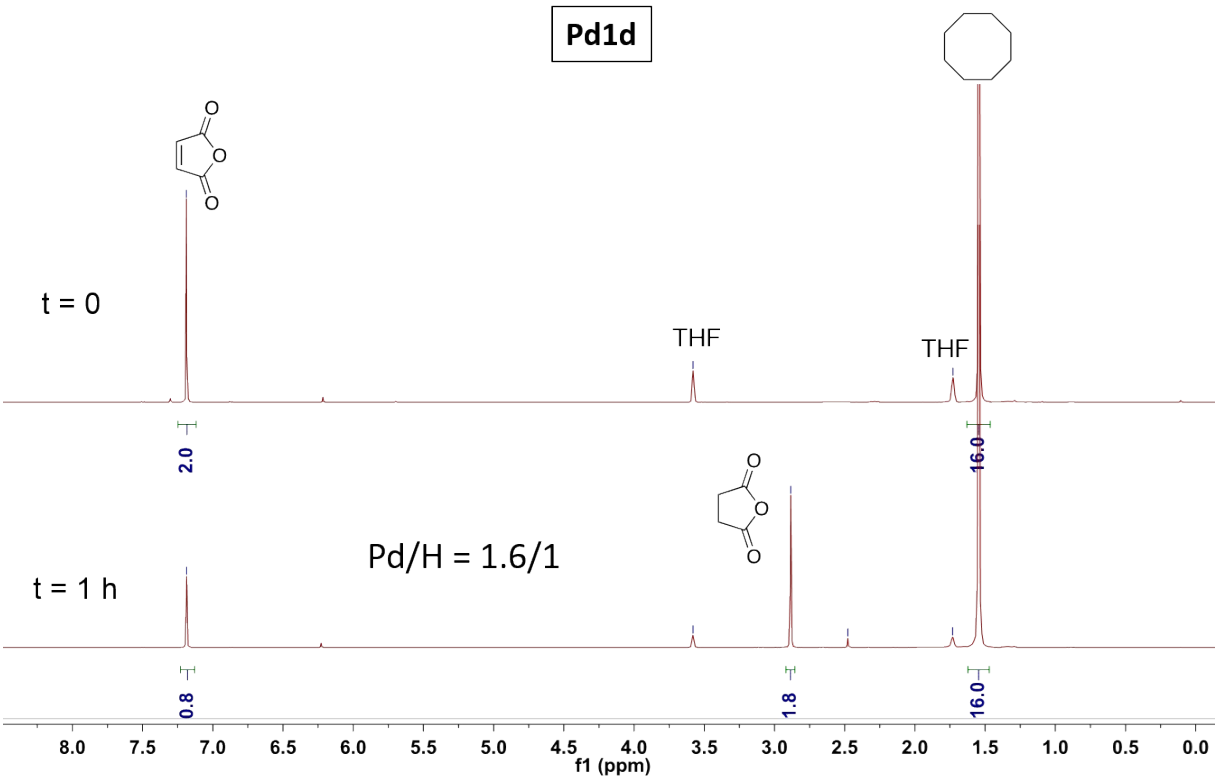

Figure S9. (a) Titration of hydrides present on **Pd1L** (s) (L = **a**, **d**) in THF-d_8 using maleic anhydride and cyclooctane as internal standard. ^{1}H NMR spectra (300 MHz, $CDCl_3$, 298 K) for **PdIa** (b) and **PdId** (c).

(a)

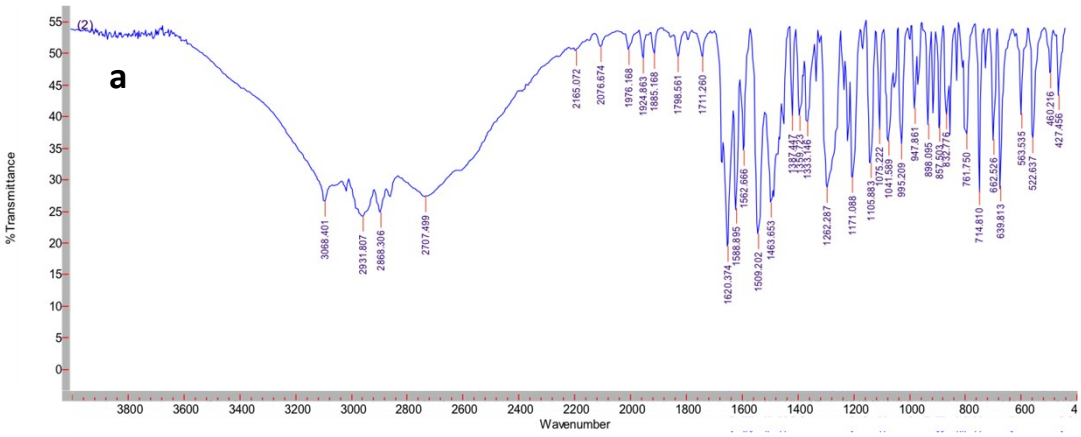
a
% Transmittance
Wavenumber

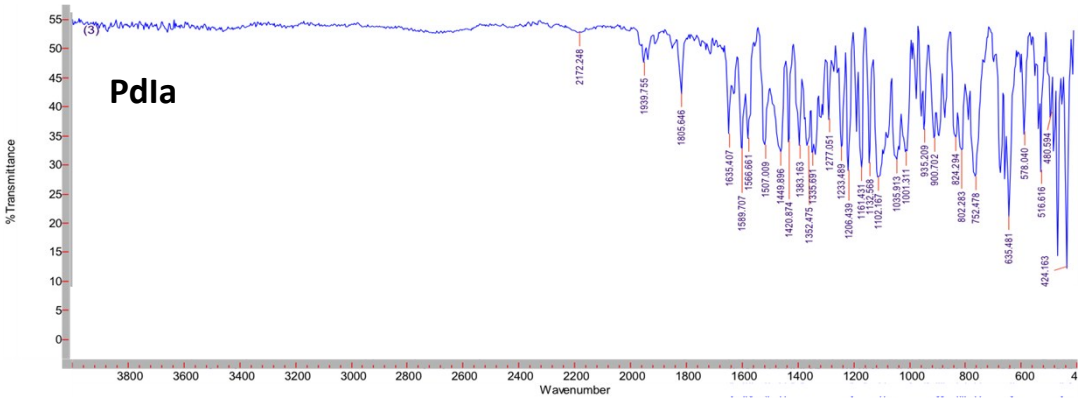
PdIa
% Transmittance
Wavenumber

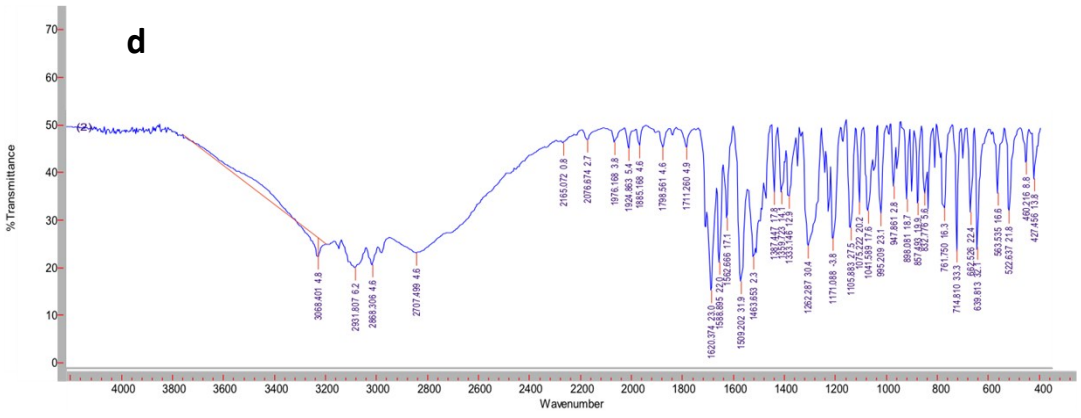
d
% Transmittance
Wavenumber

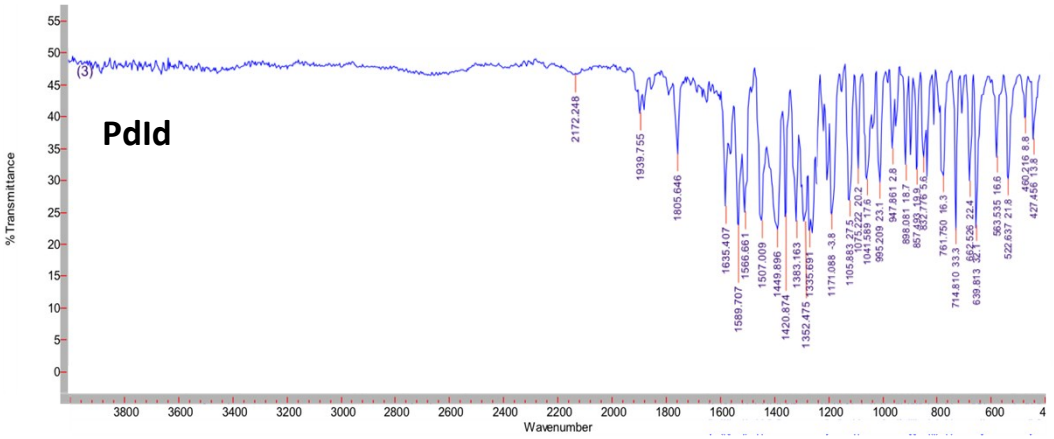
PdId
% Transmittance
Wavenumber

(b)

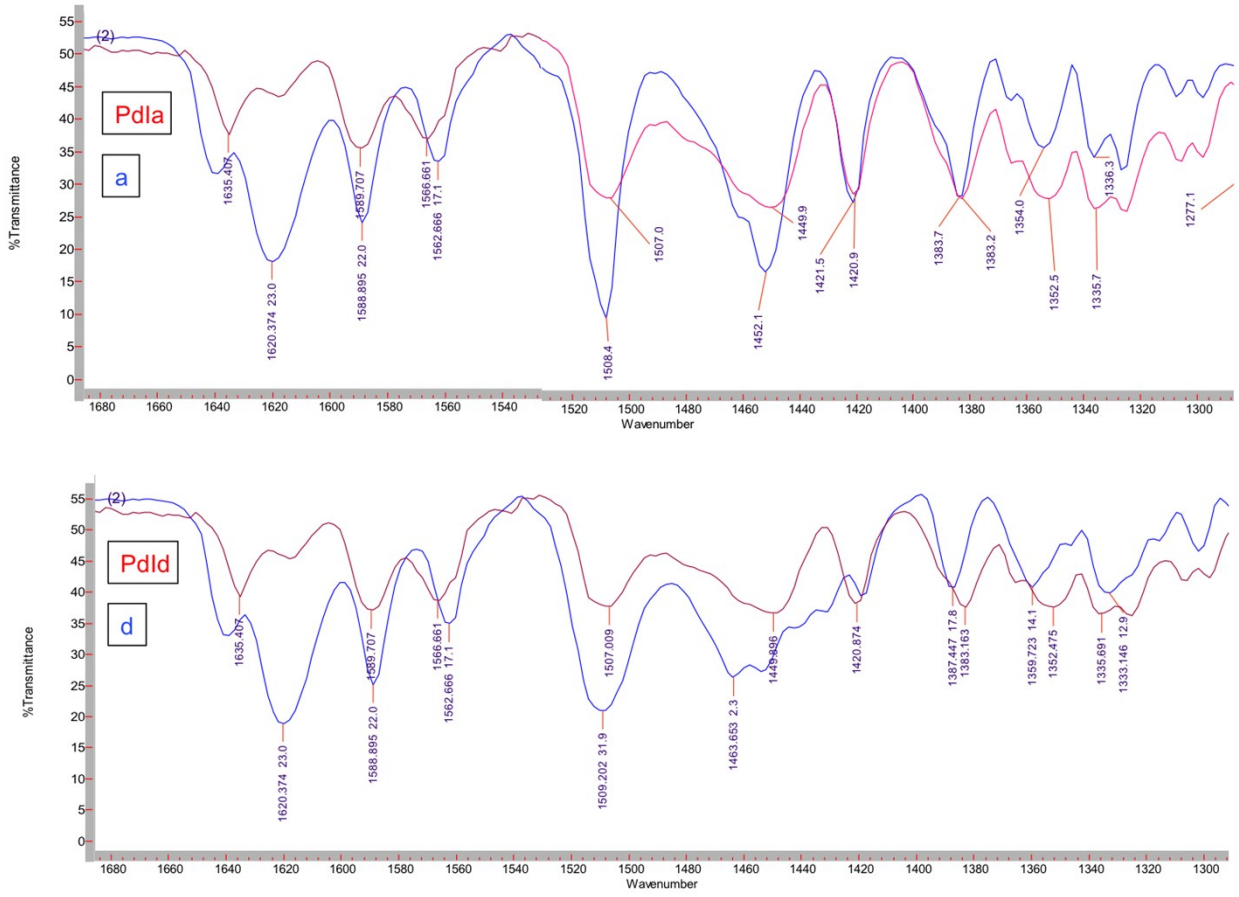

Figure S10. (a): IR spectra (KBr pellets) for cinchona-based stabilisers (**a**, **d**) with the corresponding PdNPs (**PdIa**, **PdId**); (b) IR region corresponding to the double bonds and quinuclidine fragment. The intense absorption at *ca.* 1620 cm^{-1} for the free ligands **a** and **d** corresponds to the bending of water.

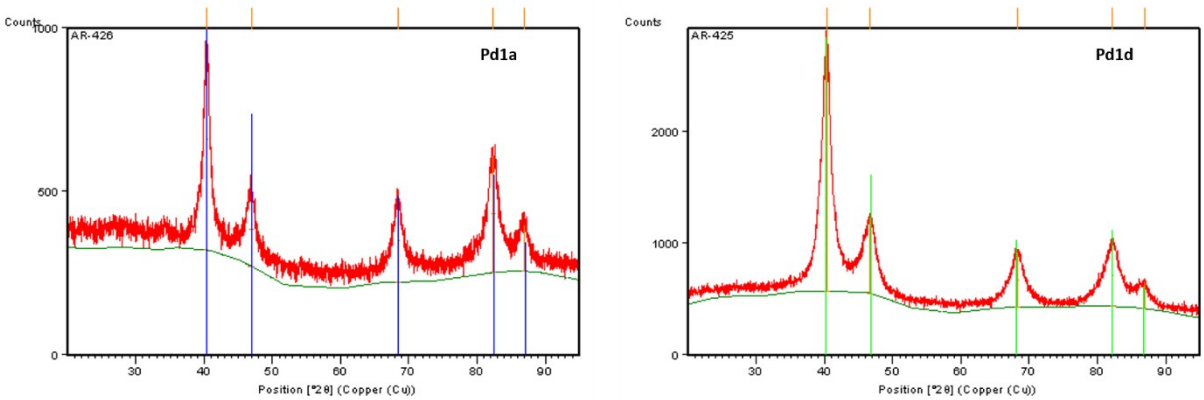

Figure S11. XRD diffractograms (red traces) for **PdIa** (left) and **PdId** (right) showing the peaks corresponding to fcc structure. Sharp lines correspond to the pattern of bulk fcc Pd(0).

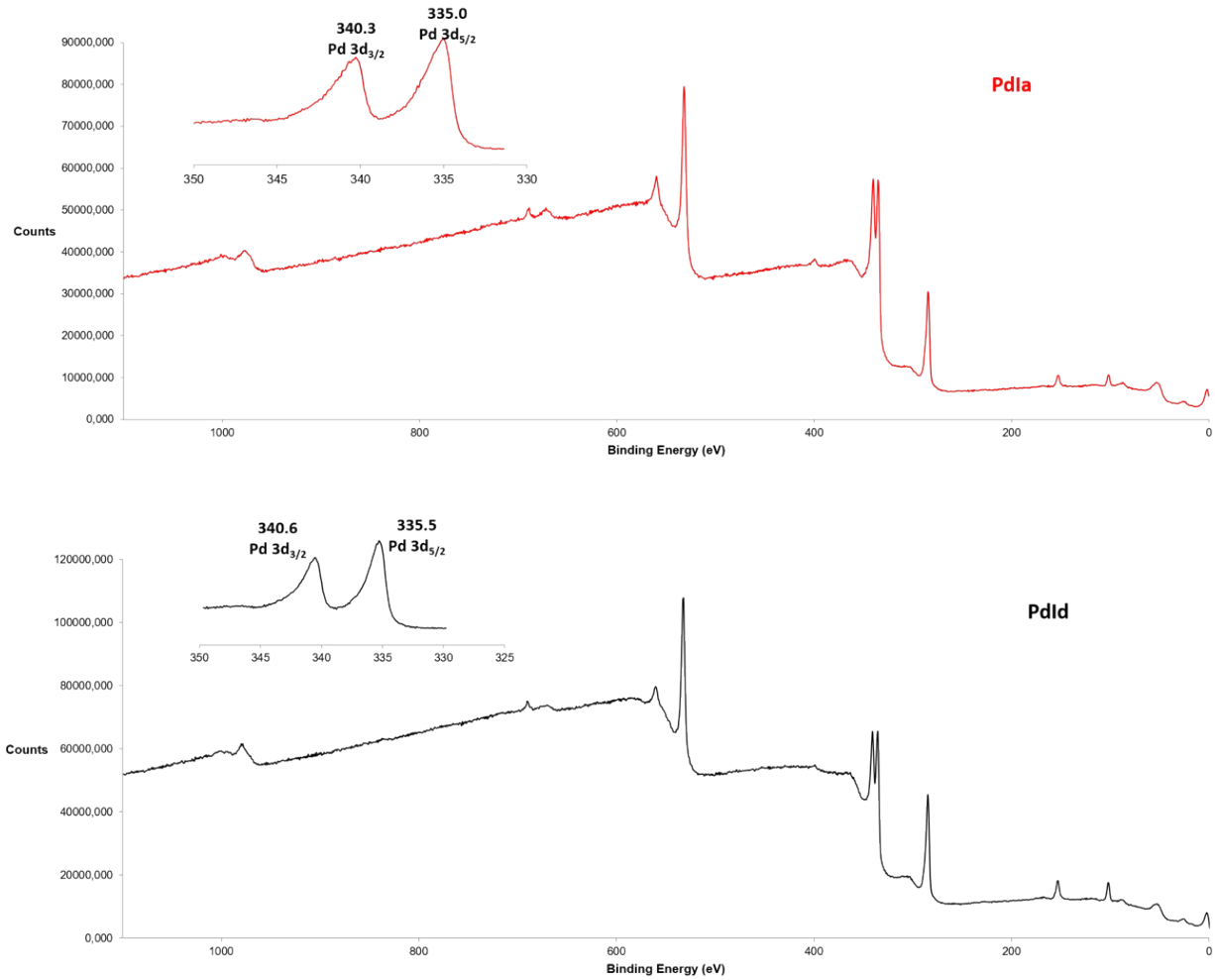

Figure S12. XPS survey spectra for **PdIa** (top) and **PdId** (bottom) at solid state. Insets correspond to high-resolution XPS spectra of Pd 3d binding region.

(a)

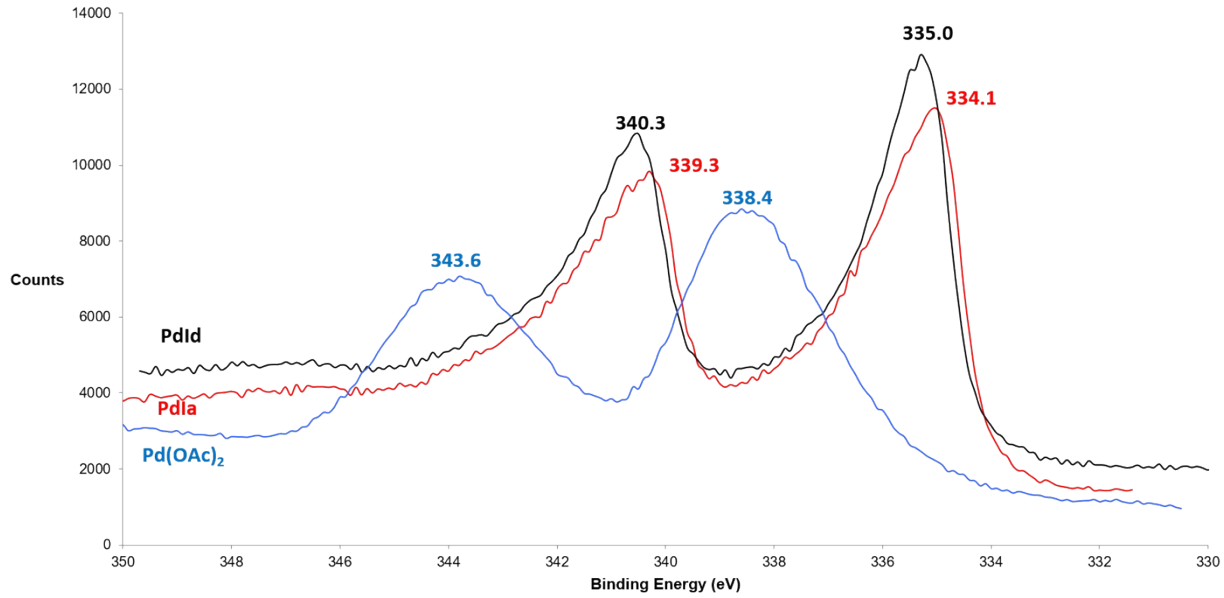

(b)

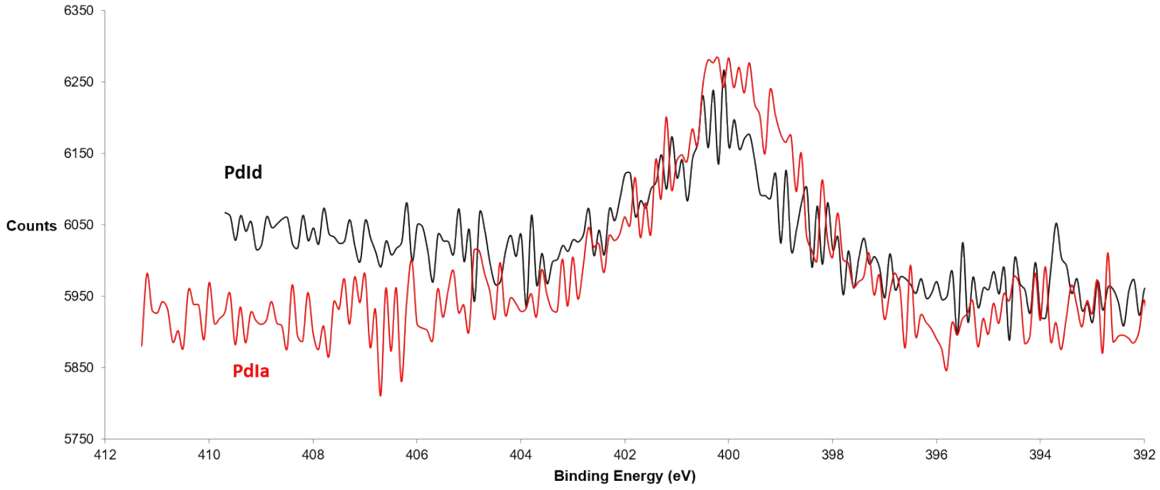

Figure S13. High-resolution XPS spectra: (a) Pd 3d binding energy region for **PdIa** and **PdId** at the solid state; the corresponding spectrum for $Pd(OAc)_2$ is included for comparison purposes. (b) N 1s binding region for **PdIa** and **PdId**.

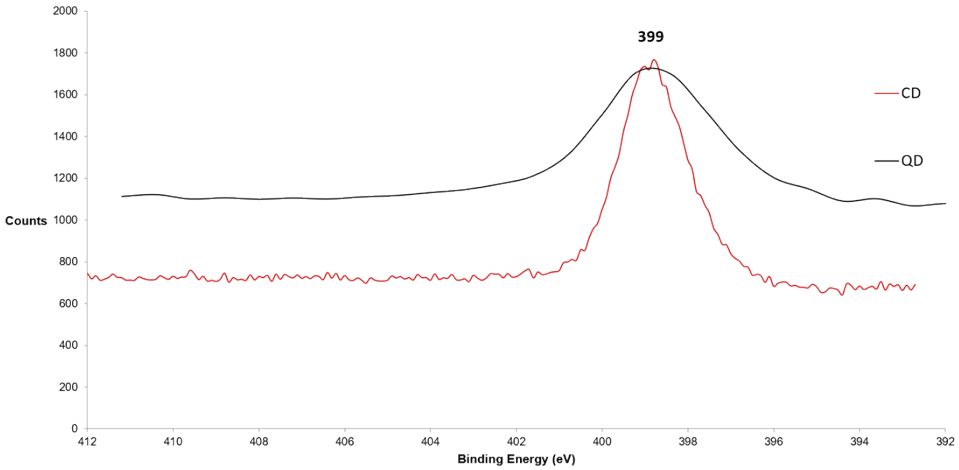

Figure S14. High-resolution XPS spectra in the N1s binding energy region for cinchonidine (**a**) and quinidine (**d**) at the solid state.

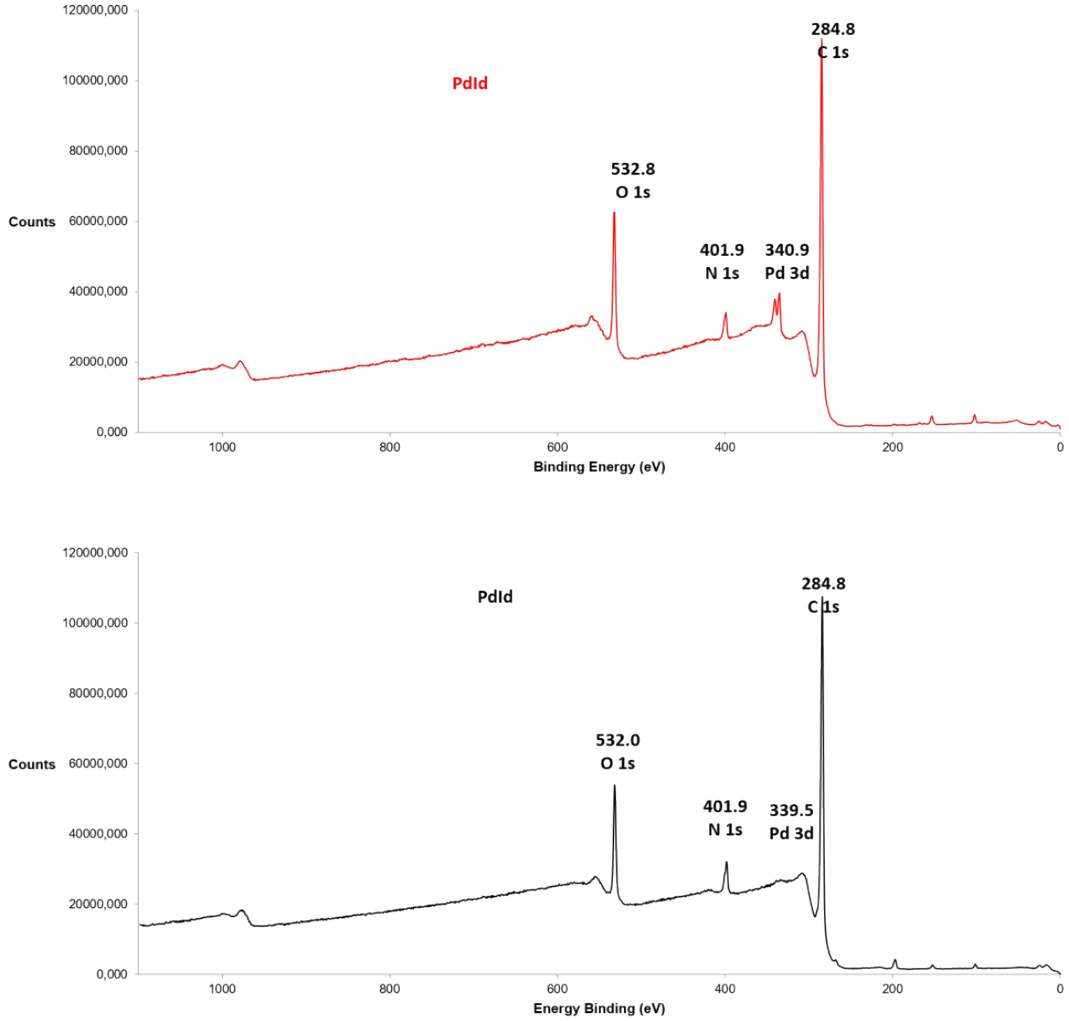

Figure S15. XPS survey spectra for **PdIa** (top) and **PdId** (bottom) in glycerol.

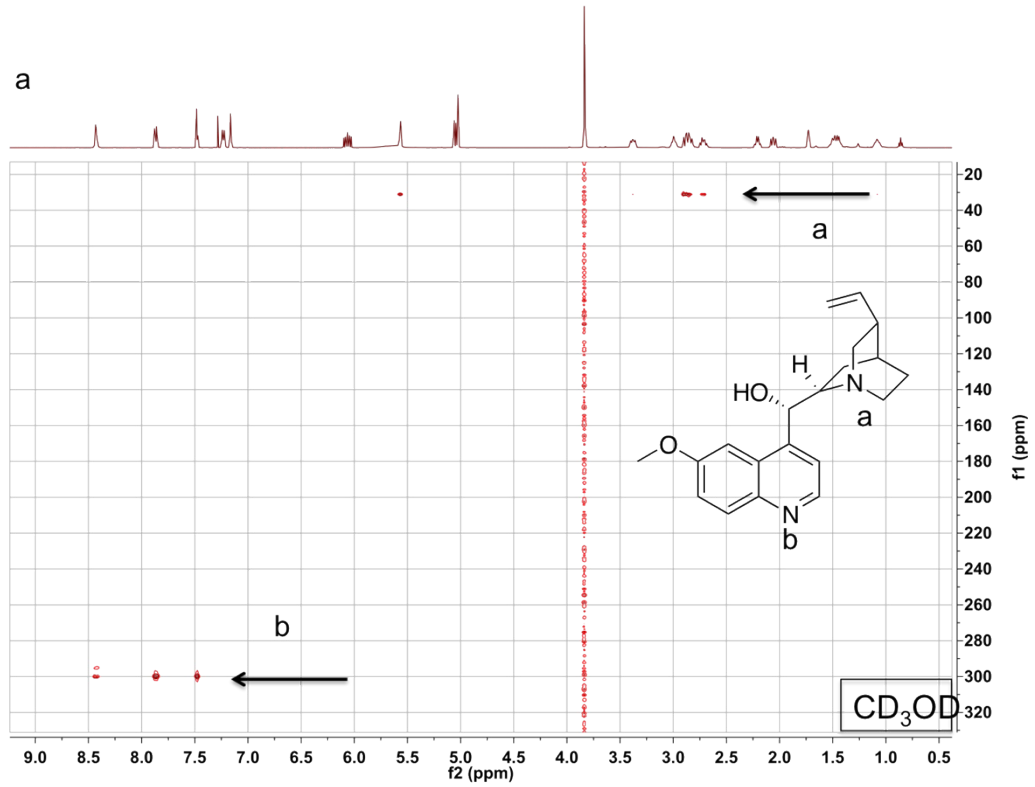
a
a
H
HO
N
a
O
N
b
b
CD3OD
f2 (ppm)
f1 (ppm)

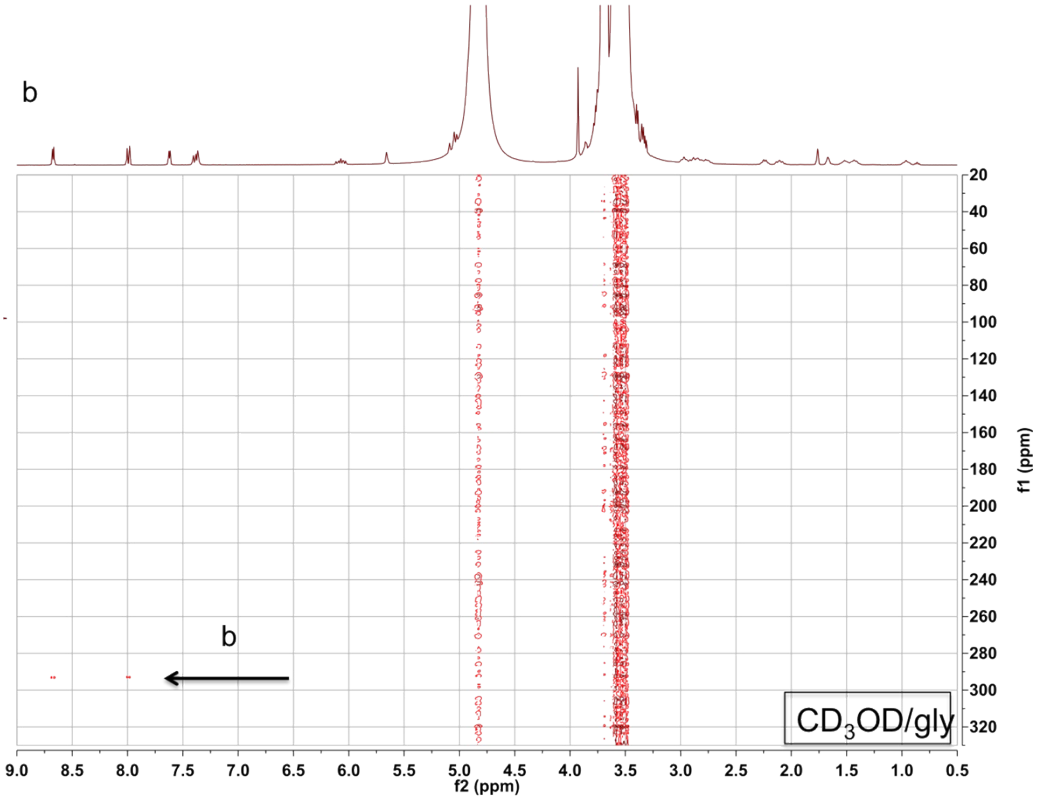
b
b
CD3OD/gly
f2 (ppm)
f1 (ppm)

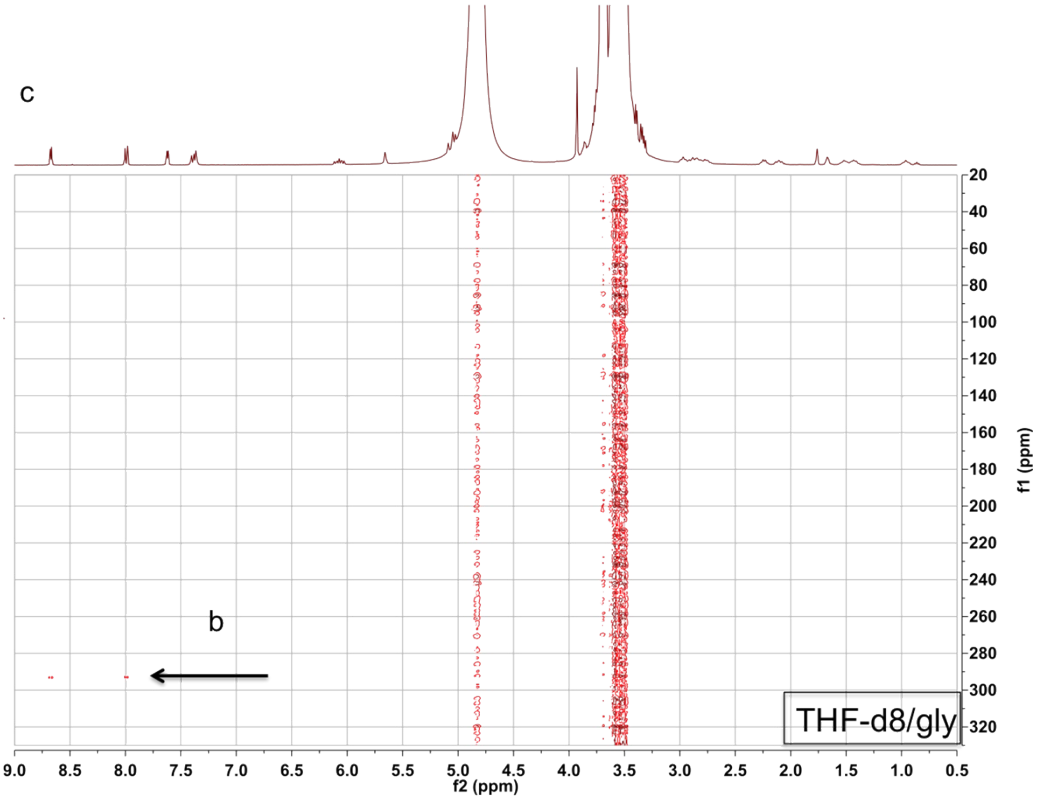

Figure S16. Heteronuclear Multiple Bond Correlation (HMBC) NMR experiment between ^{1}H and ^{15}N for quinidine (**d**) in a) CD_3OD; b) CD_3OD/glycerol (1:1) and c) THF-d_8/glycerol (1/1) at room temperature. Arrows show the quinoline and quinuclidine nitrogen atoms.

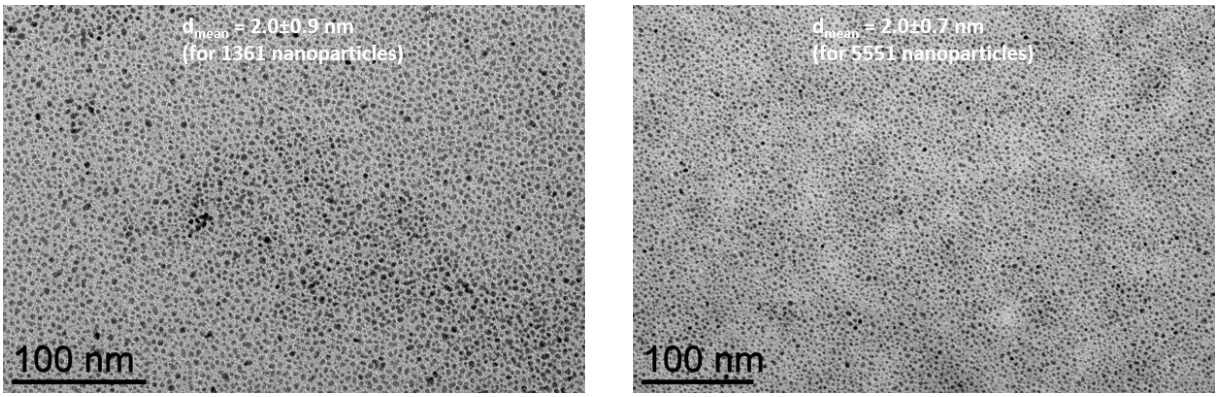

Figure S17. TEM images after the first (left) and the fourth (right) recycling of the hydrogenation of 4-phenylbut-3-en-2-one catalysed by **PdId** (see Table 1 and Fig. 4 in the main text).

(a)

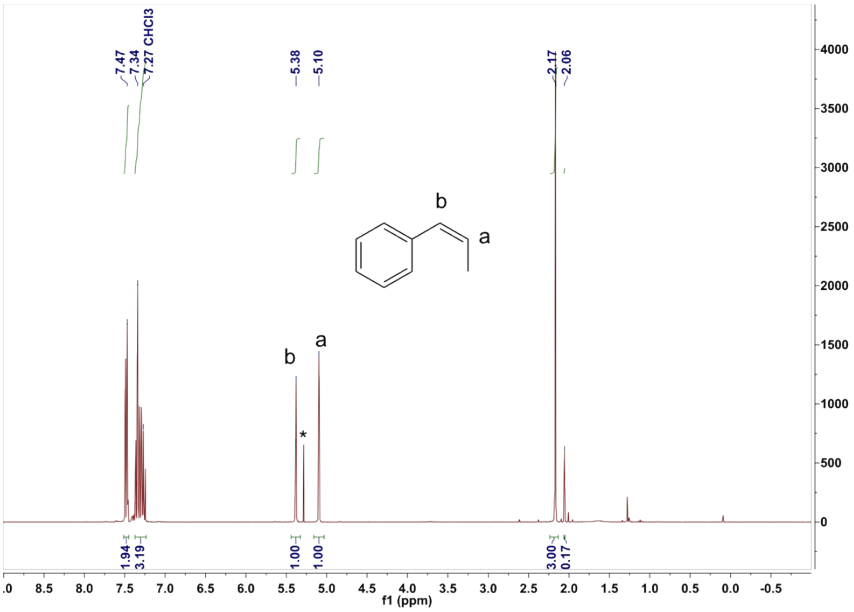

(b)

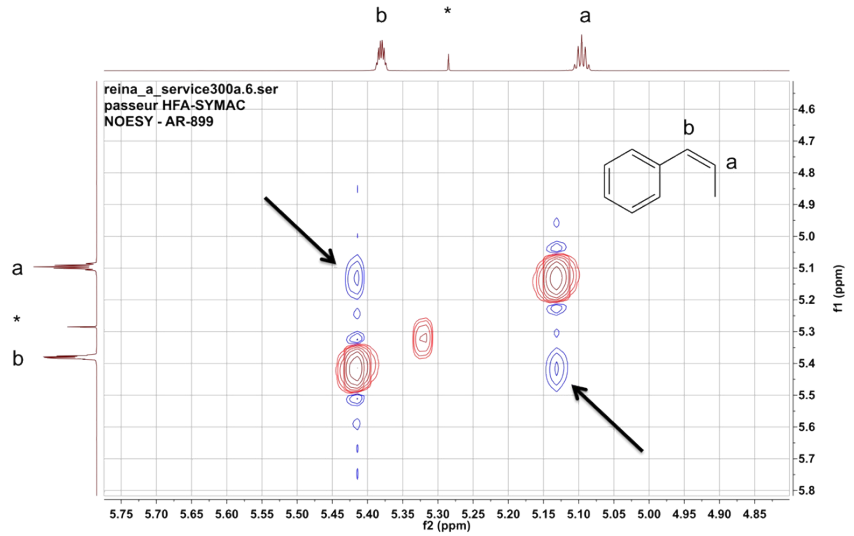

Figure S18. (a) ^{1}H NMR spectrum (300 MHz, $CDCl_3$, 298 K) corresponding to the product **12HE**; (b) NOESY-NMR analysis of **12HE** showing the exclusive formation of the (*Z*)-stereoisomer. Arrows indicate the NOE contact between both ethylenic hydrogens. * Denotes CH_2Cl_2.

(a)

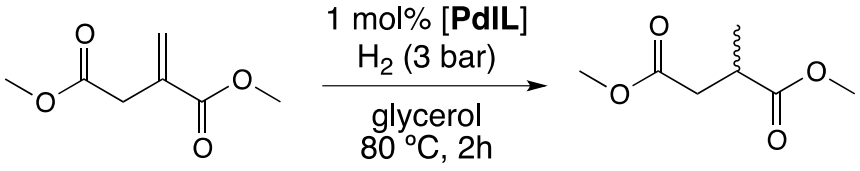

A **AH**

Conv. (yield), %	ee %
L = a, 97 (91)	0
L = d, 99 (91)	0

(b)

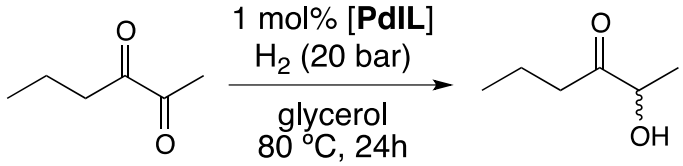

B **BH**

Conv. (yield), %	ee %
L = a, 86 (81)	0
L = d, 80 (75)	0

At milder conditions, no conversion was obtained

(c)

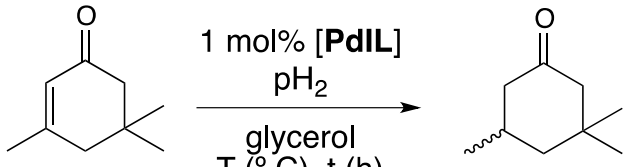

C **CH**

Entry	Catalyst	pH_2	T (º C)	t (h)	Conv. (yield) %[b]	ee %[c]
1	**PdIa**	3	100	6	90 (86)	<5
2	**PdId**	3	100	6	99 (94)	<5
3	**PdIa**	3	40	6	32 (29)	<5
4	**PdId**	3	40	6	88 (84)	<5
6	**PdId**	10	40	6	>99 (95)	<5
7	**PdId**	15	40	6	>99 (94)	<5

[a] Results from duplicated experiments. Reaction conditions: 1 mmol of substrate (**A-C**) and 1 mL of the catalytic glycerol solution of PdIa (10-2 molL-1, 0.01 mmol of total Pd). [b] Determined by GC and GC-MS using decane as internal standard. [c] Enantiomeric excess determined by chiral GC using a FS-Cyclodex beta I/P column. The addition of L-proline did not favour the asymmetric induction.

Figure S19. Pd-catalysed hydrogenation of prochiral substrates dimethyl itaconate **A** (a), ethyl pyruvate **B** (b) and isophorone **C** (c) by **PdIa** and **PdId**. Conversions and yields were determined by GC and GC-MS using decane as internal standard and enantiomeric excesses were determined by chiral GC (FS-Cyclodex beta I/P column).

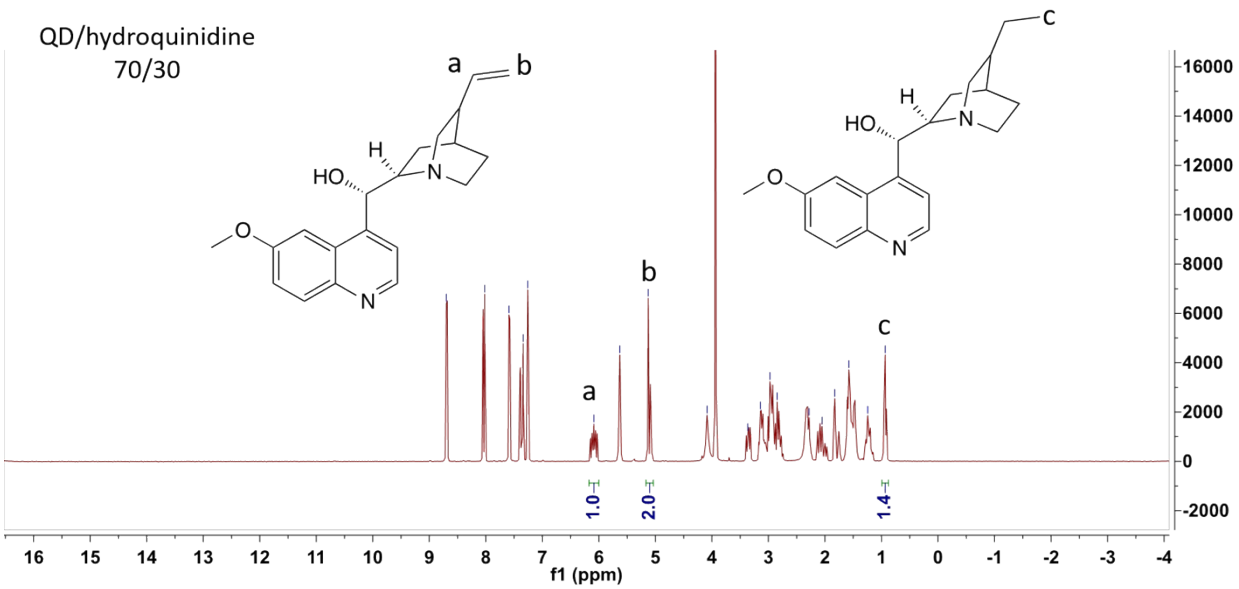

Figure S20. ^{1}H NMR spectrum (300 MHz, $CDCl_3$, 298 K) corresponding to the extraction of stabiliser from the catalytic glycerol phase **PdId**, after hydrodehalogenation of 4-bromophenol.

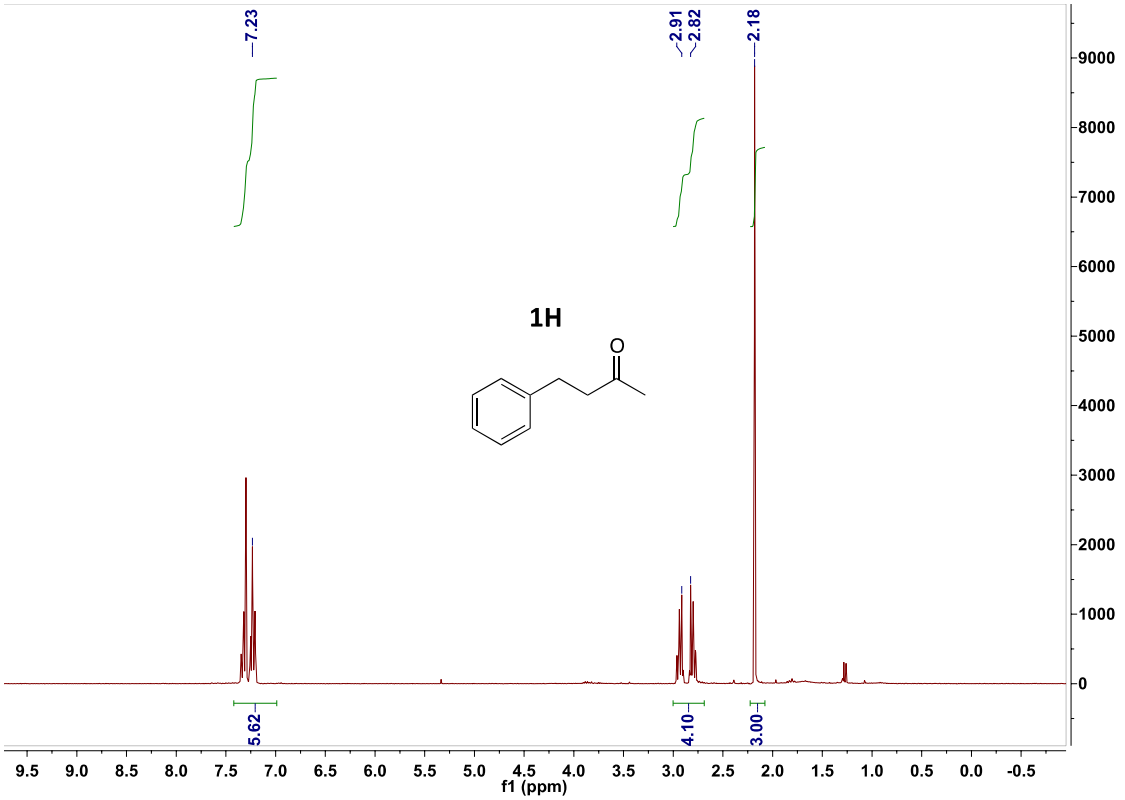

^{1}H NMR (300 MHz, 298 K) spectrum in $CDCl_3$ for **1H**.

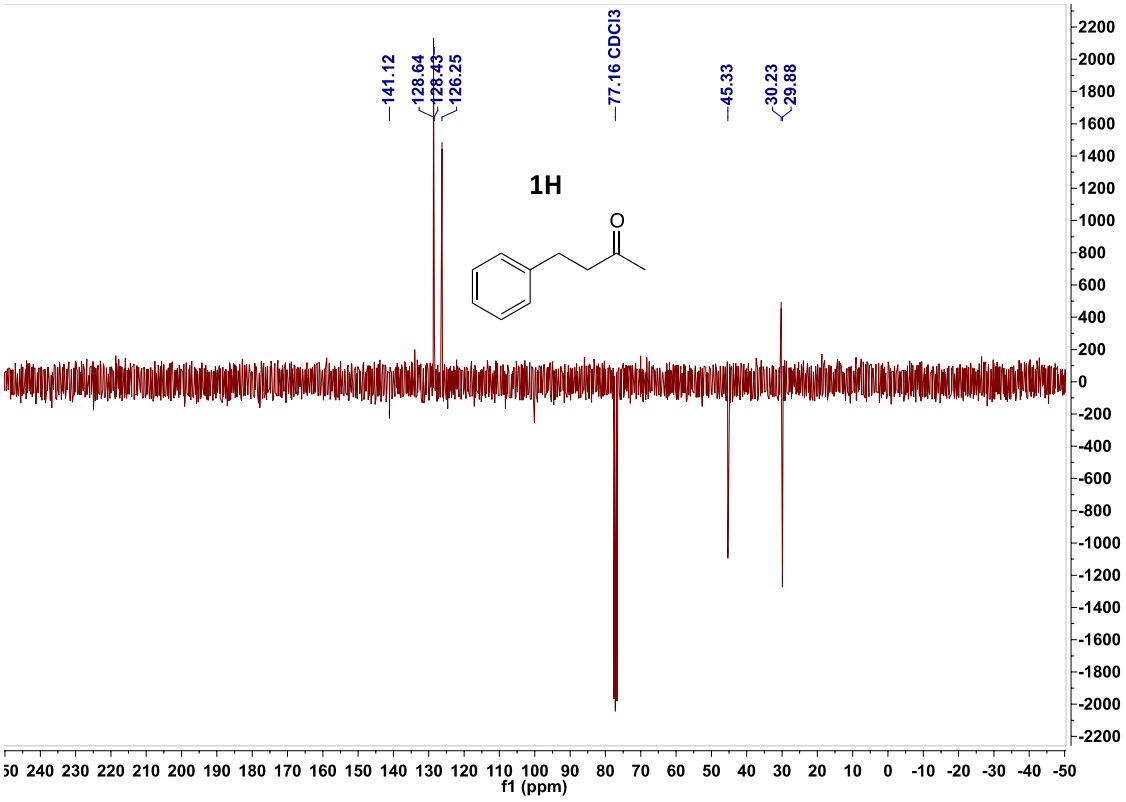

$^{13}C\{^{1}H\}$ Jmod NMR (75 MHz, 298 K) spectrum in $CDCl_3$ for **1H**.

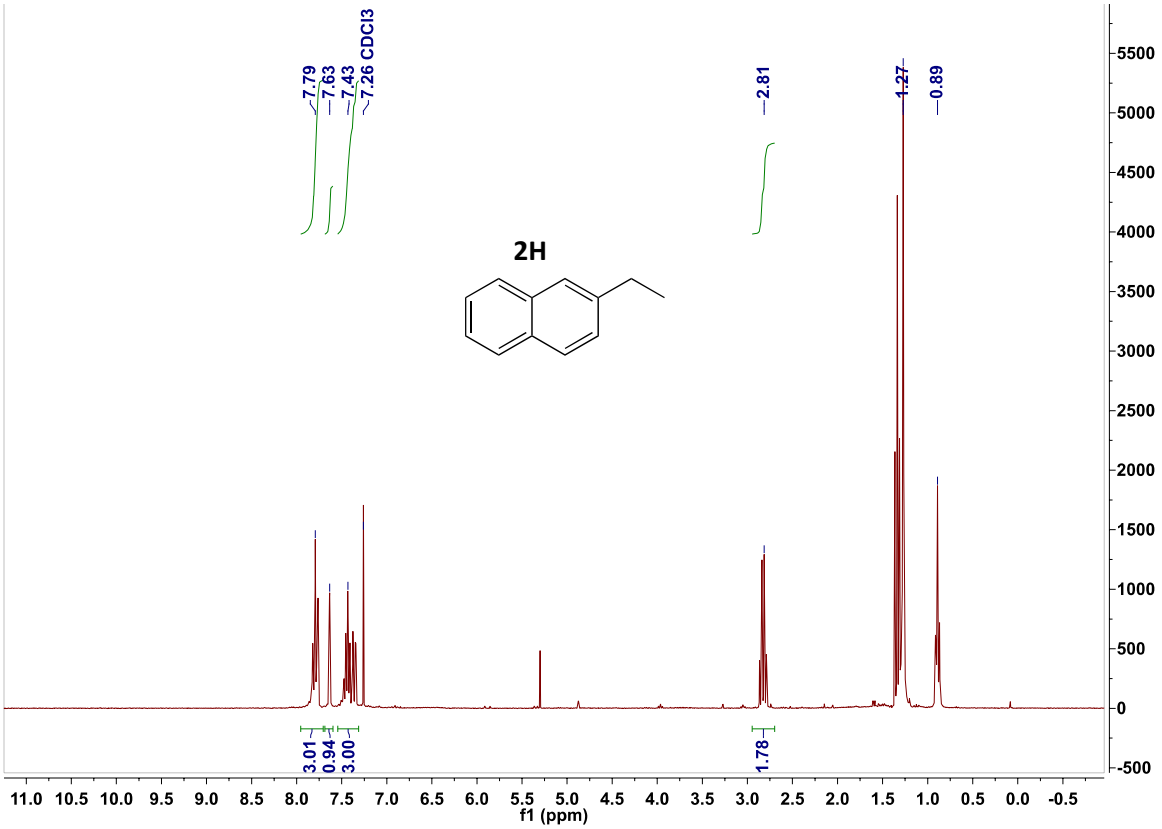

^{1}H NMR (300 MHz, 298 K) spectrum in $CDCl_3$ for **2H**.

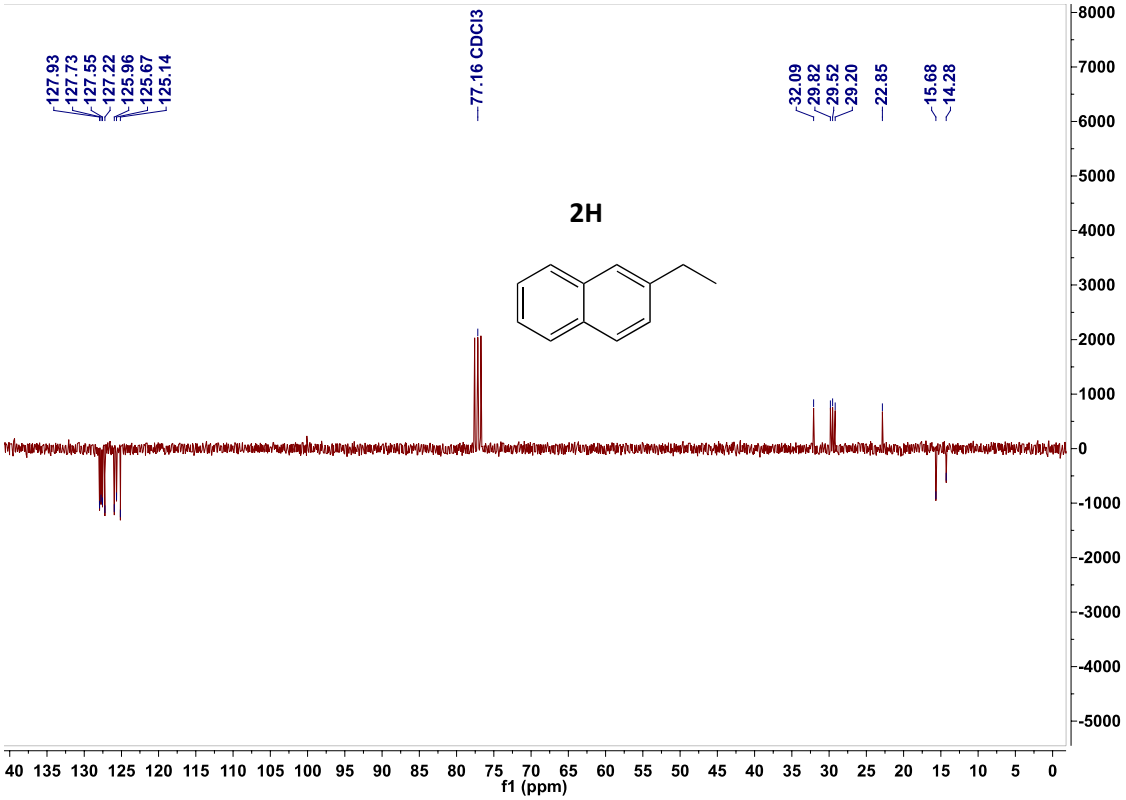

$^{13}C\{^{1}H\}$ Jmod NMR (75 MHz, 298 K) spectrum in $CDCl_3$ for **2H**.

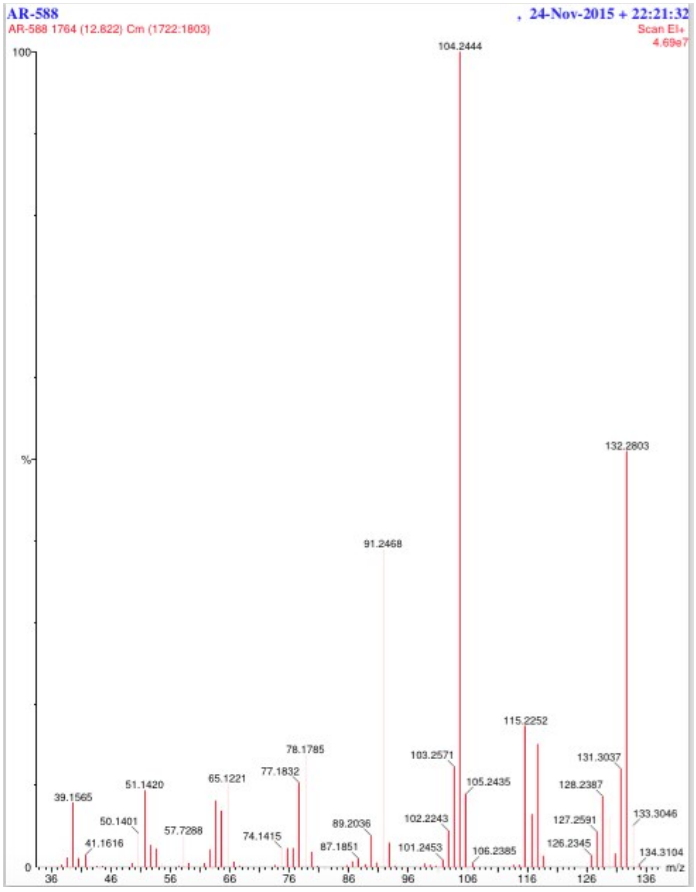

3H

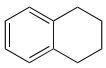

GC-MS chromatogram for **3H**.

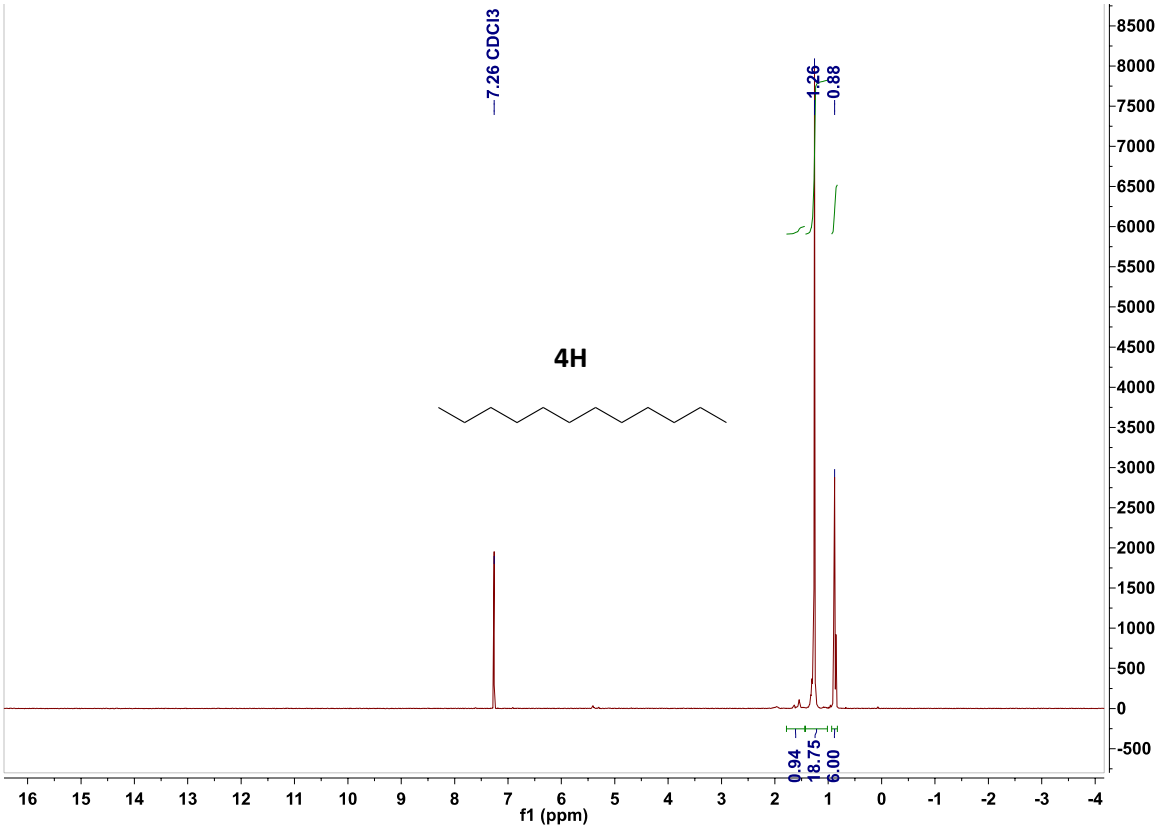

^{1}H NMR (300 MHz, 298 K) spectrum in $CDCl_3$ for **4H**.

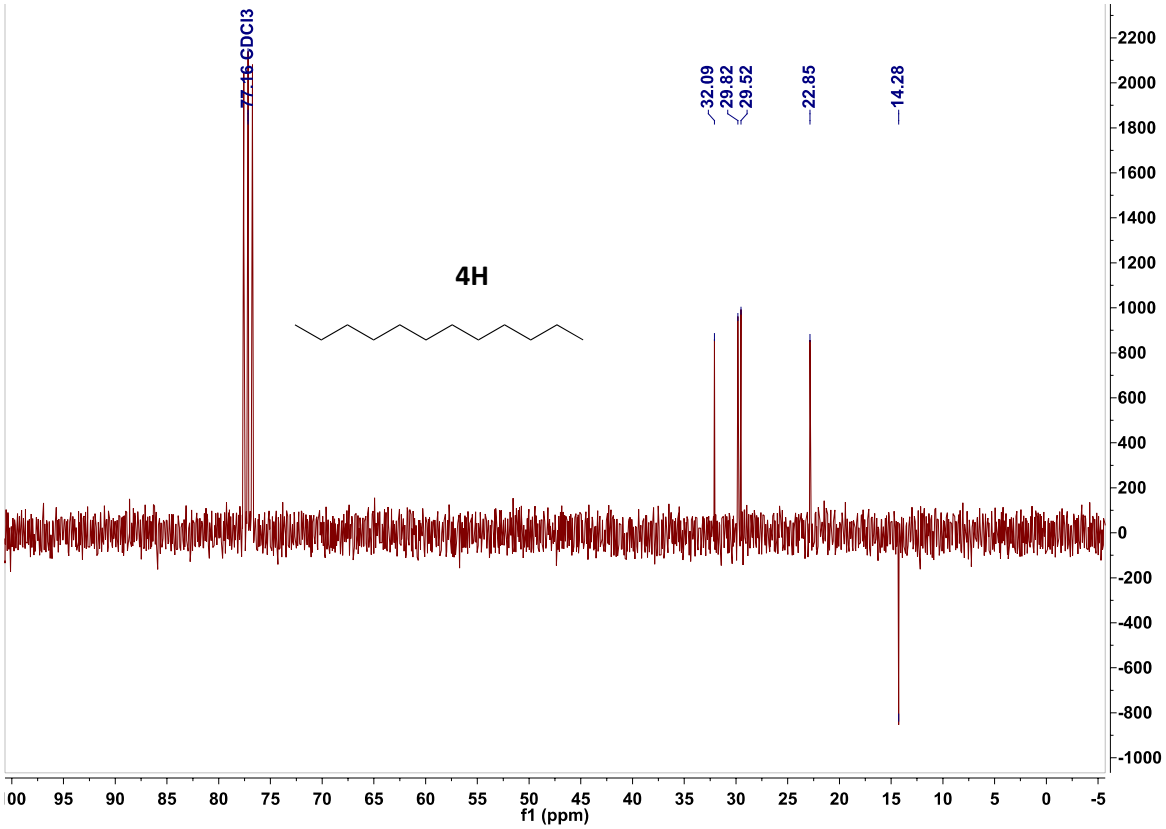

$^{13}C\{^{1}H\}$ Jmod NMR (75 MHz, 298 K) spectrum in $CDCl_3$ for **4H**.

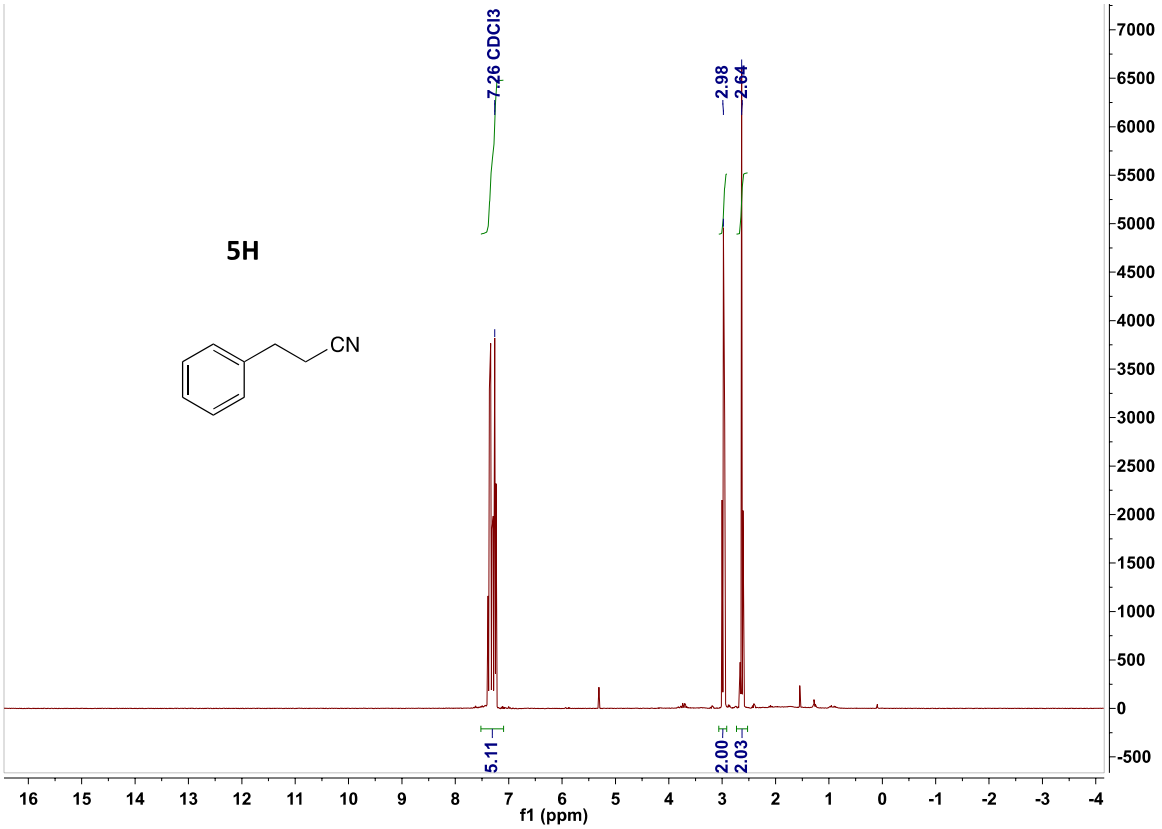

^{1}H NMR (300 MHz, 298 K) spectrum in $CDCl_3$ for **5H**.

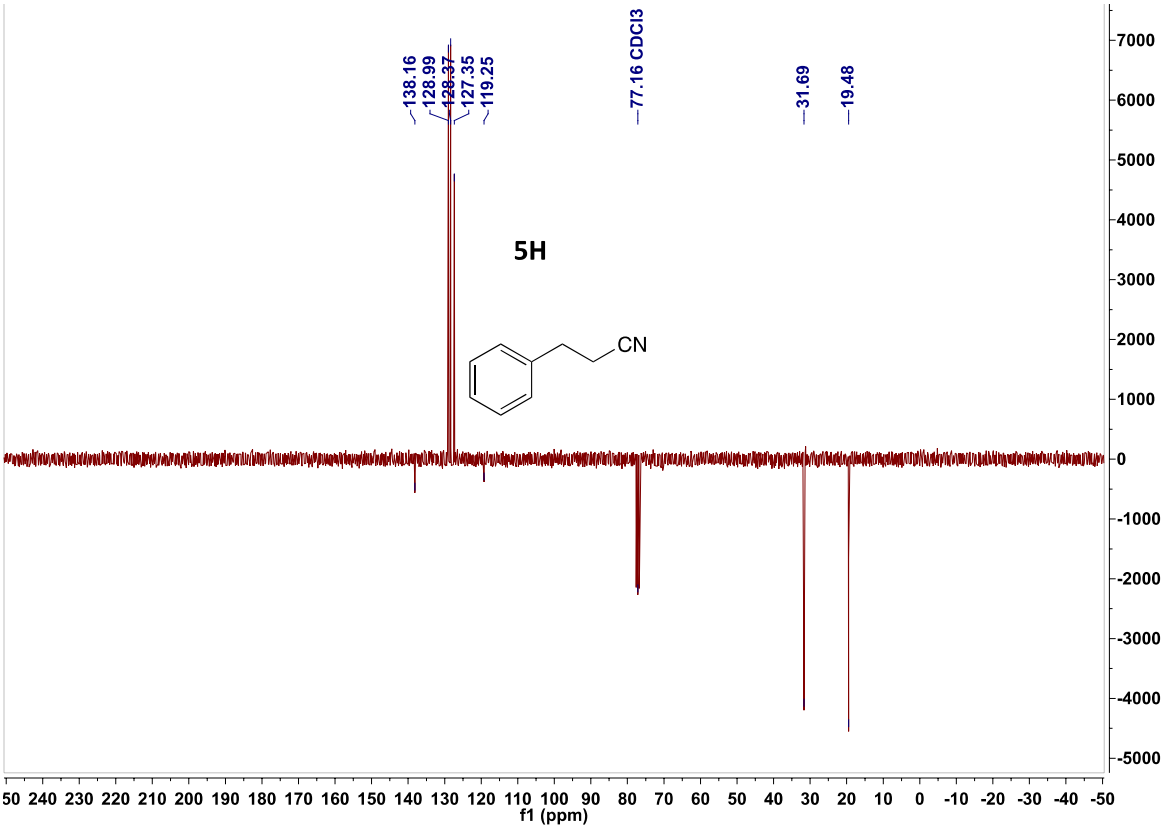

$^{13}C\{^{1}H\}$ Jmod NMR (75 MHz, 298 K) spectrum in $CDCl_3$ for **5H**.

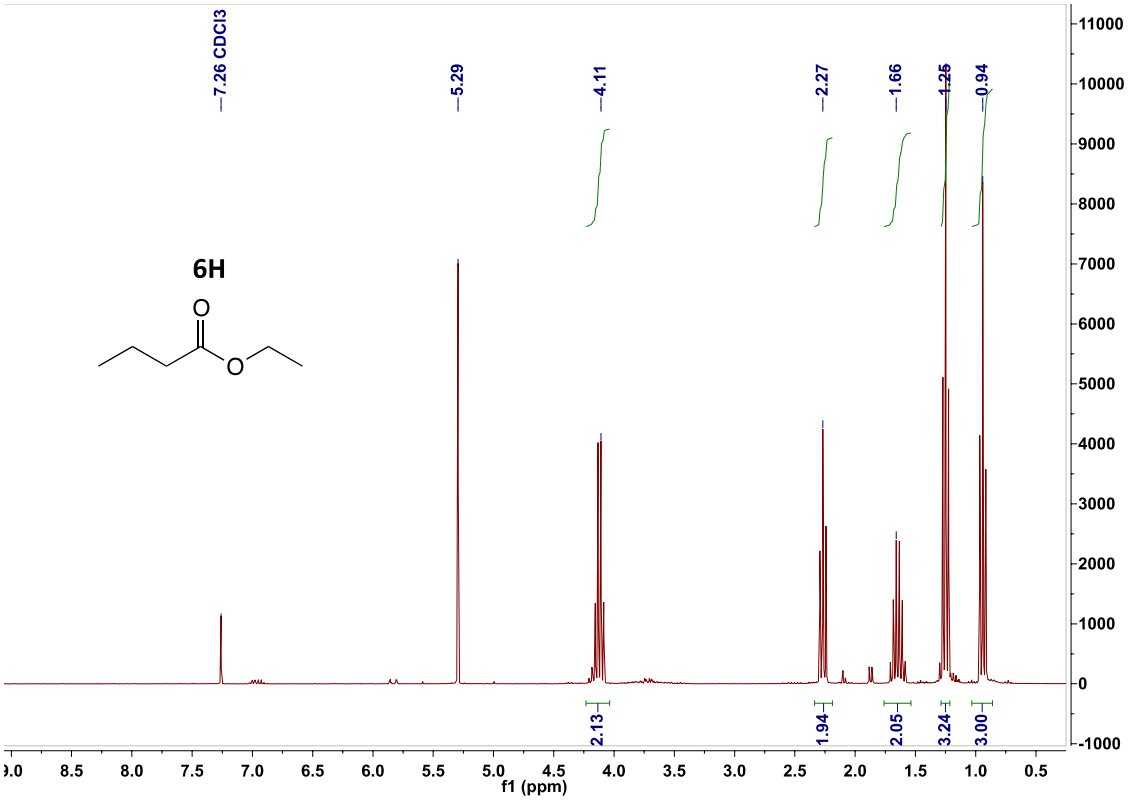

^{1}H NMR (300 MHz, 298 K) spectrum in $CDCl_3$ for **6H**.

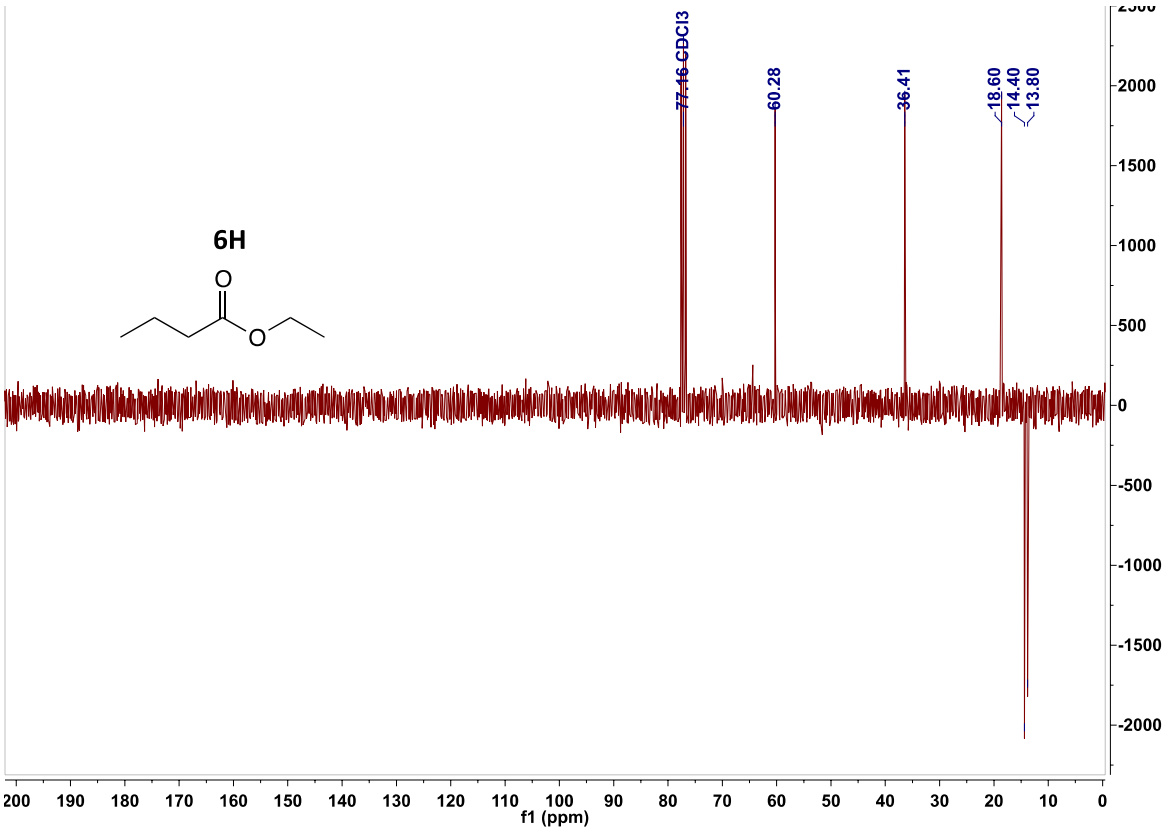

$^{13}C\{^{1}H\}$ Jmod NMR (75 MHz, 298 K)spectrum in $CDCl_3$ for **6H**.

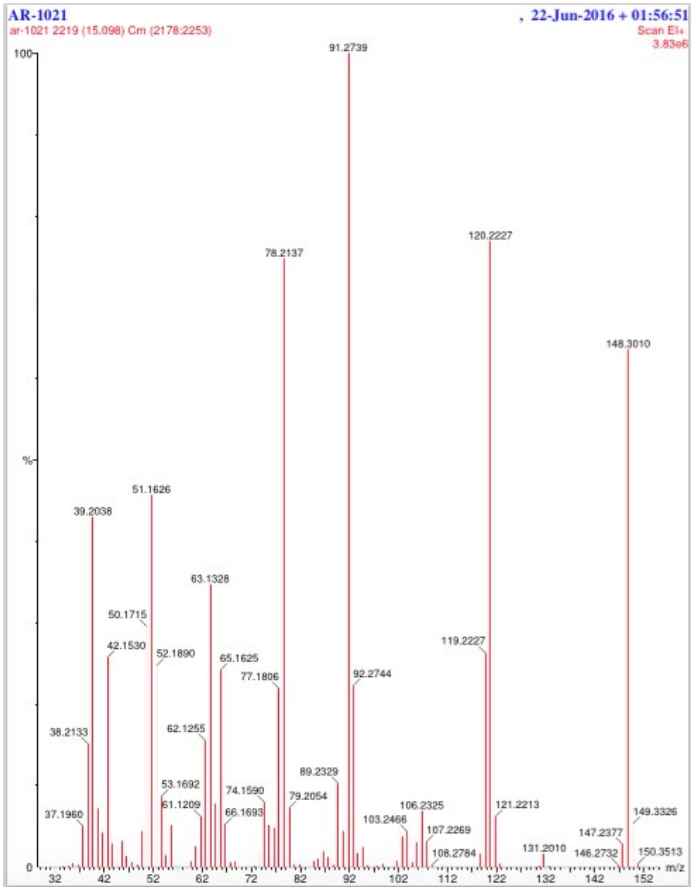

7H

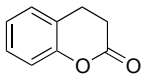

GC-MS chromatogram for **7H**.

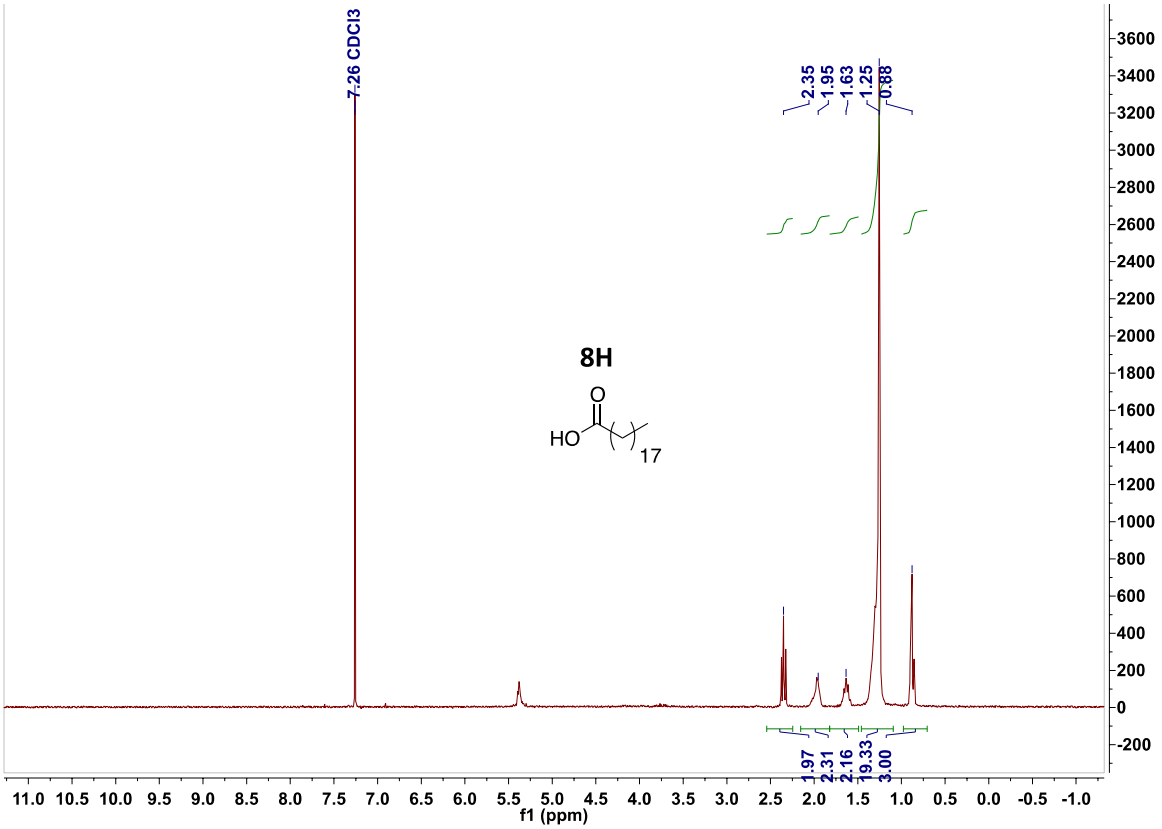

^{1}H NMR (300 MHz, 298 K) spectrum in $CDCl_3$ for **8H**.

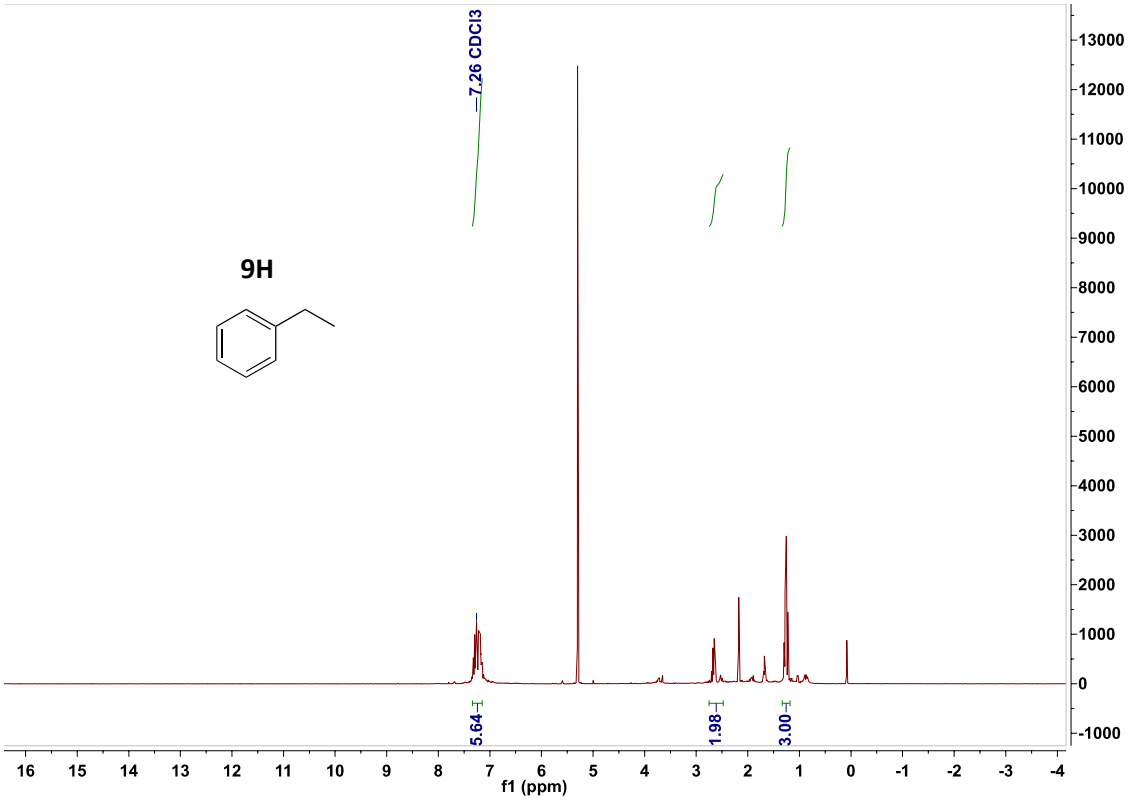

^{1}H NMR (300 MHz, 298 K) spectrum in $CDCl_3$ for **9H**.

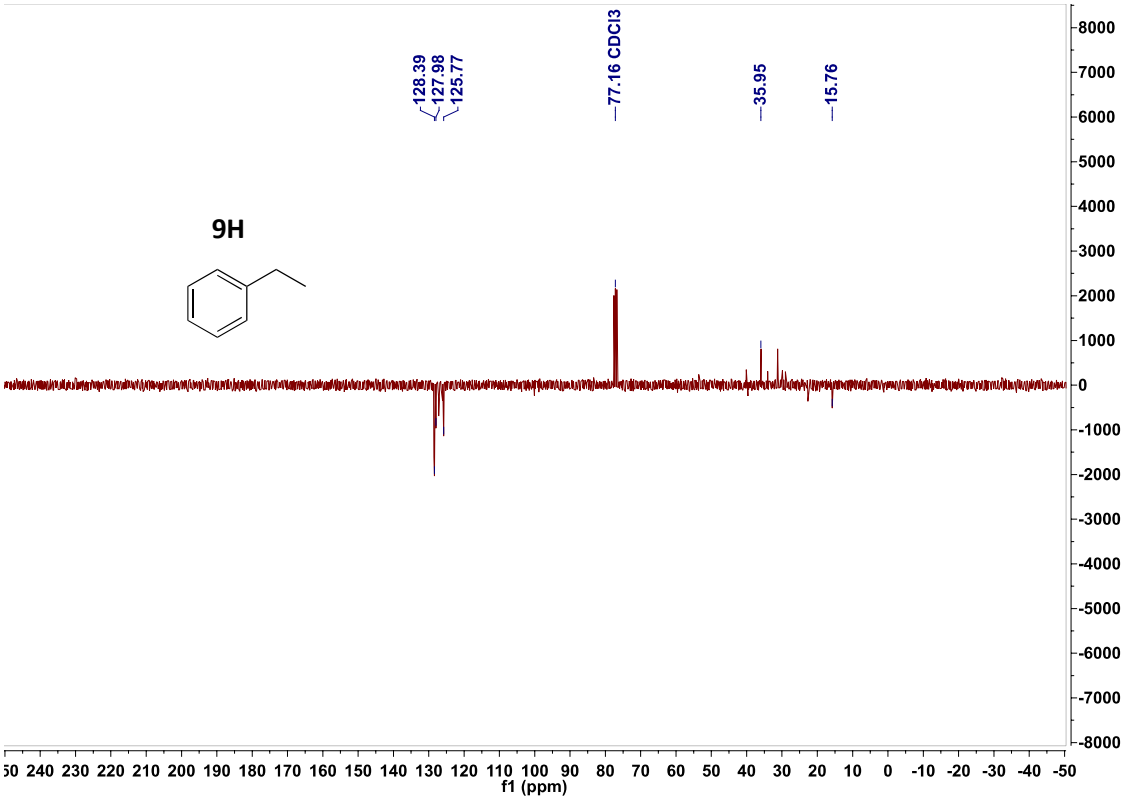

$^{13}C\{^{1}H\}$ Jmod NMR (75 MHz, 298 K) spectrum in $CDCl_3$ for **9H**.

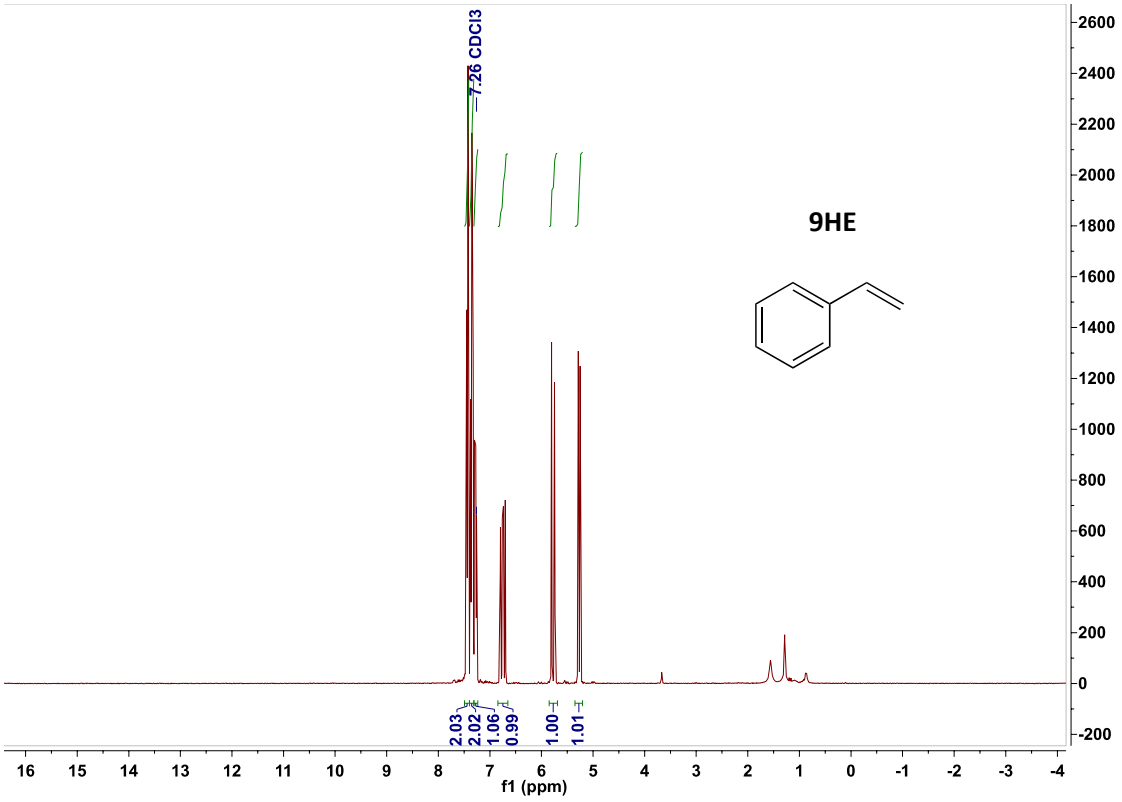

^{1}H NMR (300 MHz, 298 K) spectrum in $CDCl_3$ for **9HE**.

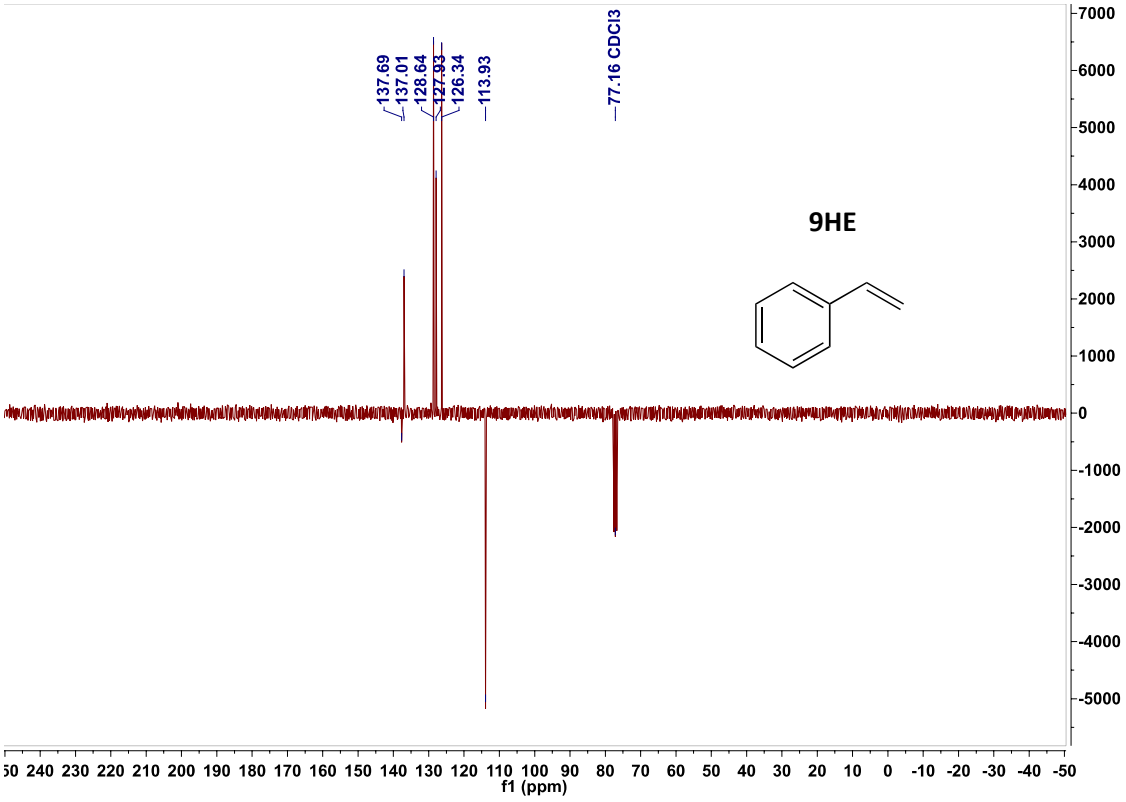

$^{13}C\{^{1}H\}$ Jmod NMR (75 MHz, 298 K) spectrum in $CDCl_3$ for **9HE**.

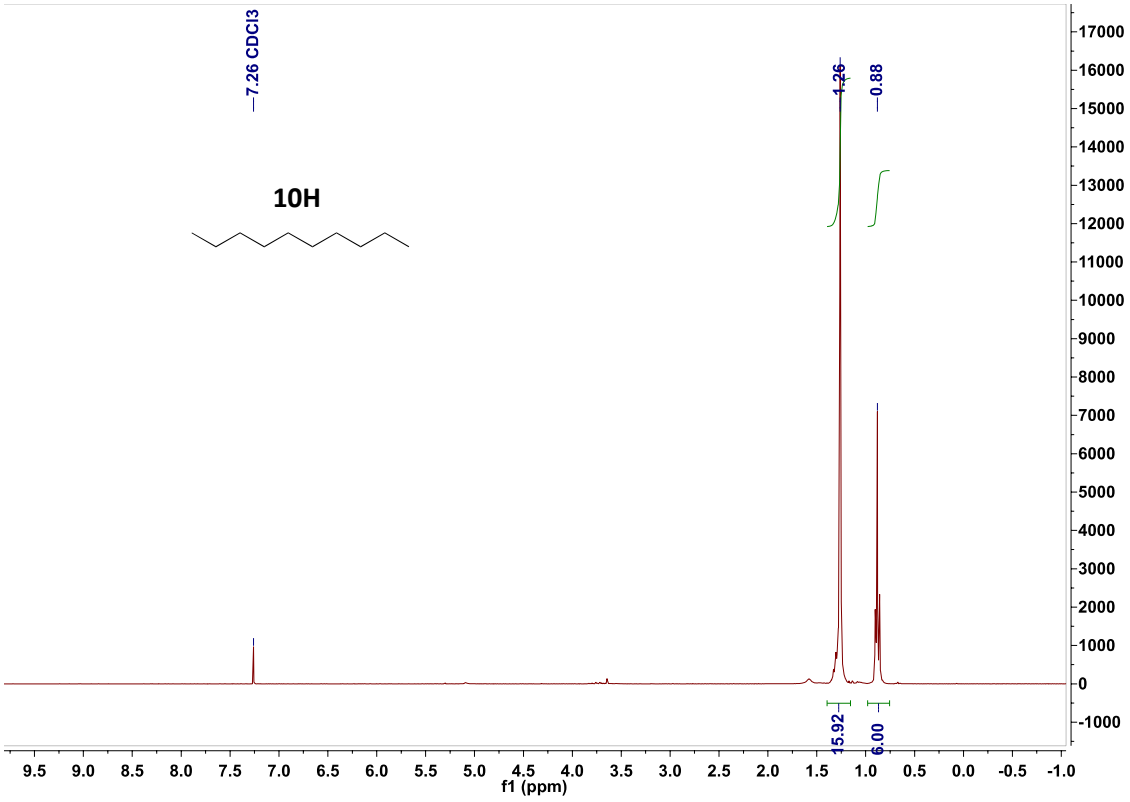

^{1}H NMR (300 MHz, 298 K) spectrum in $CDCl_3$ for **10H**.

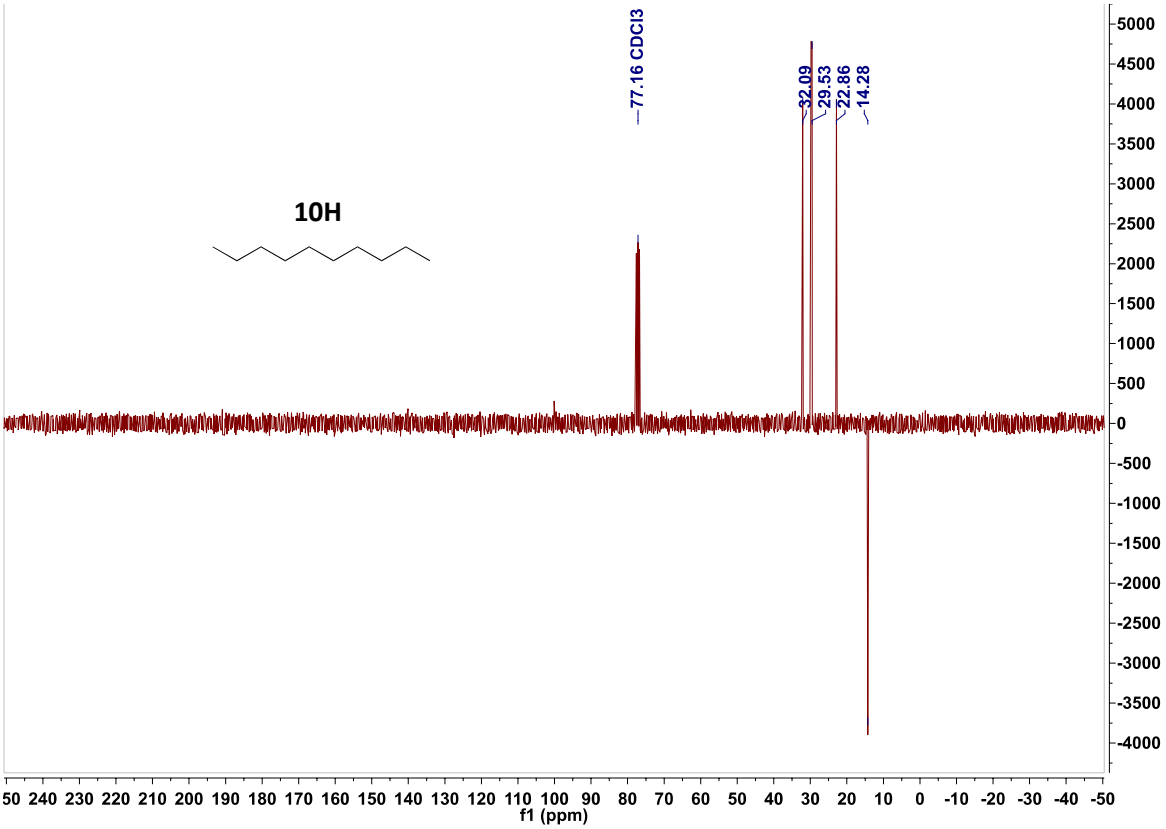

$^{13}C\{^{1}H\}$ Jmod NMR (75 MHz, 298 K) spectrum in $CDCl_3$ for **10H**.

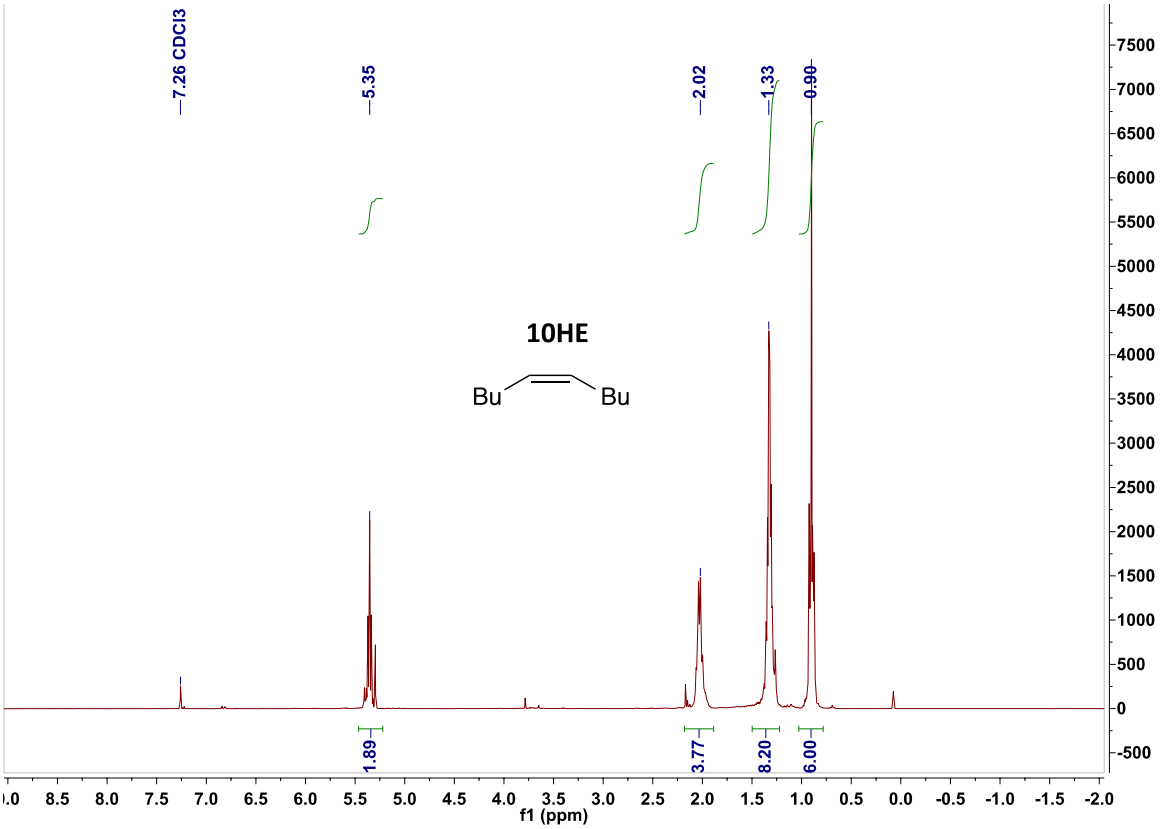

^{1}H NMR (300 MHz, 298 K) spectrum in $CDCl_3$ for **10HE**.

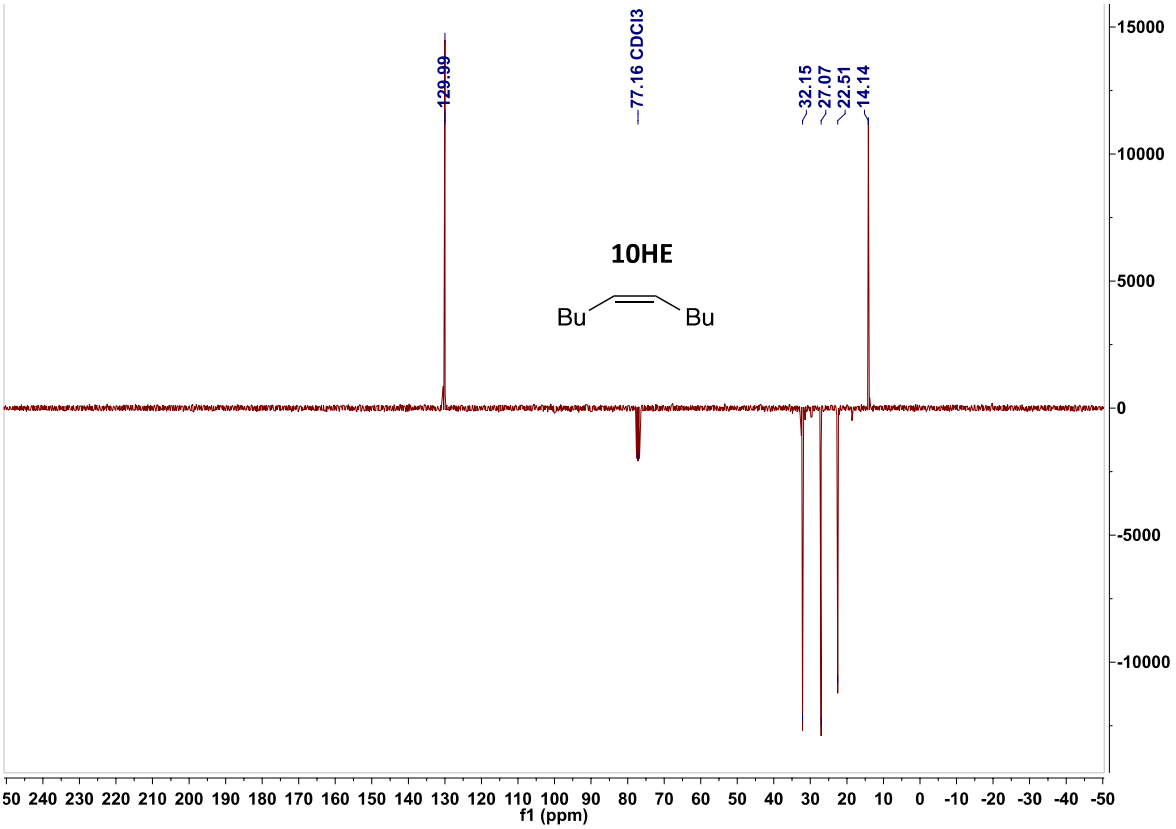

$^{13}C\{^{1}H\}$ Jmod NMR (75 MHz, 298 K) spectrum in $CDCl_3$ for **10HE**.

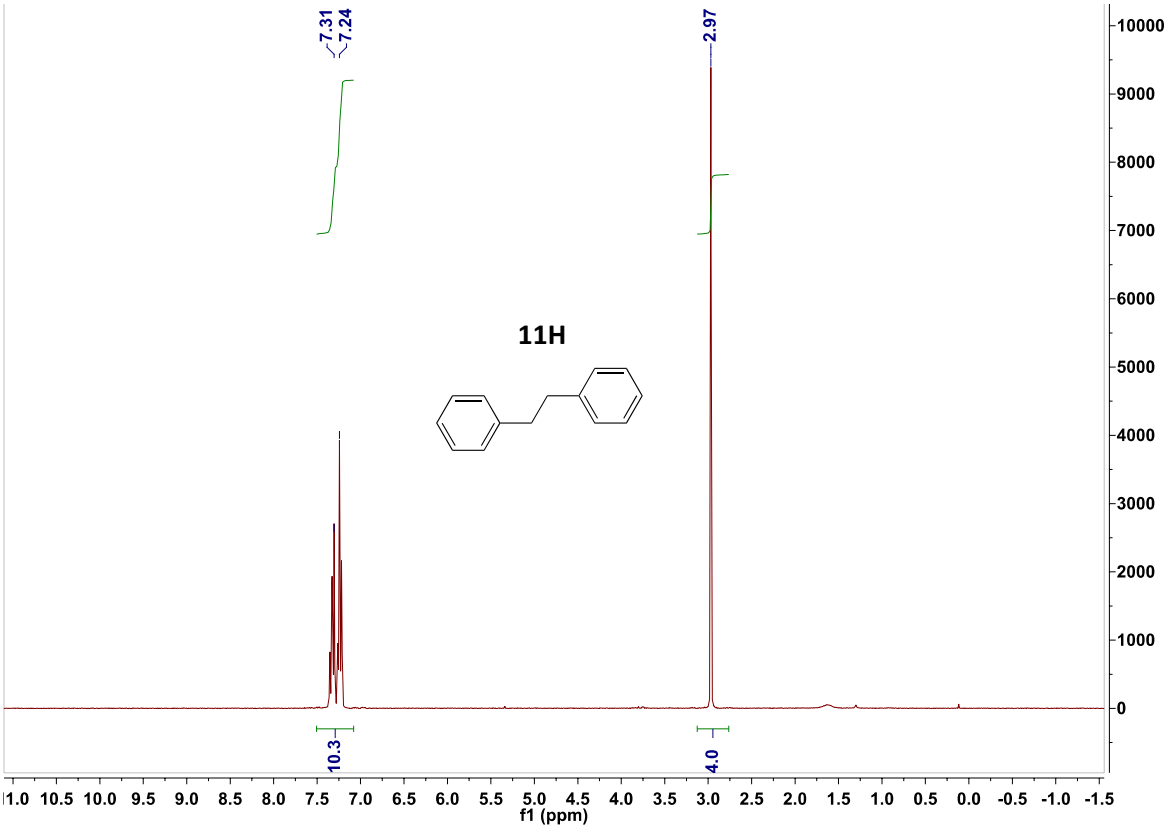

^{1}H NMR (300 MHz, 298 K) spectrum in $CDCl_3$ for **11H**.

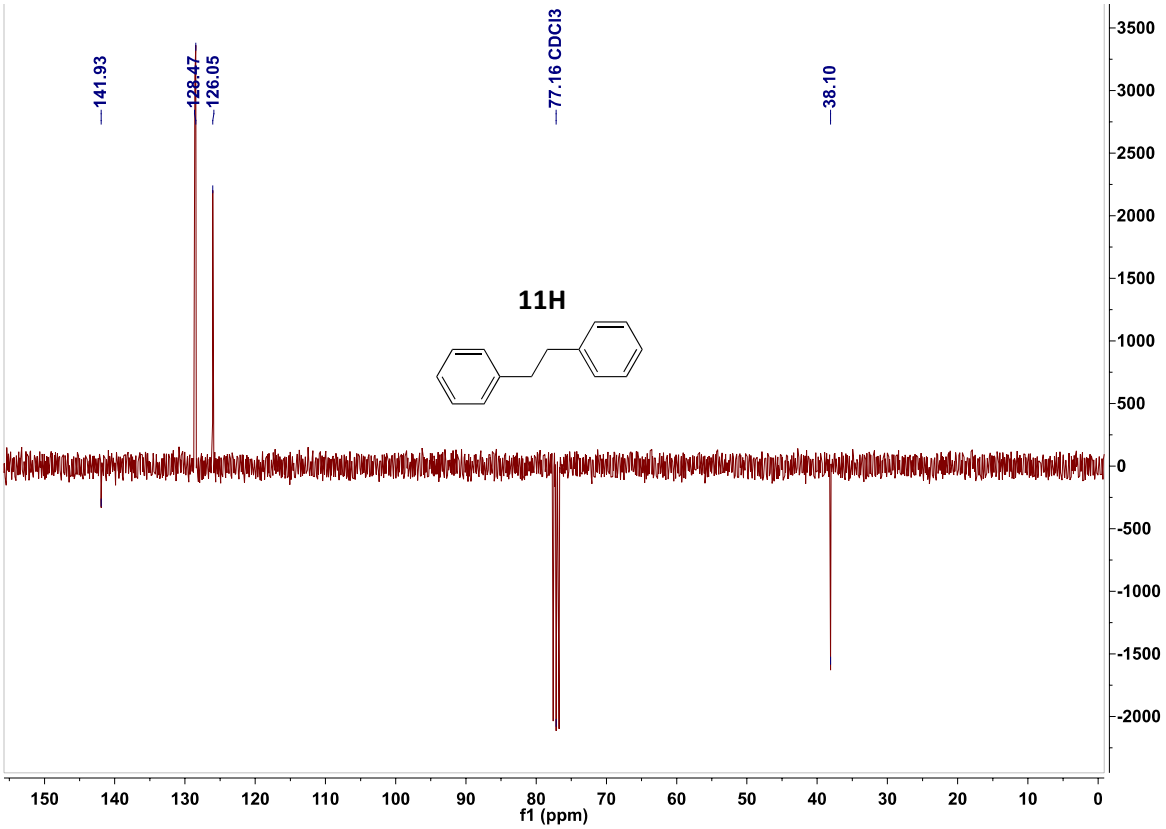

$^{13}C\{^{1}H\}$ Jmod NMR (75 MHz, 298 K) spectrum in $CDCl_3$ for **11H**.

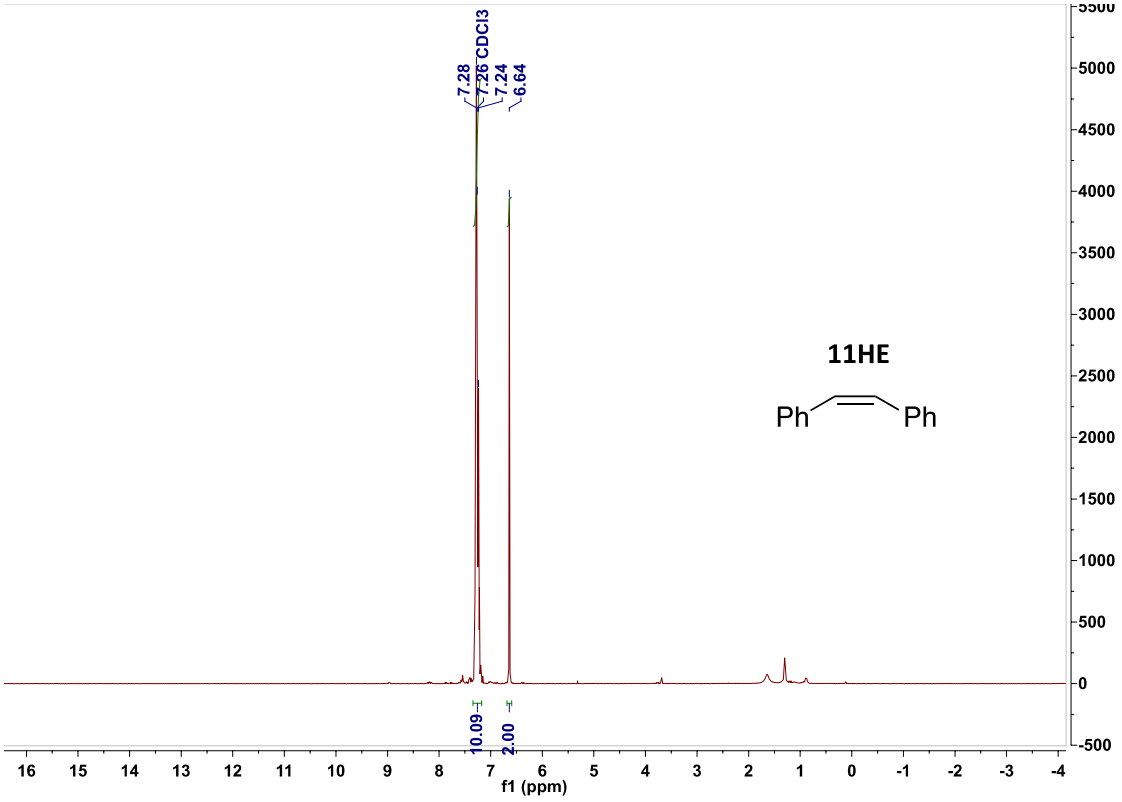

^{1}H NMR (300 MHz, 298 K) spectrum in $CDCl_3$ for **11HE**.

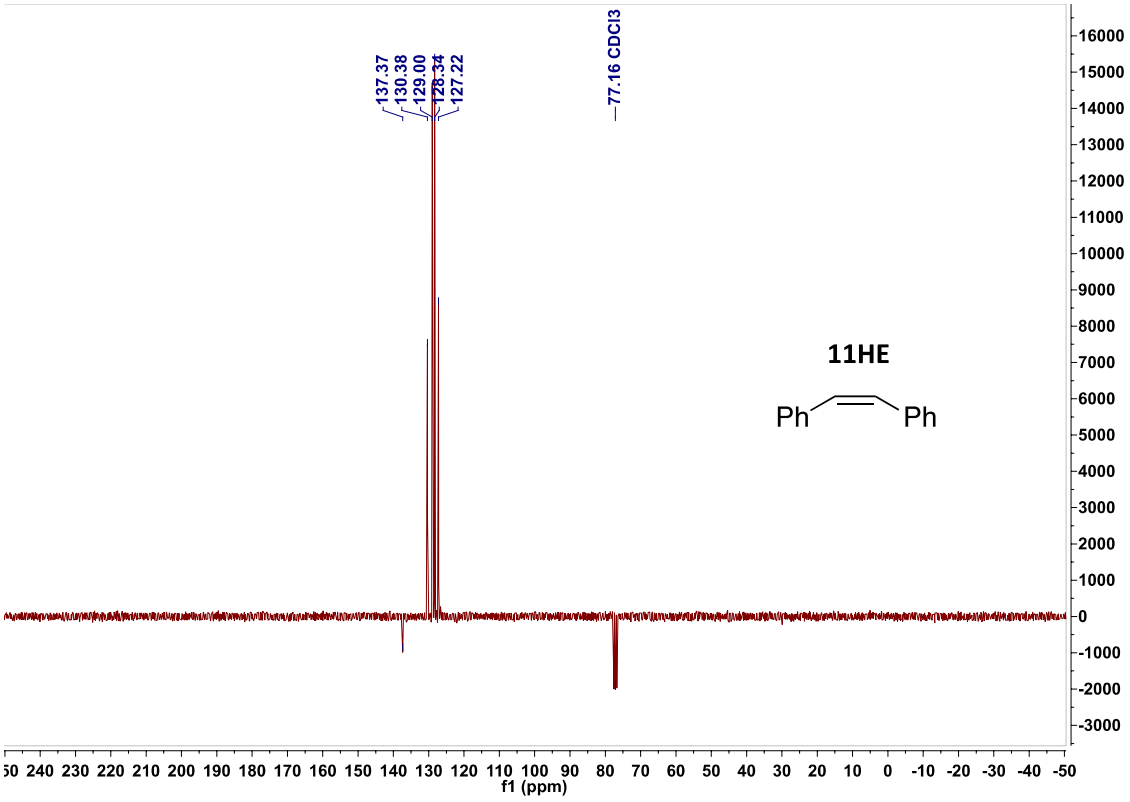

$^{13}C\{^{1}H\}$ Jmod NMR (75 MHz, 298 K) spectrum in $CDCl_3$ for **11HE**.

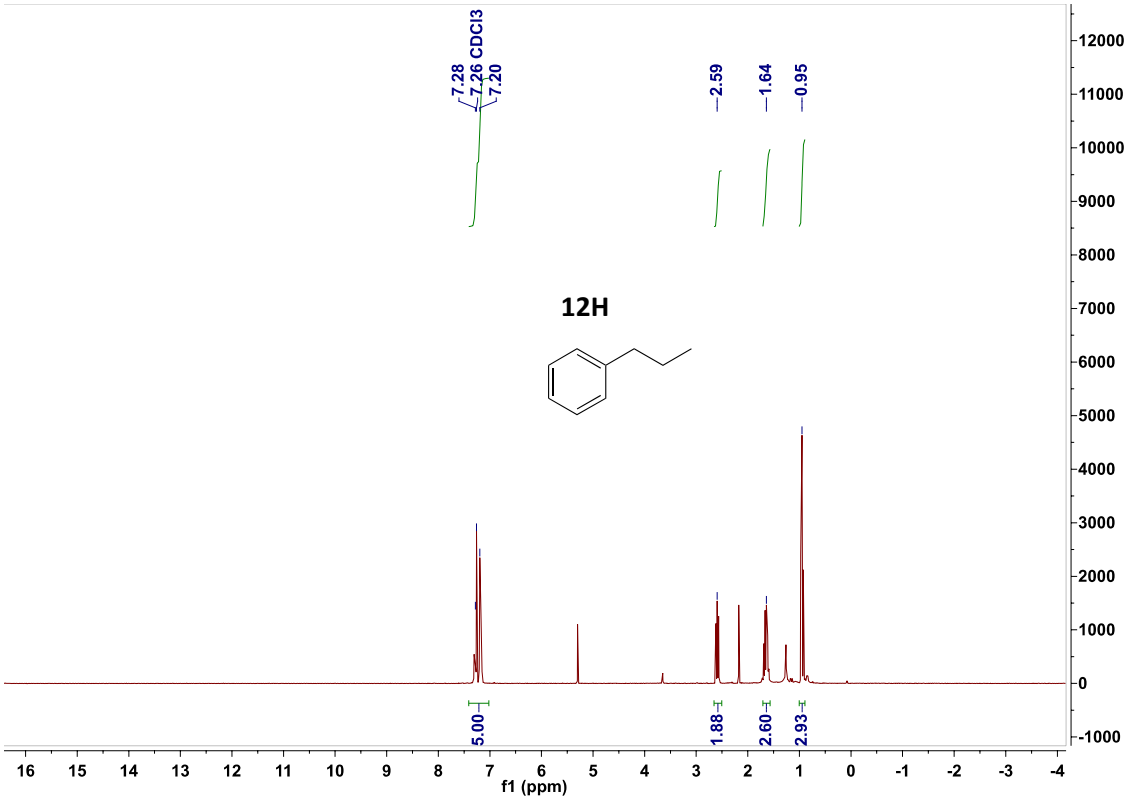

^{1}H NMR (300 MHz, 298 K) spectrum in $CDCl_3$ for **12H**.

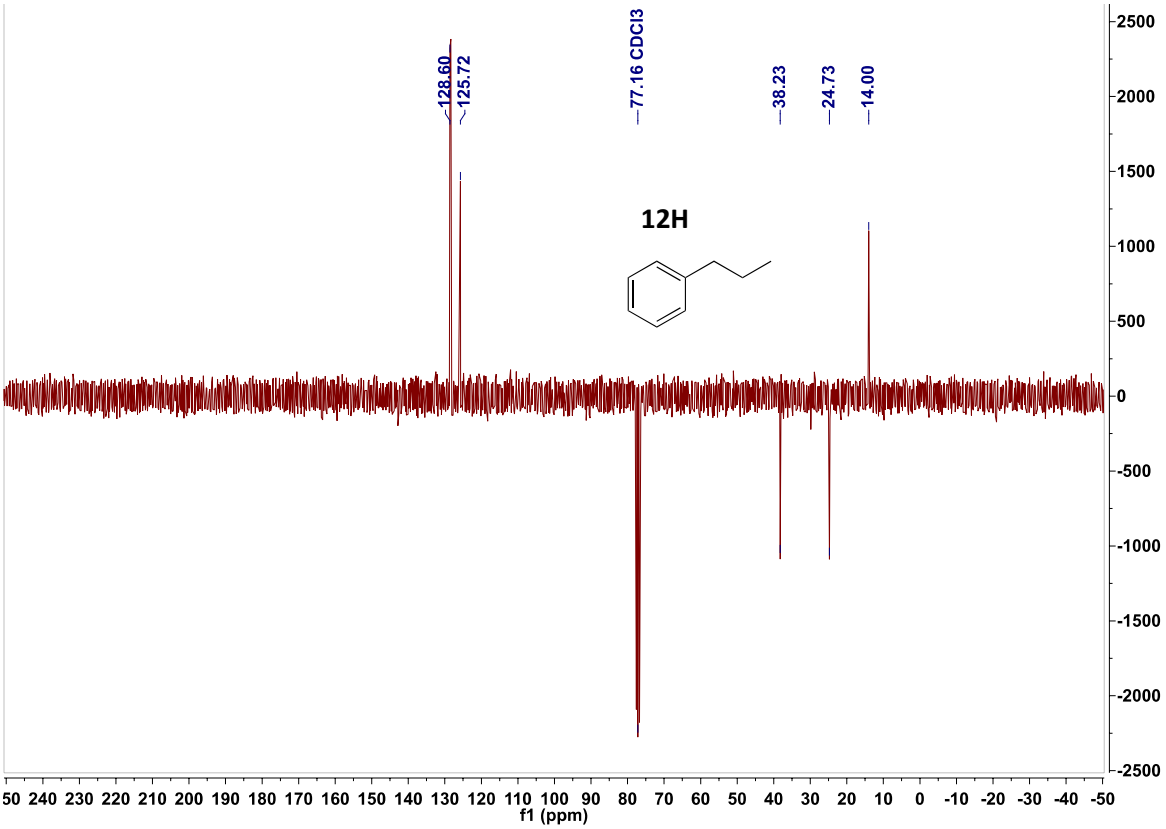

$^{13}C\{^{1}H\}$ Jmod NMR (75 MHz, 298 K) spectrum in $CDCl_3$ for **12H**.

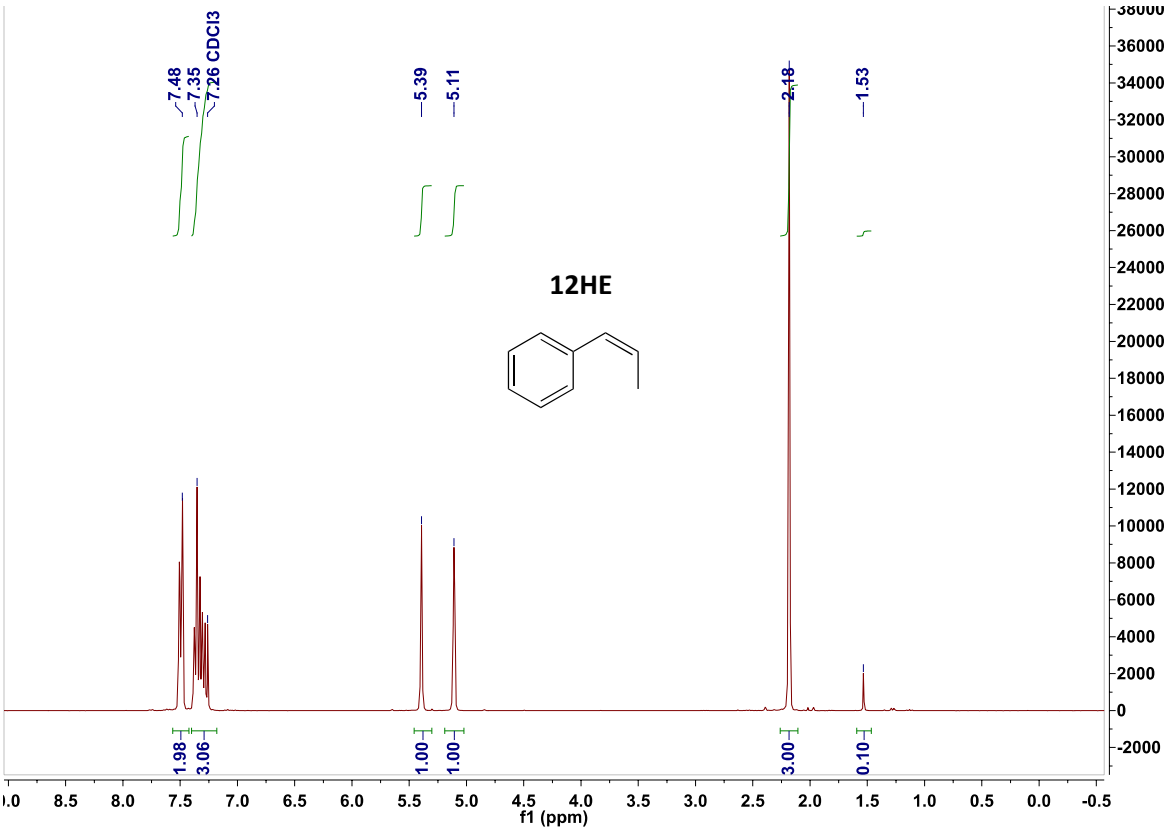

^{1}H NMR (300 MHz, 298 K) spectrum in $CDCl_3$ for **12HE**.

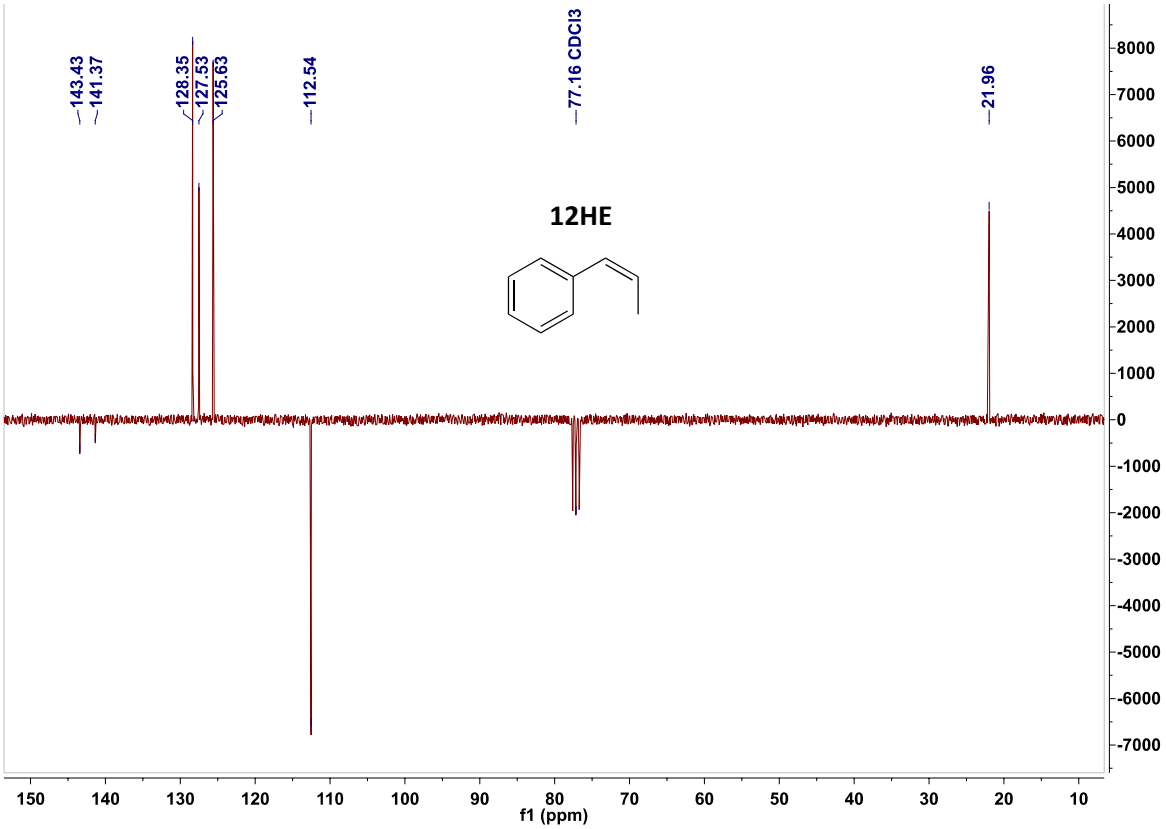

$^{13}C\{^{1}H\}$ Jmod NMR (75 MHz, 298 K) spectrum in $CDCl_3$ for **12HE**.

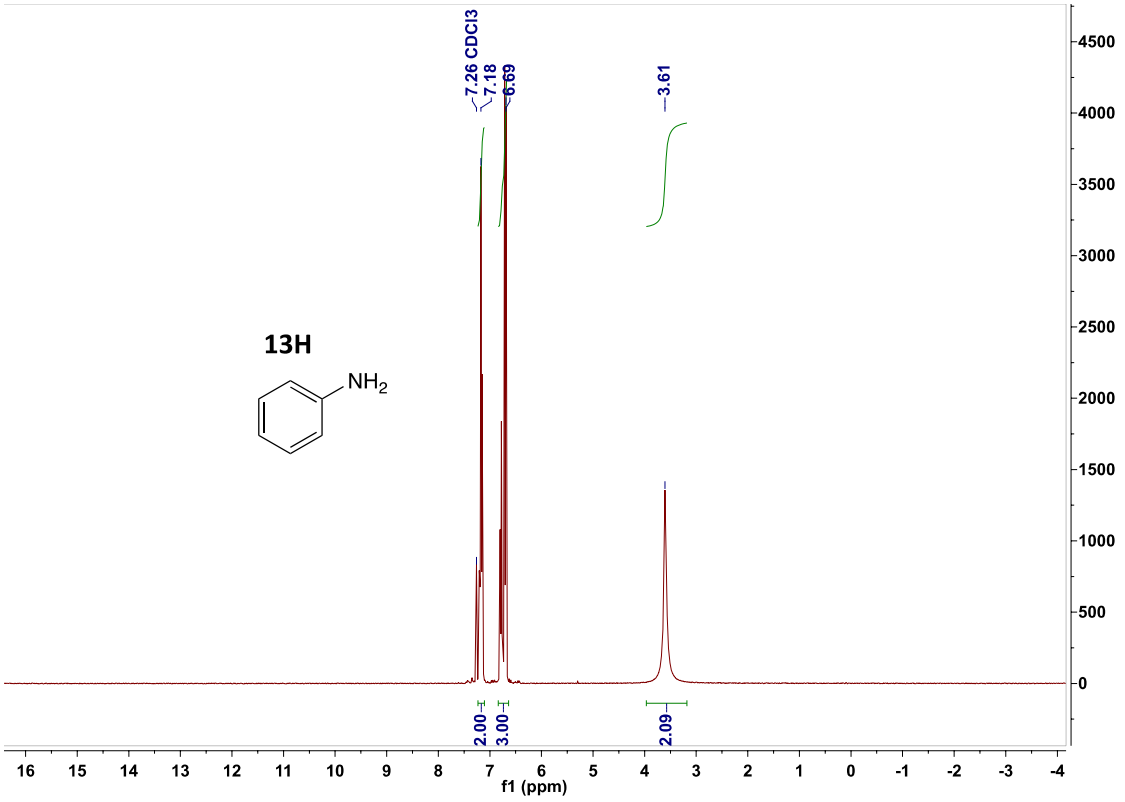

^{1}H NMR (300 MHz, 298 K) spectrum in $CDCl_3$ for **13H**.

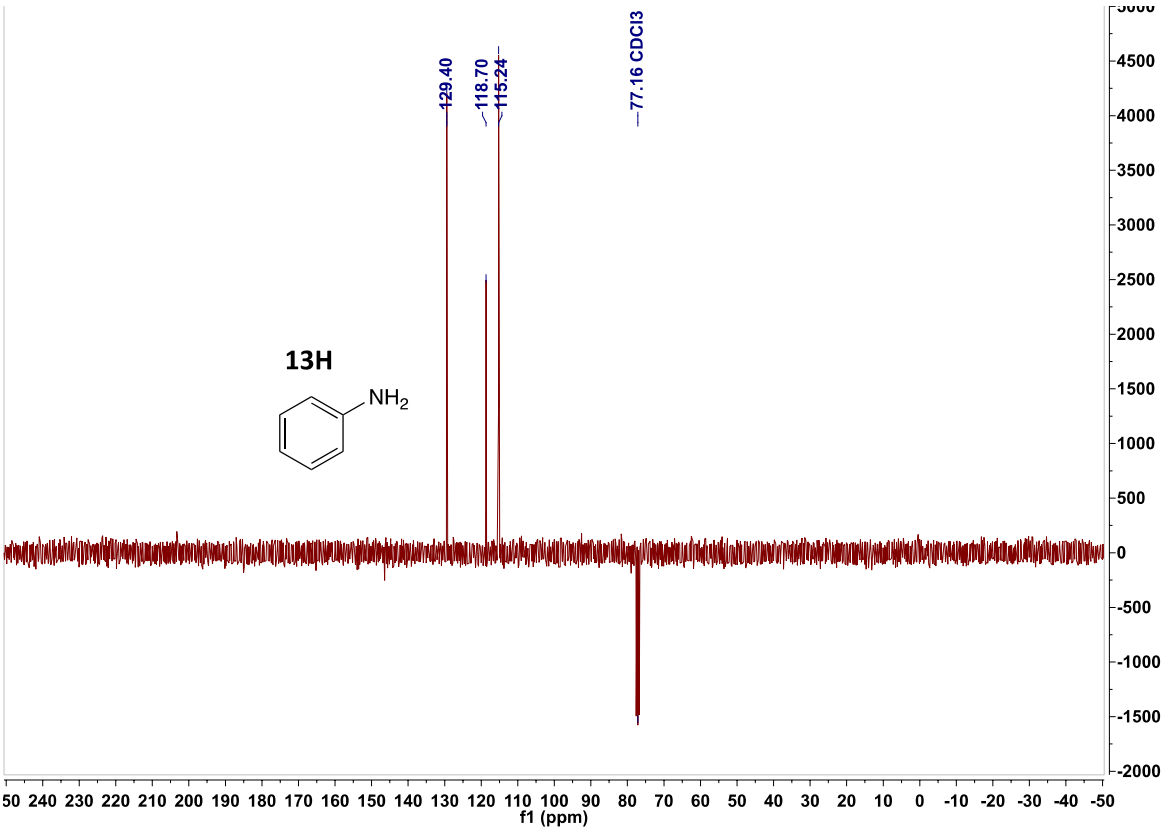

$^{13}C\{^{1}H\}$ Jmod NMR (75 MHz, 298 K) spectrum in $CDCl_3$ for **13H**.

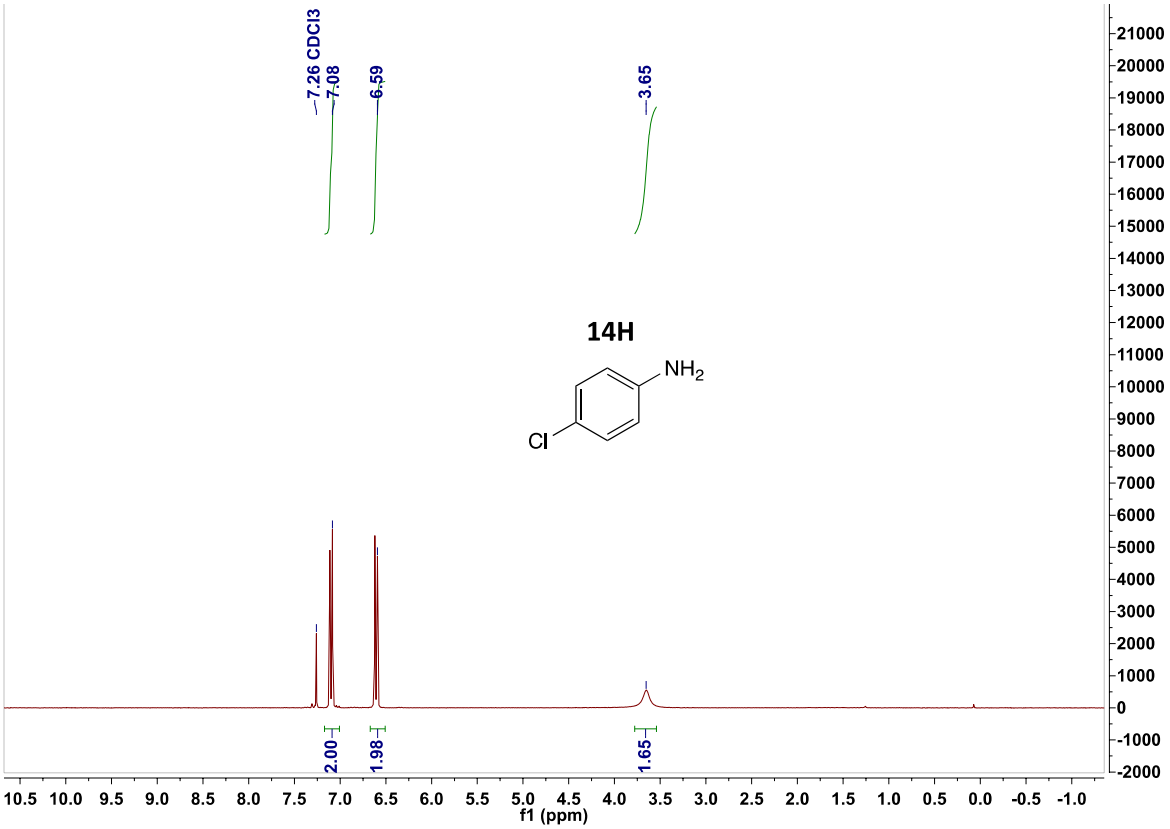

^{1}H NMR (300 MHz, 298 K) spectrum in $CDCl_3$ for **14H**.

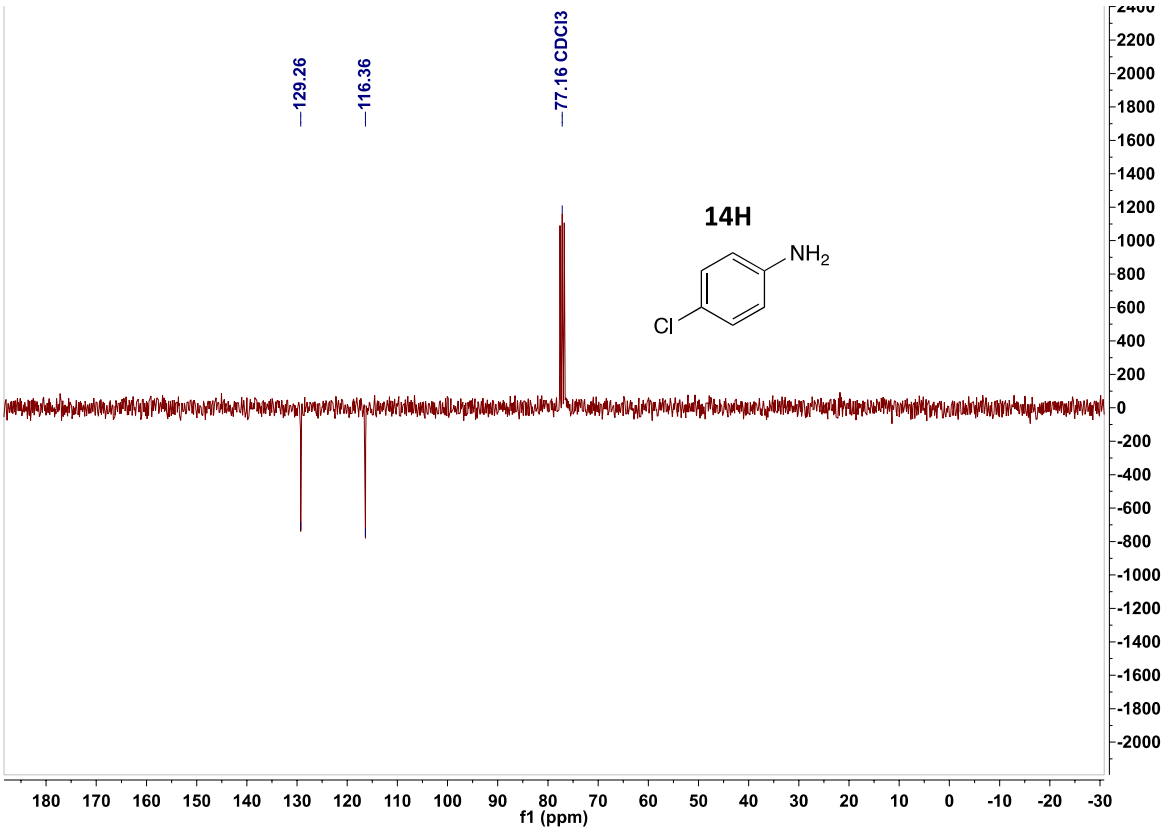

$^{13}C\{^{1}H\}$ Jmod NMR (75 MHz, 298 K) spectrum in $CDCl_3$ for **14H**.

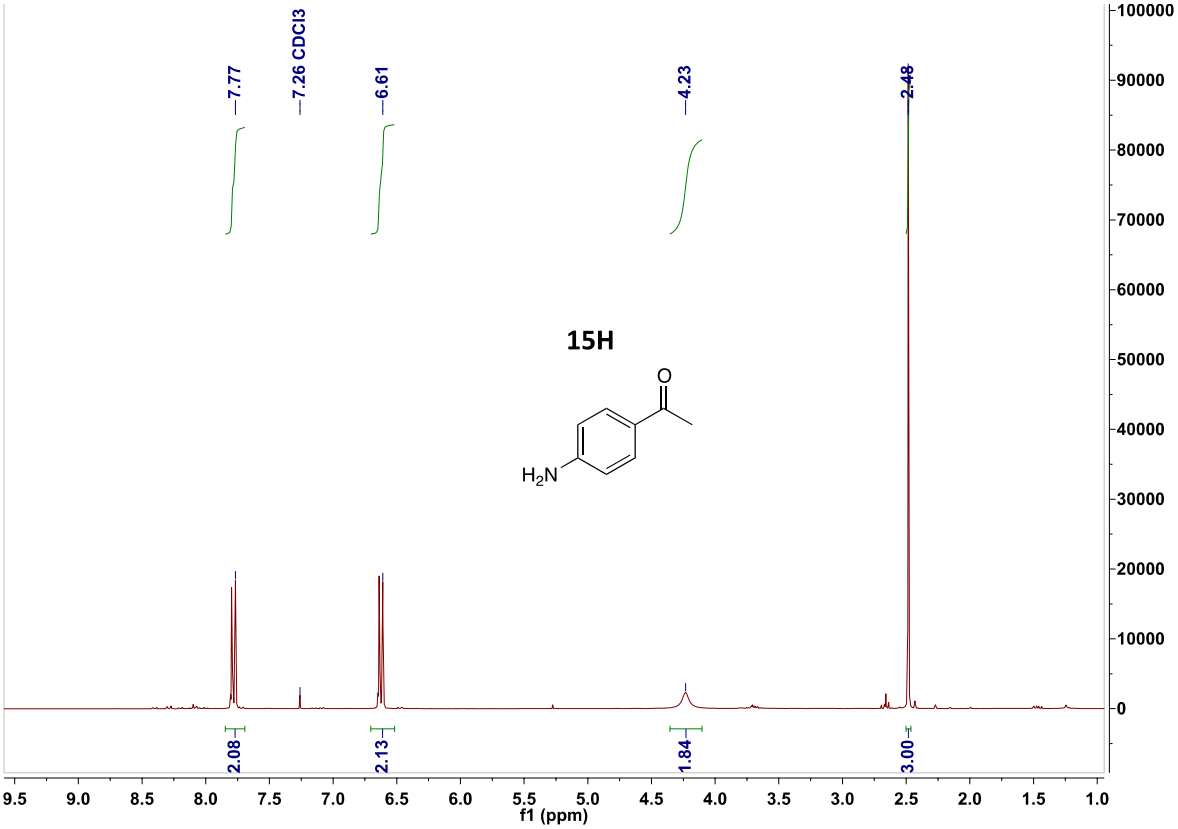

^{1}H NMR (300 MHz, 298 K) spectrum in $CDCl_3$ for **15H**.

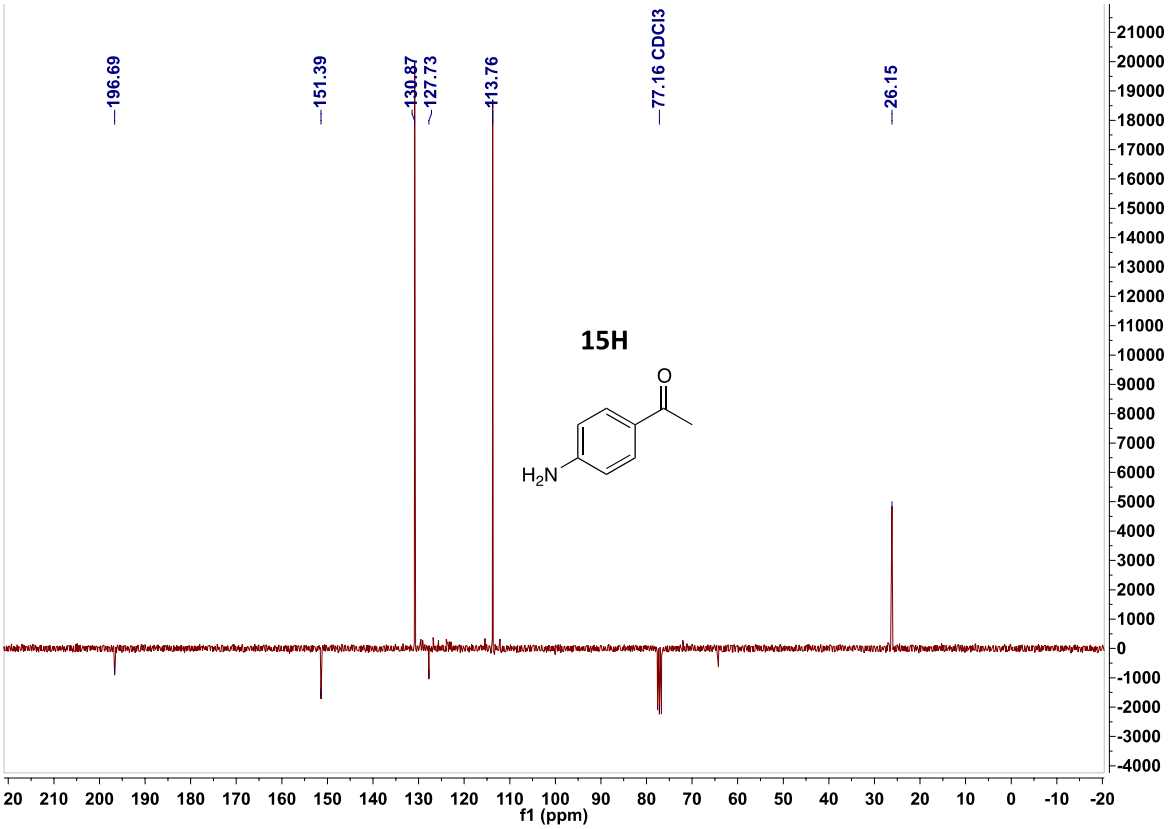

$^{13}C\{^{1}H\}$ Jmod NMR (75 MHz, 298 K) spectrum in $CDCl_3$ for **15H**.

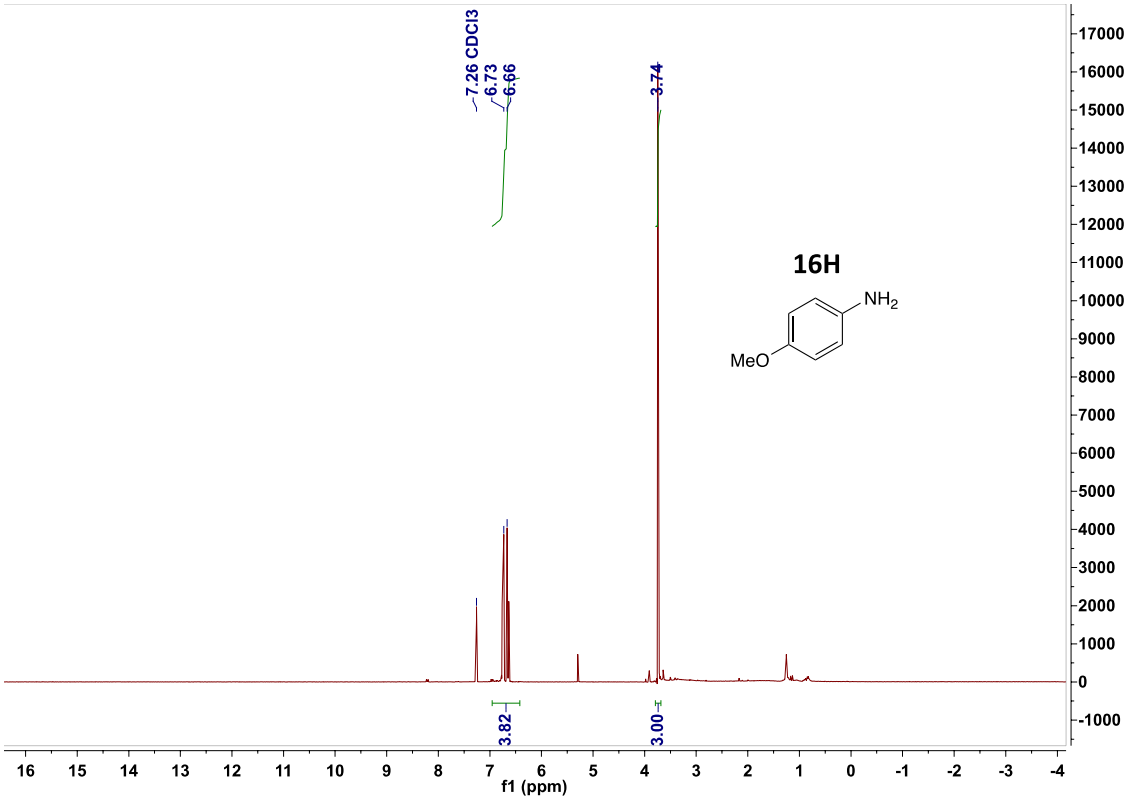

^{1}H NMR (300 MHz, 298 K) spectrum in $CDCl_3$ for **16H**.

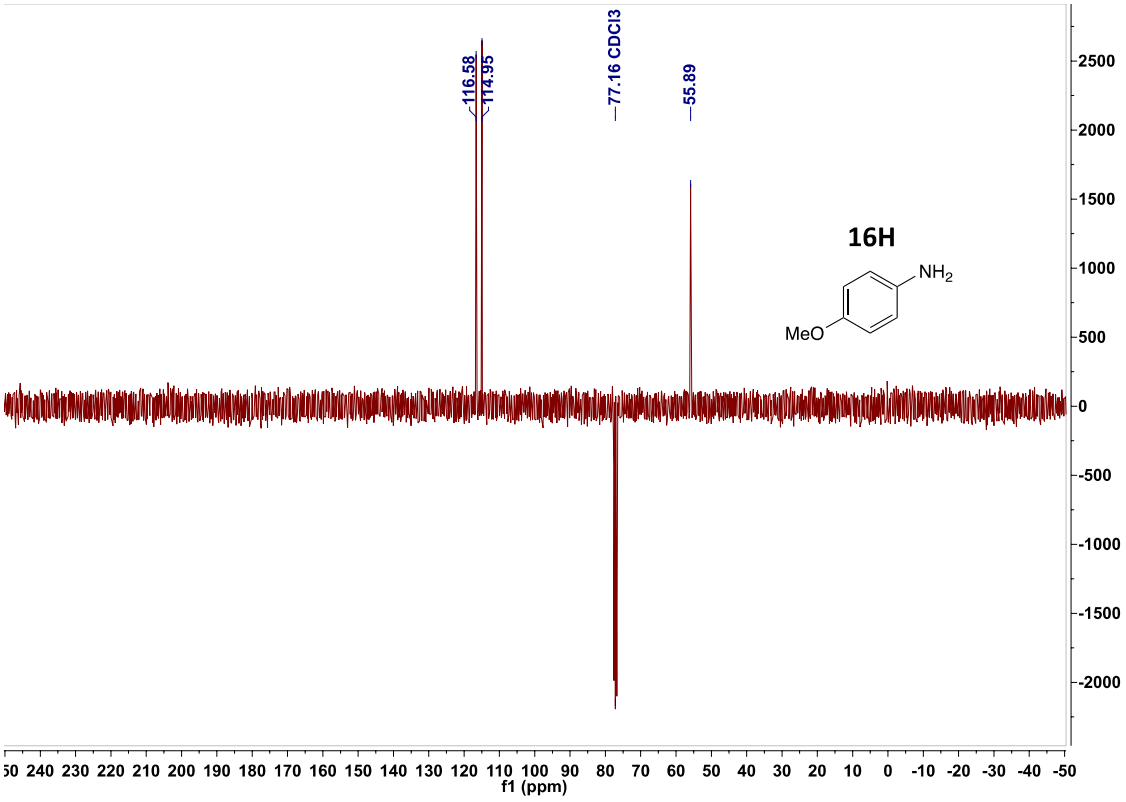

$^{13}C\{^{1}H\}$ Jmod NMR (75 MHz, 298 K) spectrum in $CDCl_3$ for **16H**.

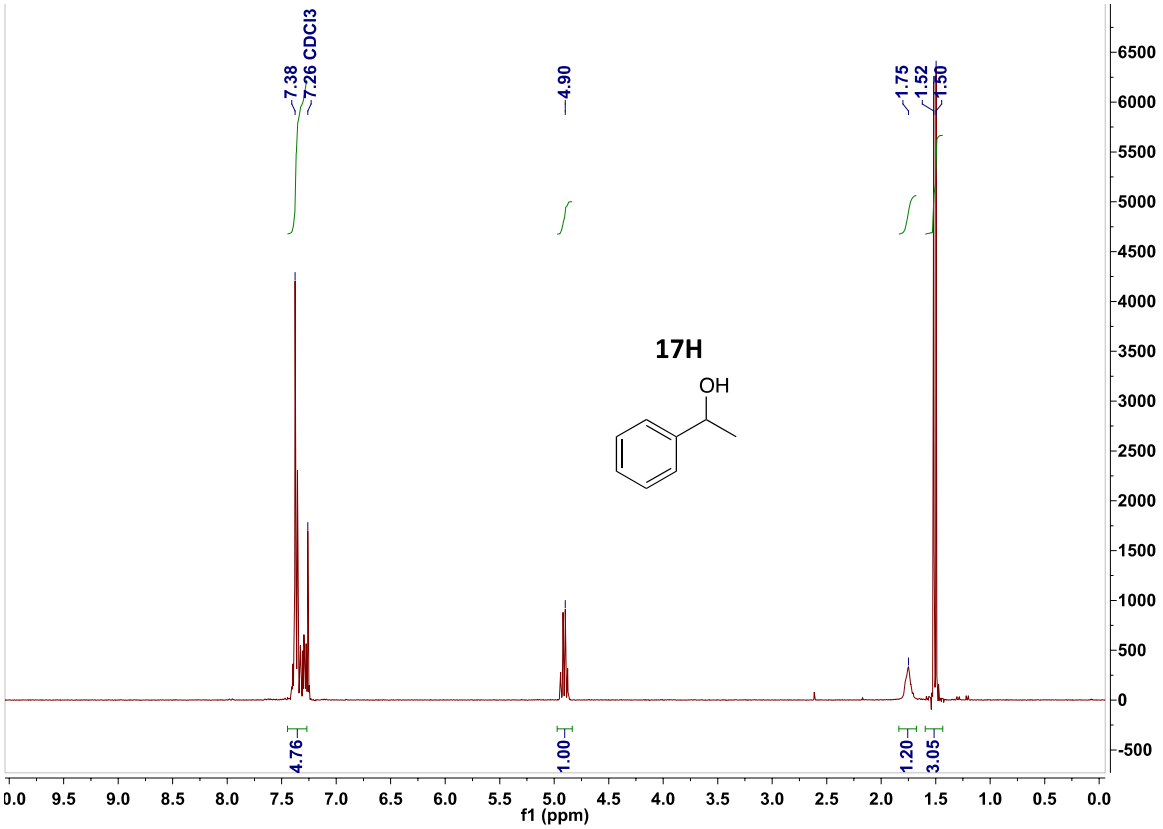

^{1}H NMR (300 MHz, 298 K) spectrum in $CDCl_3$ for **17H**.

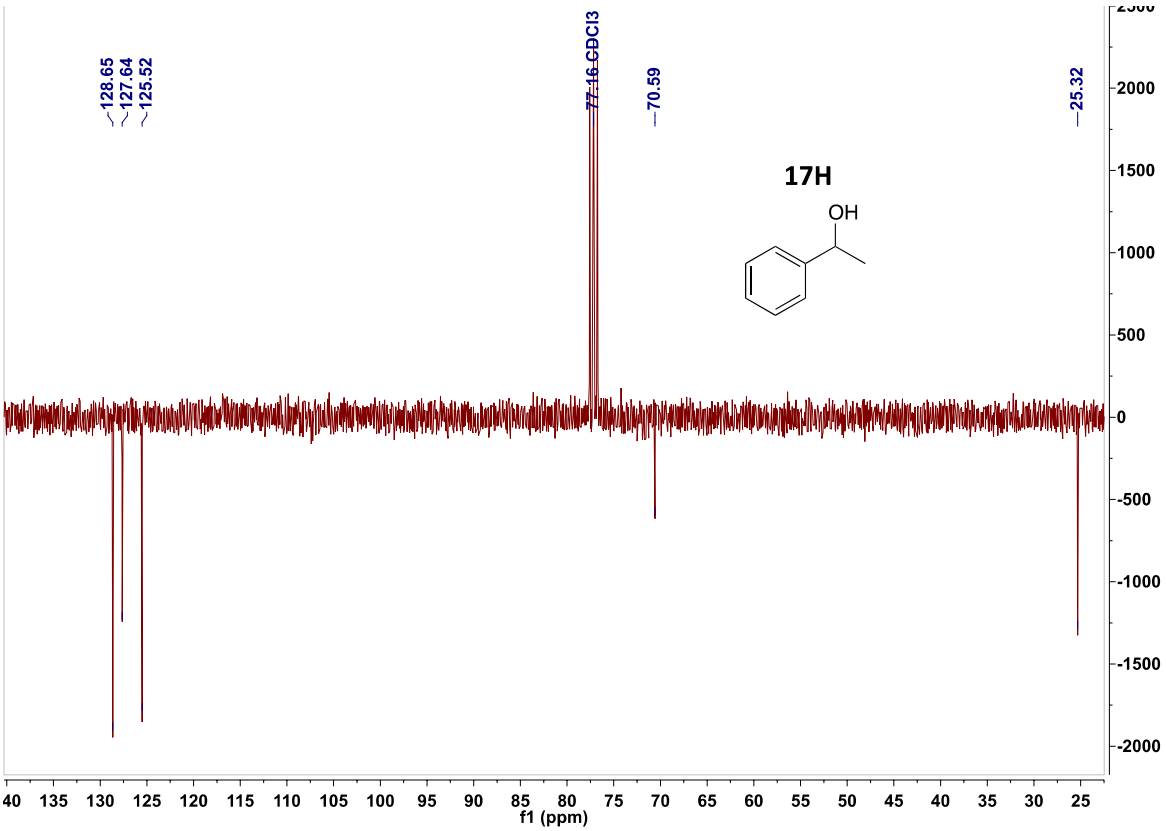

$^{13}C\{^{1}H\}$ Jmod NMR (75 MHz, 298 K) spectrum in $CDCl_3$ for **17H**.

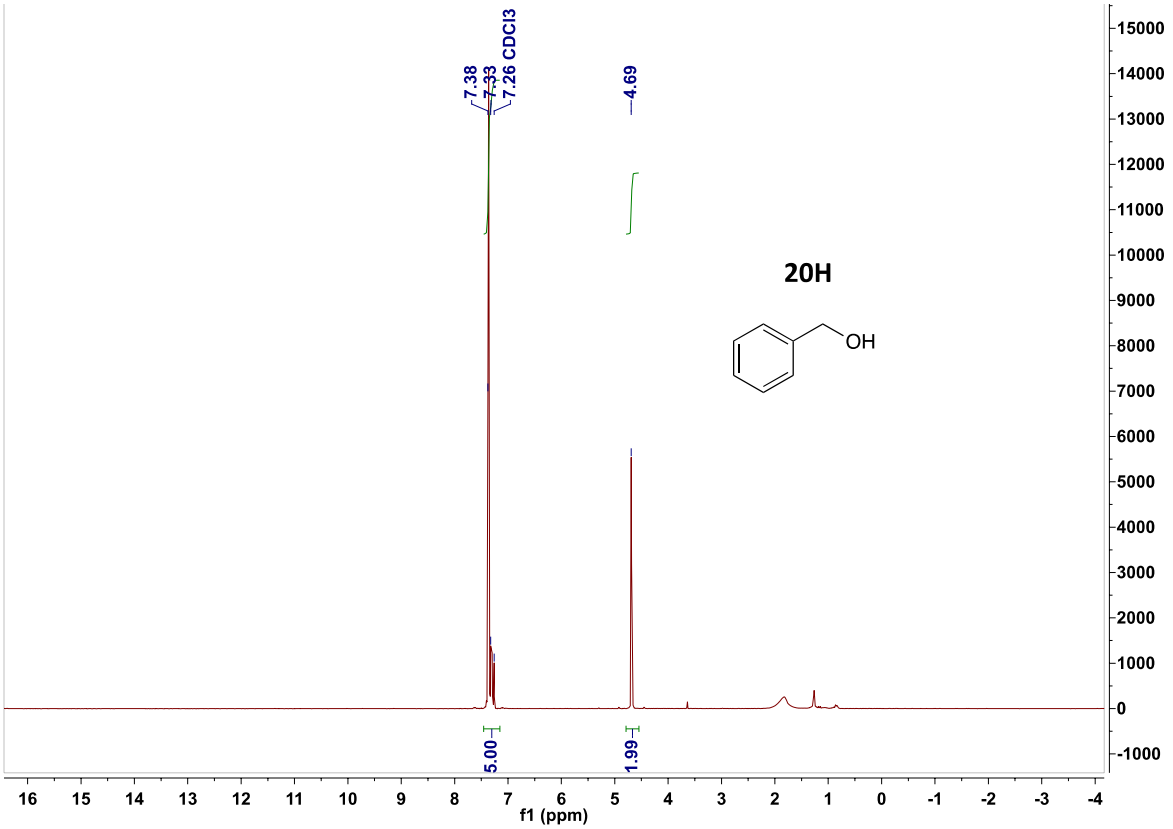

^{1}H NMR (300 MHz, 298 K) spectrum in $CDCl_3$ for **20H**.

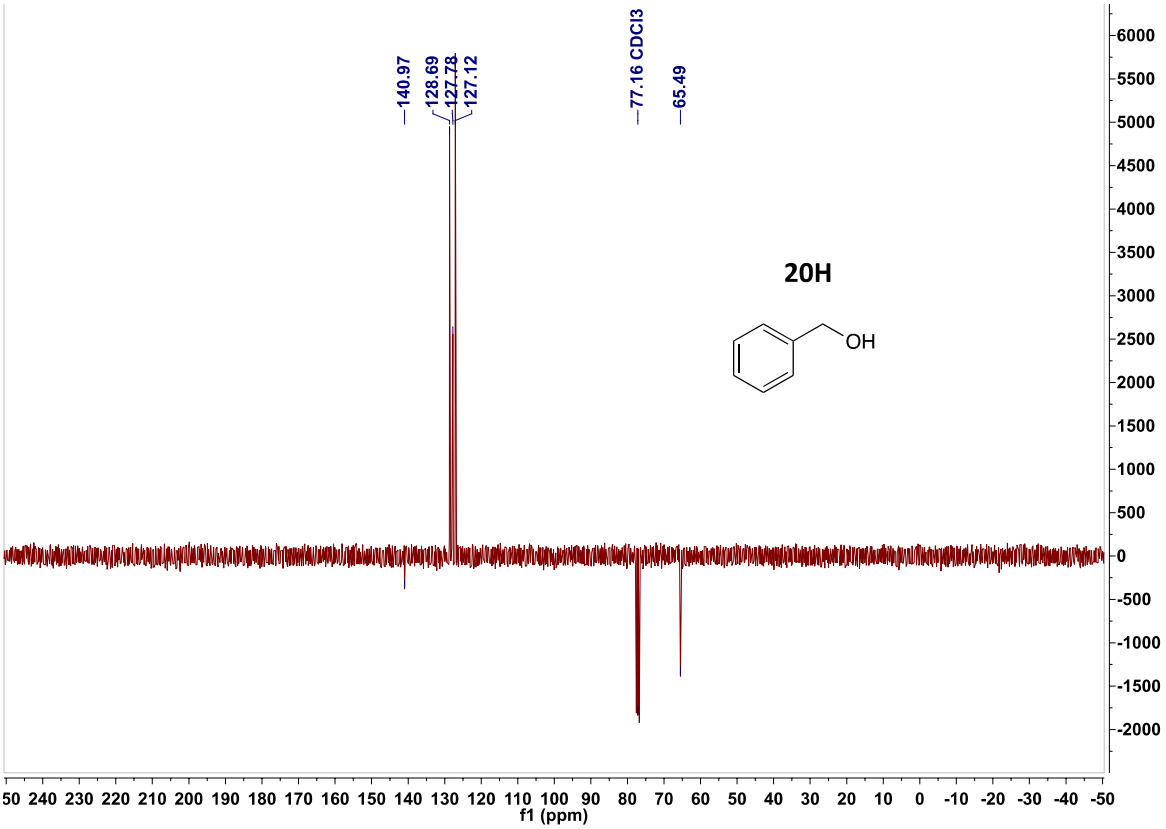

$^{13}C\{^{1}H\}$ Jmod NMR (75 MHz, 298 K) spectrum in $CDCl_3$ for **20H**.

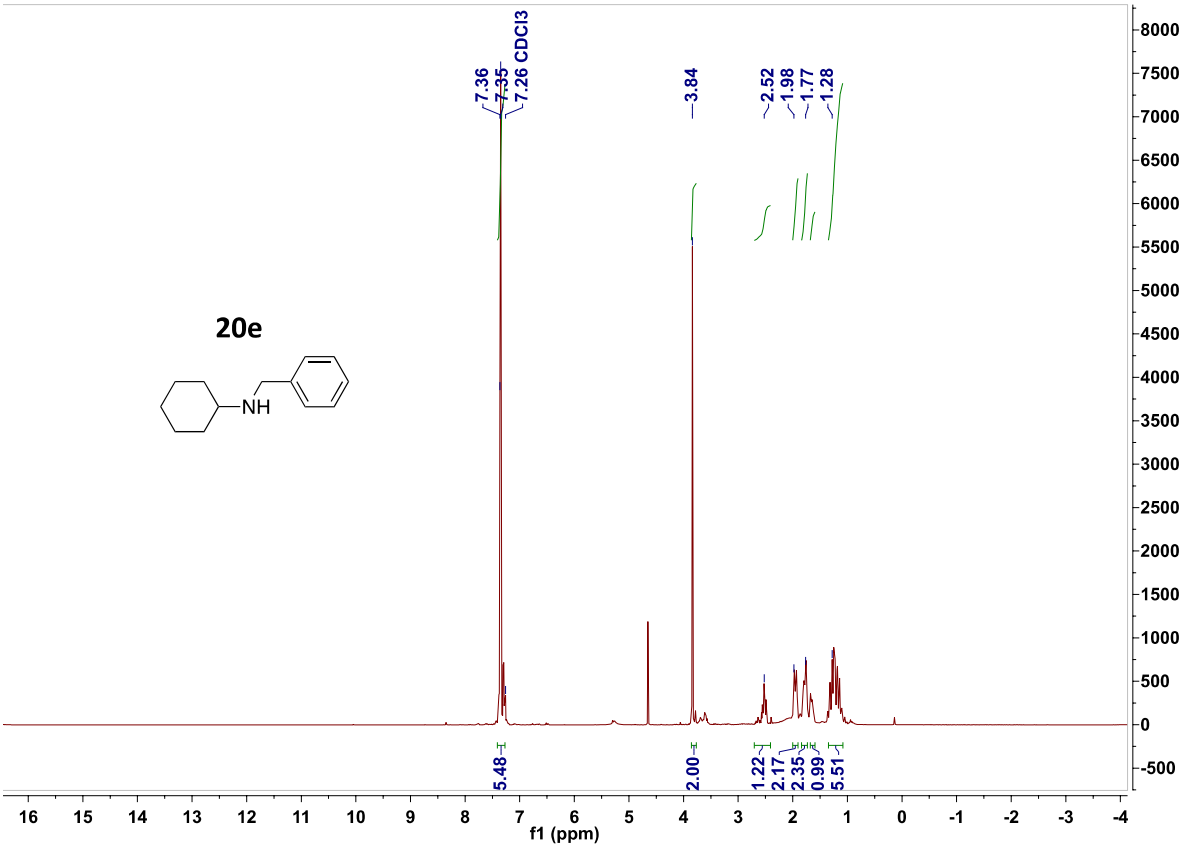

^{1}H NMR (300 MHz, 298 K) spectrum in $CDCl_3$ for **20e**.

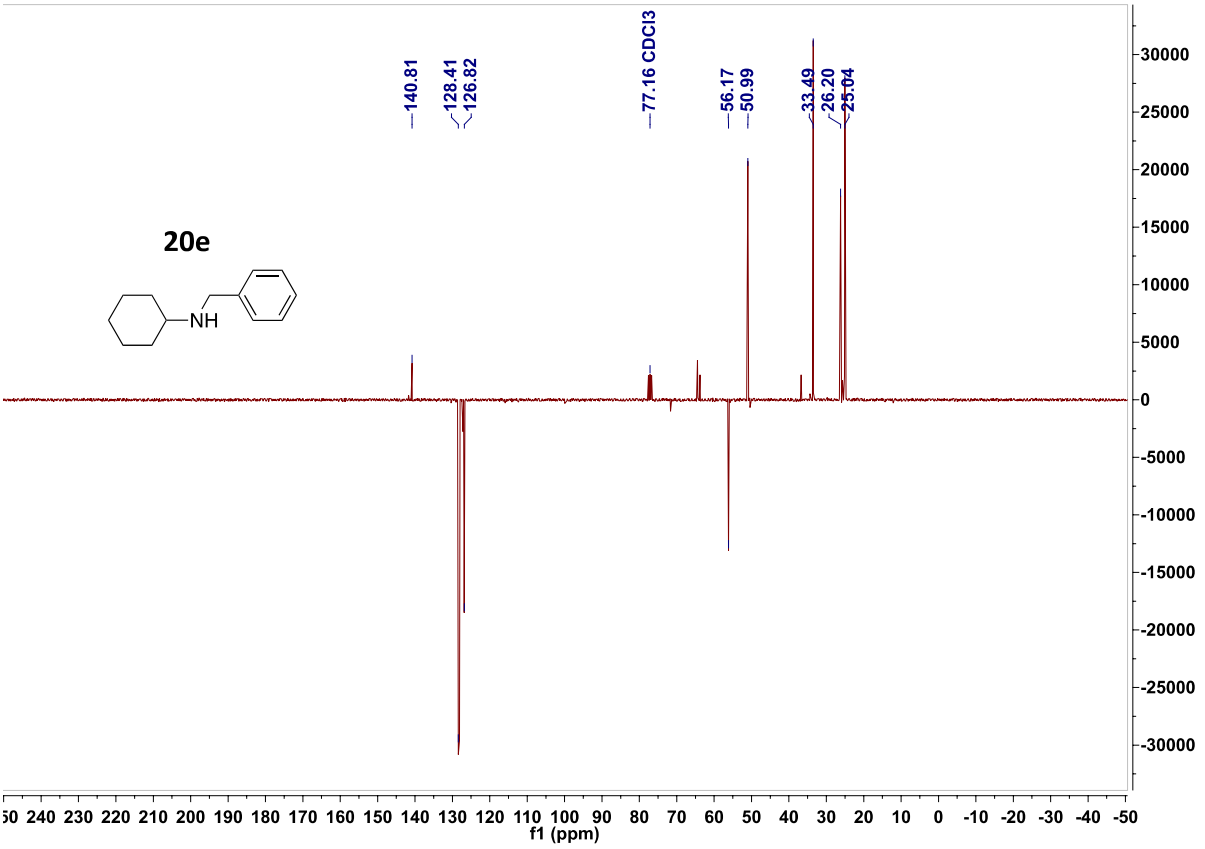

$^{13}C\{^{1}H\}$ Jmod NMR (75 MHz, 298 K) spectrum in $CDCl_3$ for **20e**.

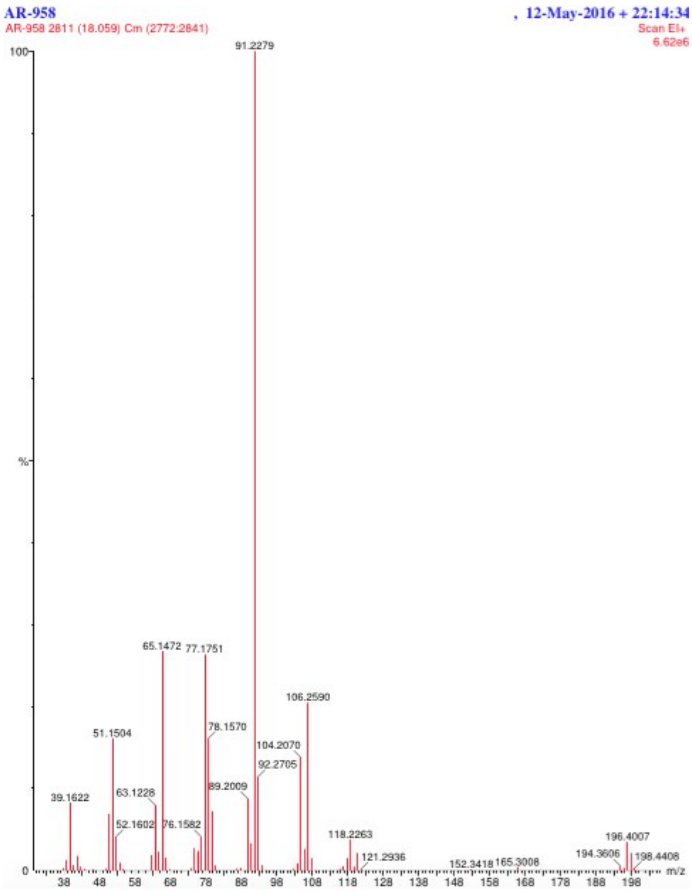

20h

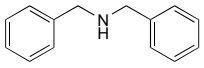

GC-MS chromatogram for **20h**.

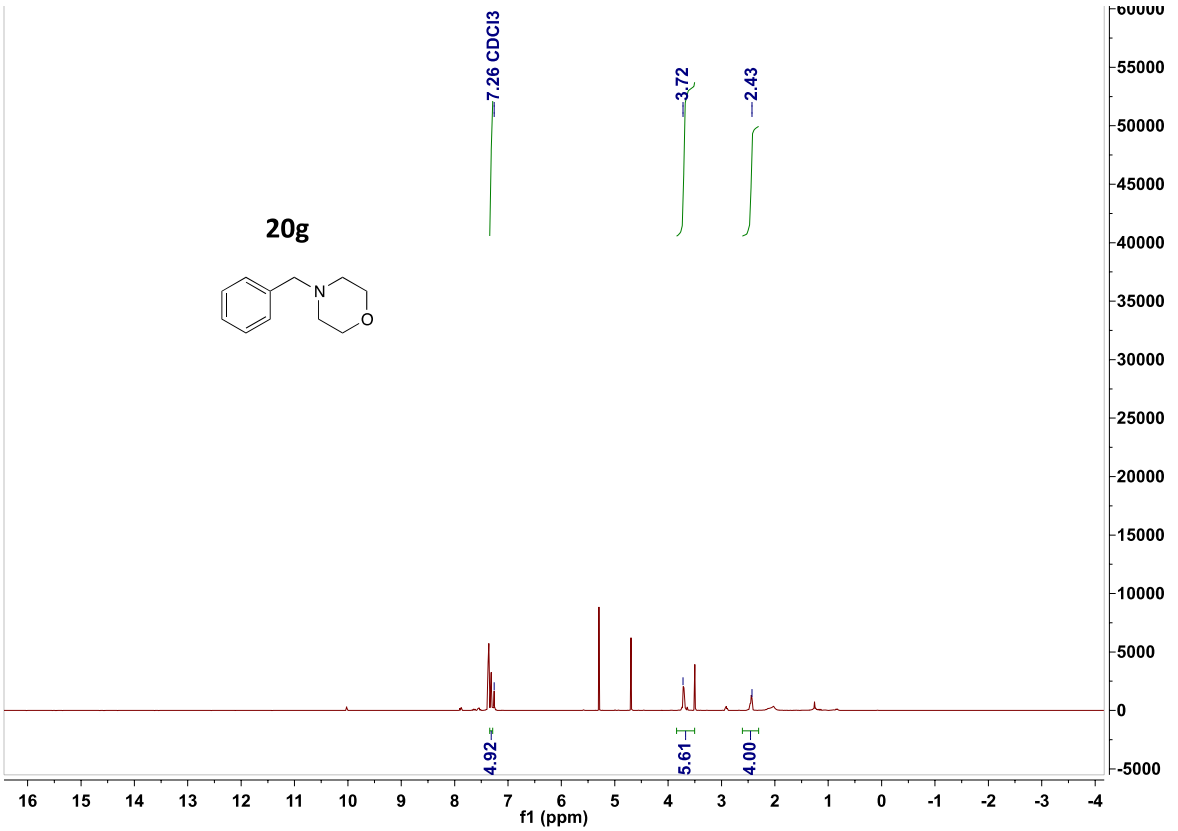

^{1}H NMR (300 MHz, 298 K) spectrum in $CDCl_3$ for **20g**.

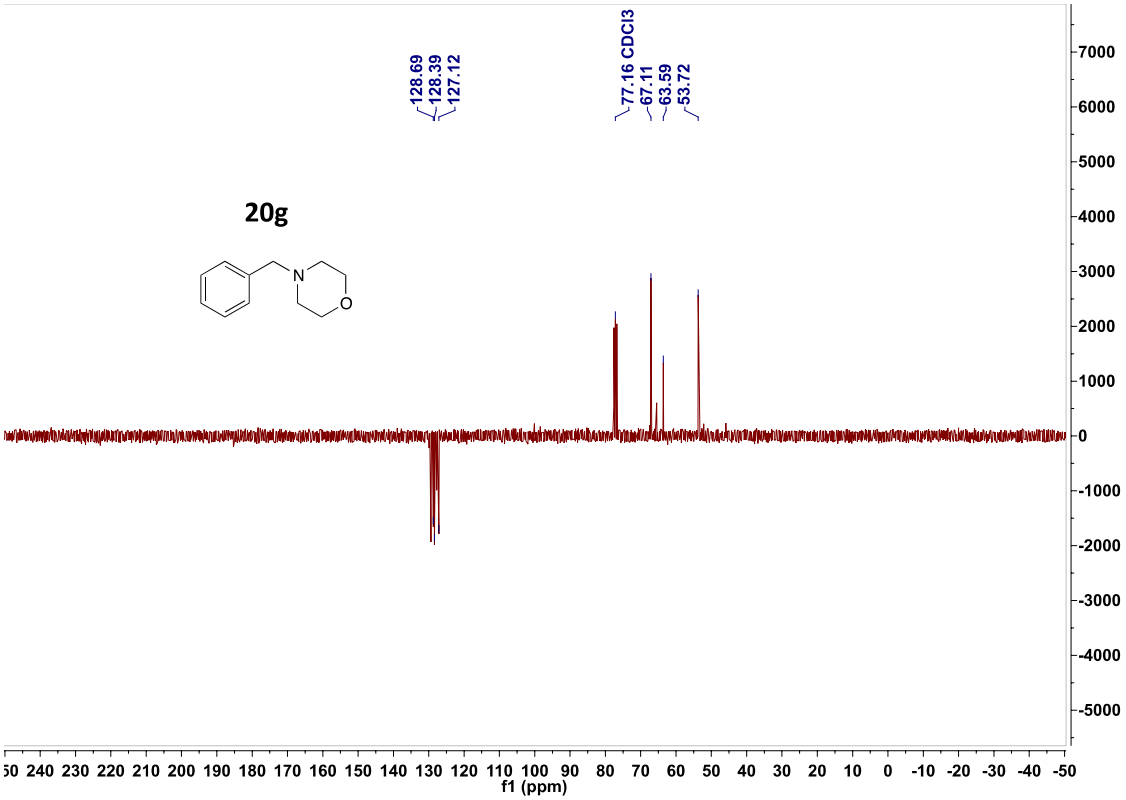

$^{13}C\{^{1}H\}$ Jmod NMR (75 MHz, 298 K) spectrum in $CDCl_3$ for **20g**.

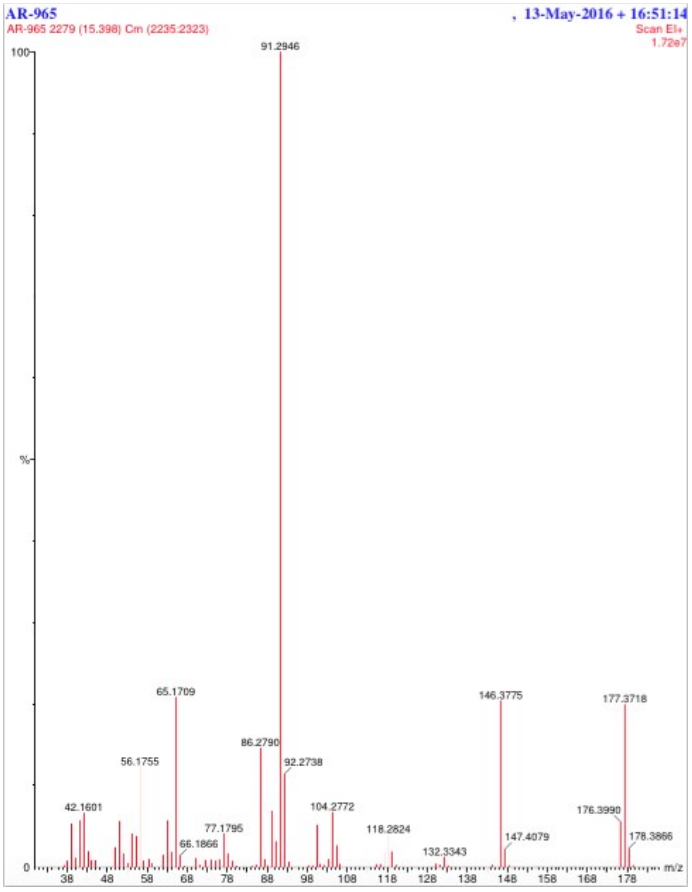

20g

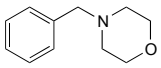

GC-MS chromatogram for **20g**.

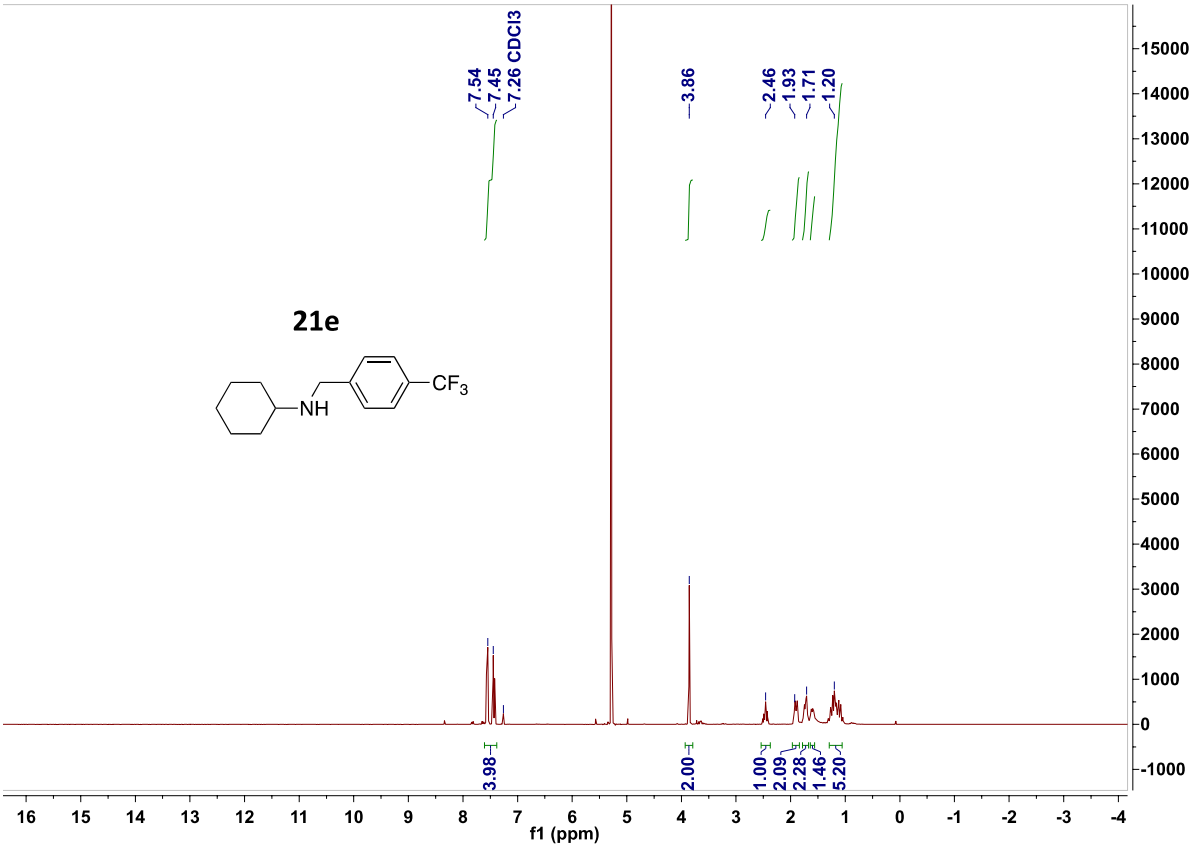

^{1}H NMR (300 MHz, 298 K) spectrum in $CDCl_3$ for **21e**.

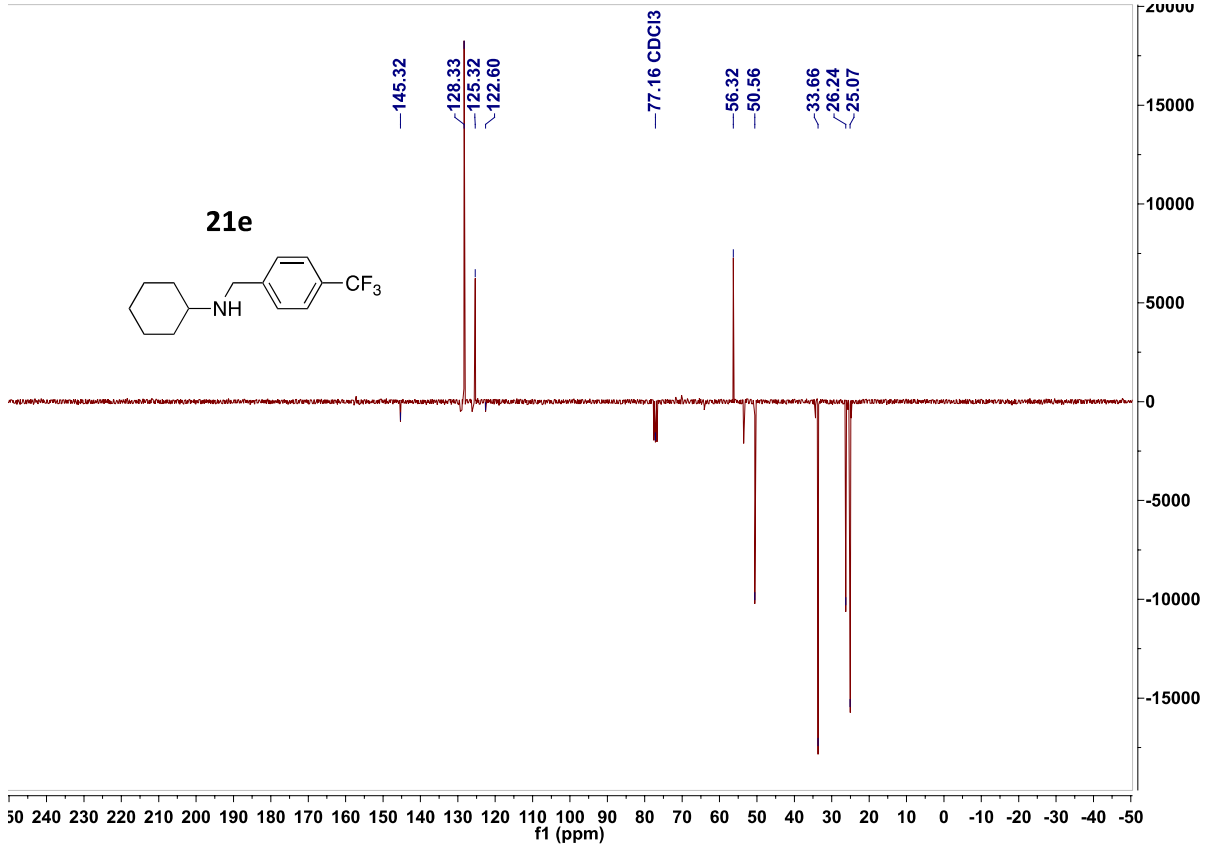

$^{13}C\{^{1}H\}$ Jmod NMR (75 MHz, 298 K) spectrum in $CDCl_3$ for **21e**.

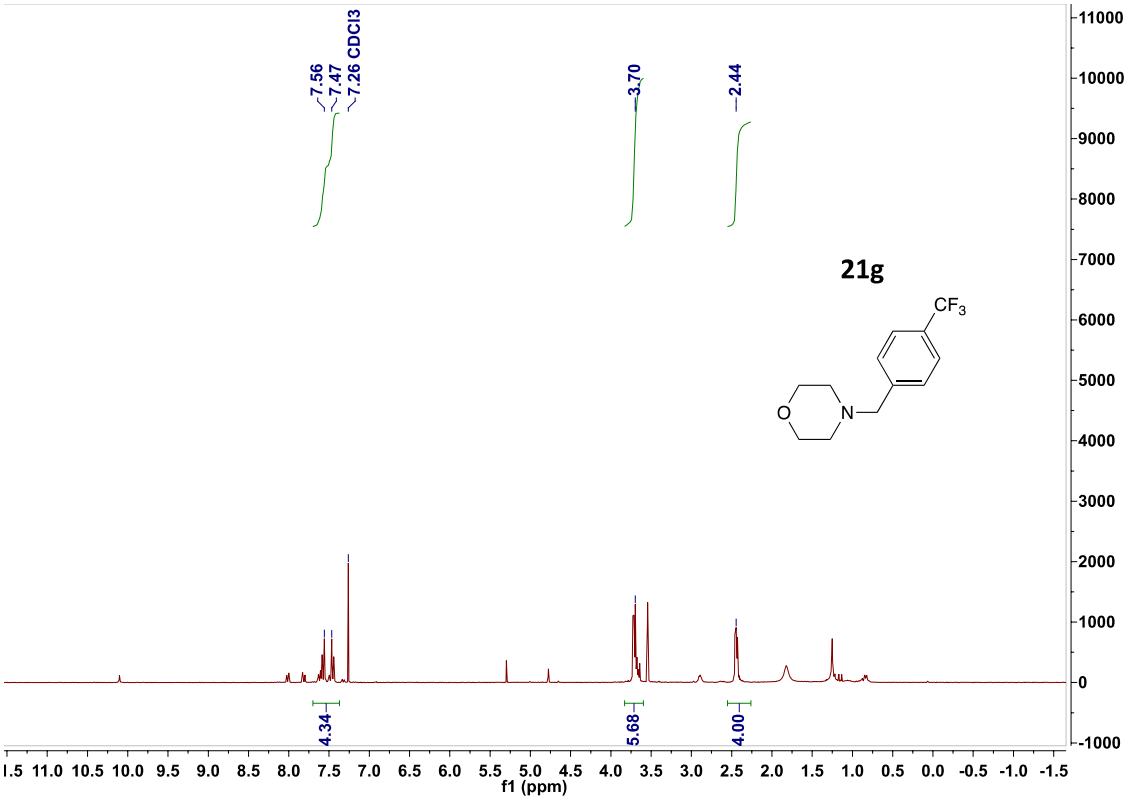

^{1}H NMR (300 MHz, 298 K) spectrum in $CDCl_3$ for **21g**.

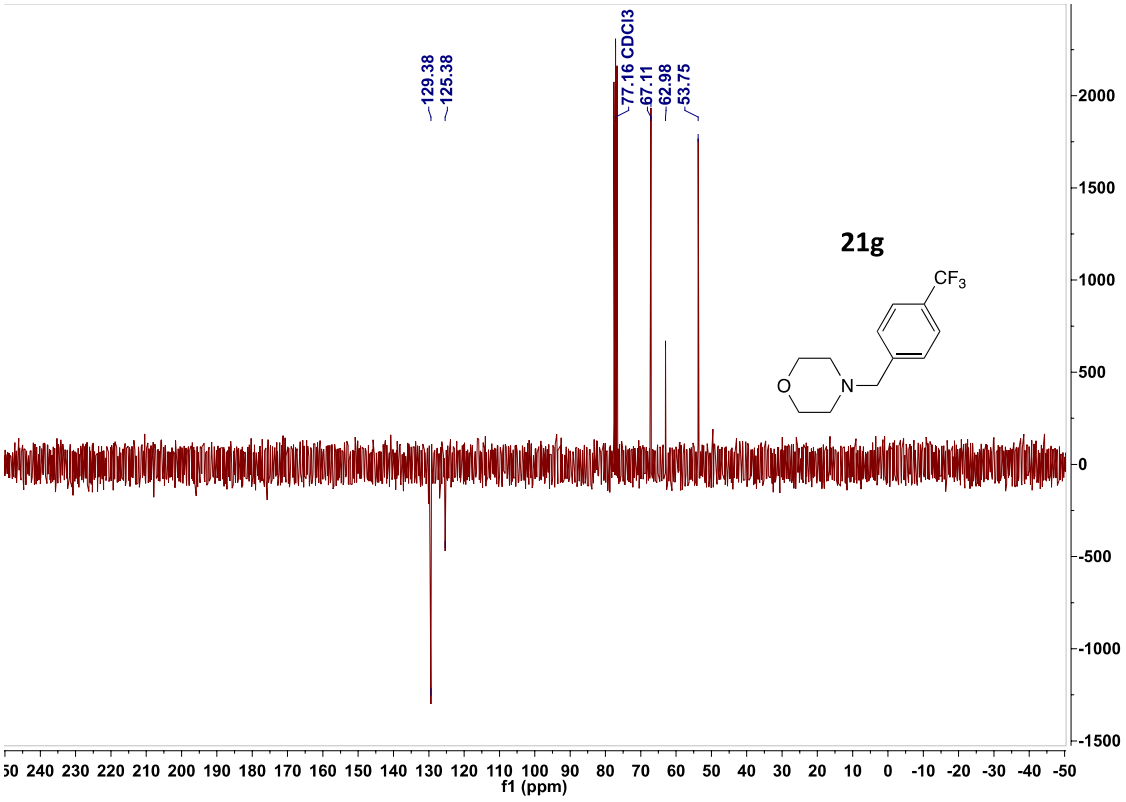

$^{13}C\{^{1}H\}$ Jmod NMR (75 MHz, 298 K) spectrum in $CDCl_3$ for **21g**.

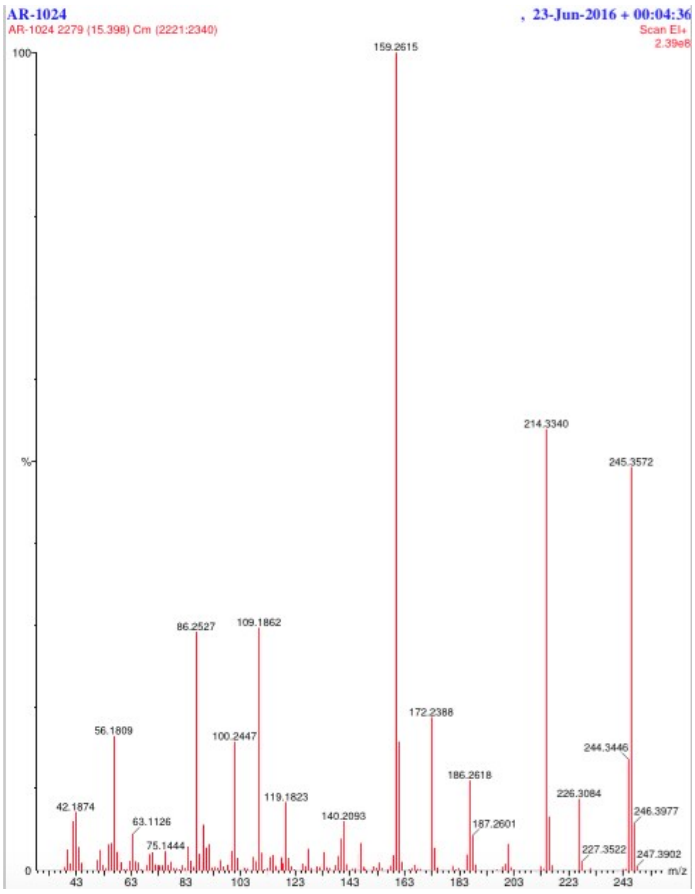

21g

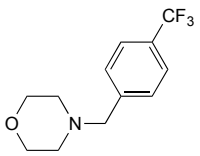

GC-MS chromatogram for **21g**.

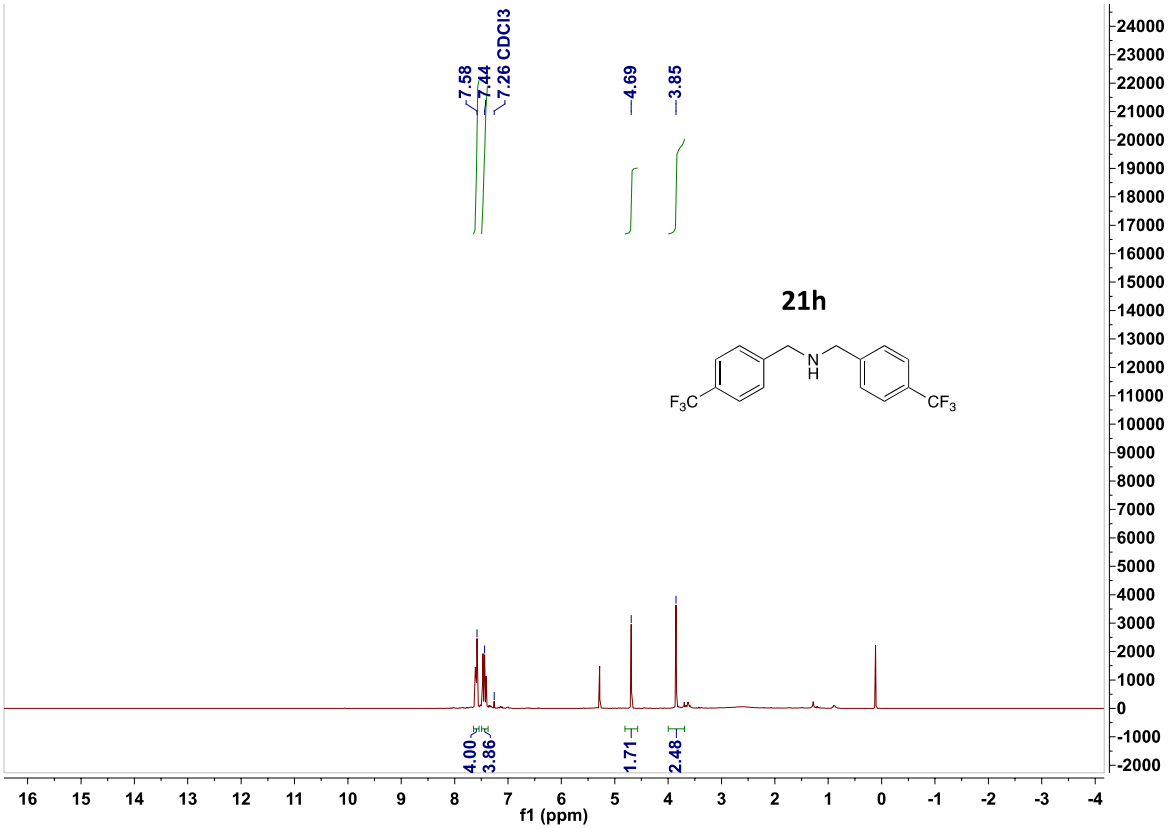

^{1}H NMR (300 MHz, 298 K) spectrum in $CDCl_3$ for **21h**.

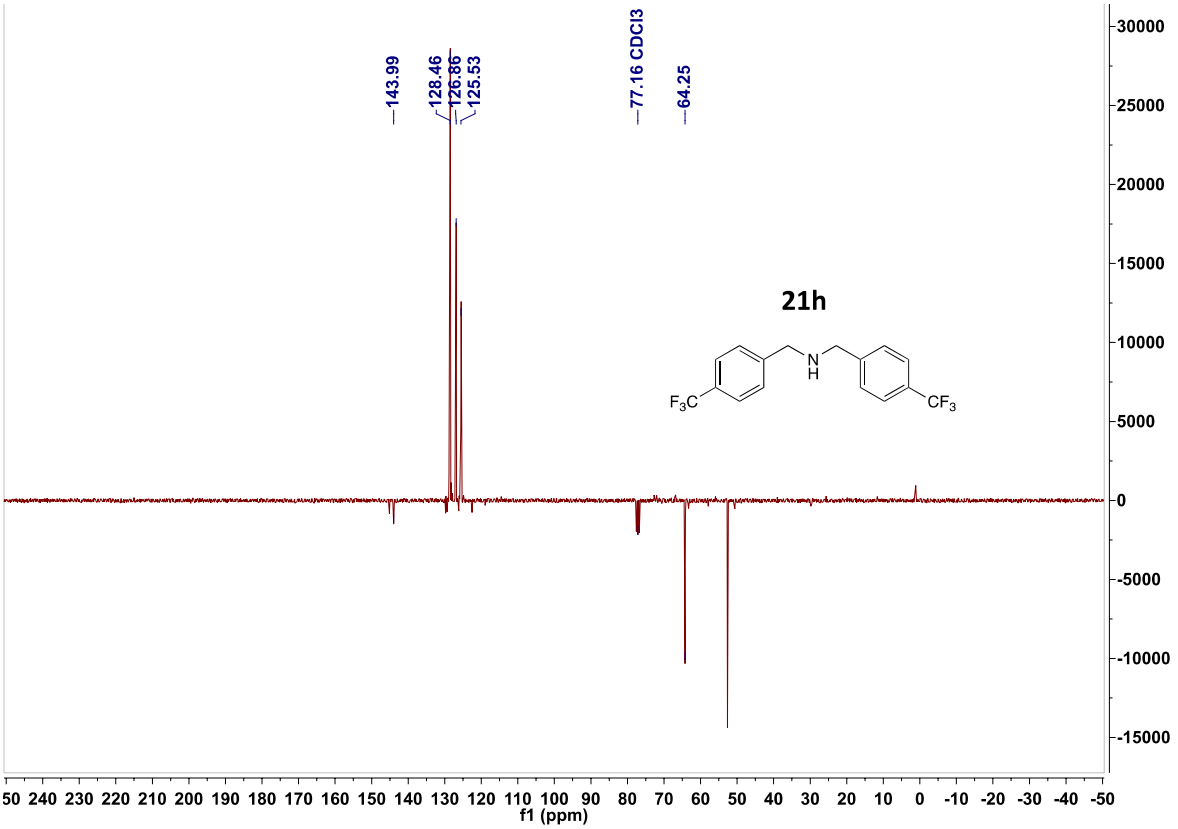

$^{13}C\{^{1}H\}$ Jmod NMR (75 MHz, 298 K) spectrum in $CDCl_3$ for **21h**.

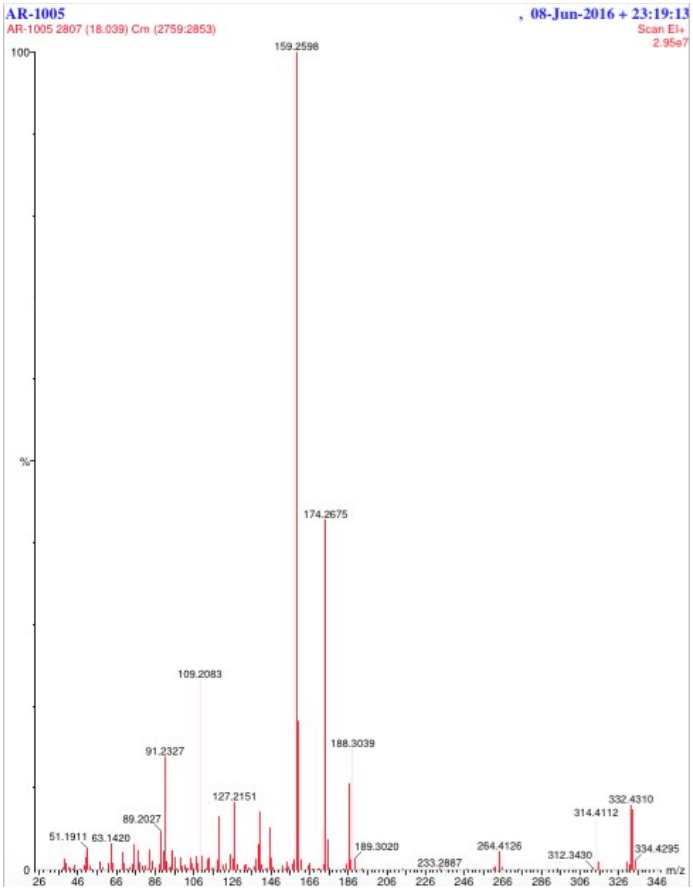

21h

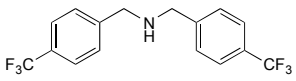

GC-MS chromatogram for **21h**.

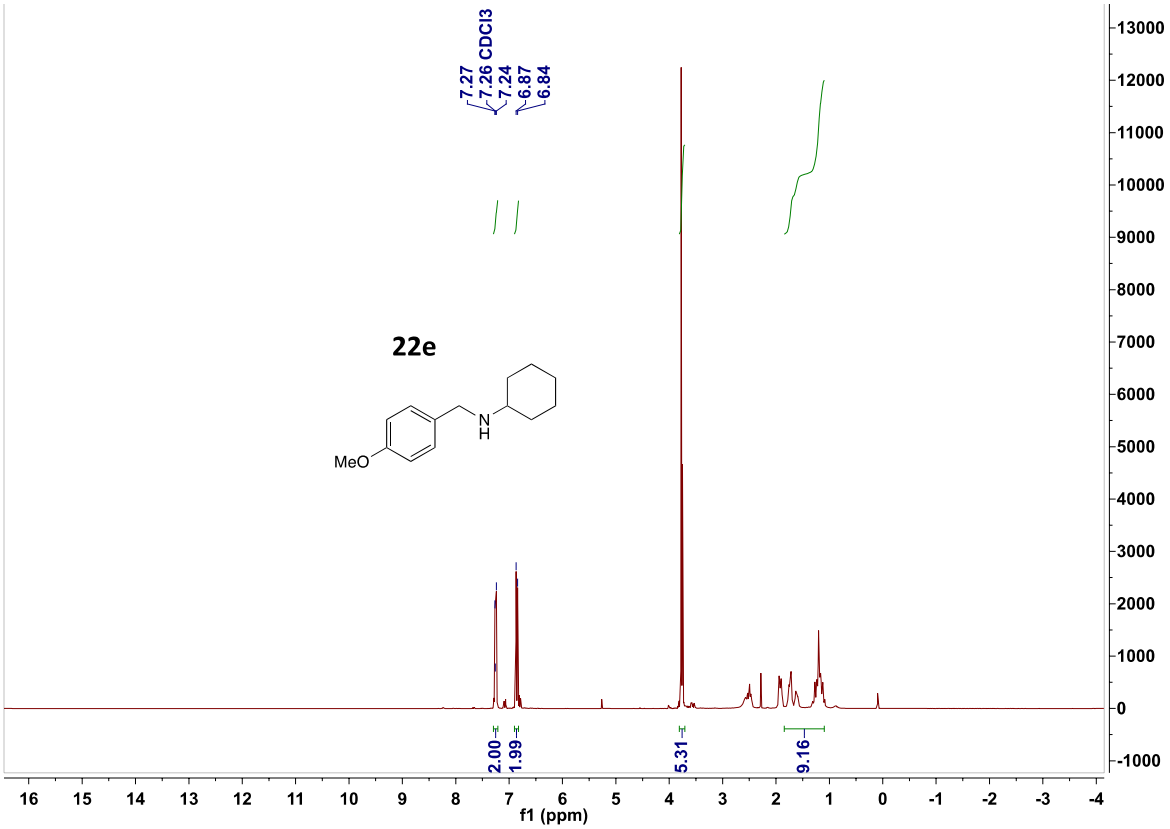

^{1}H NMR (300 MHz, 298 K) spectrum in $CDCl_3$ for **22e**.

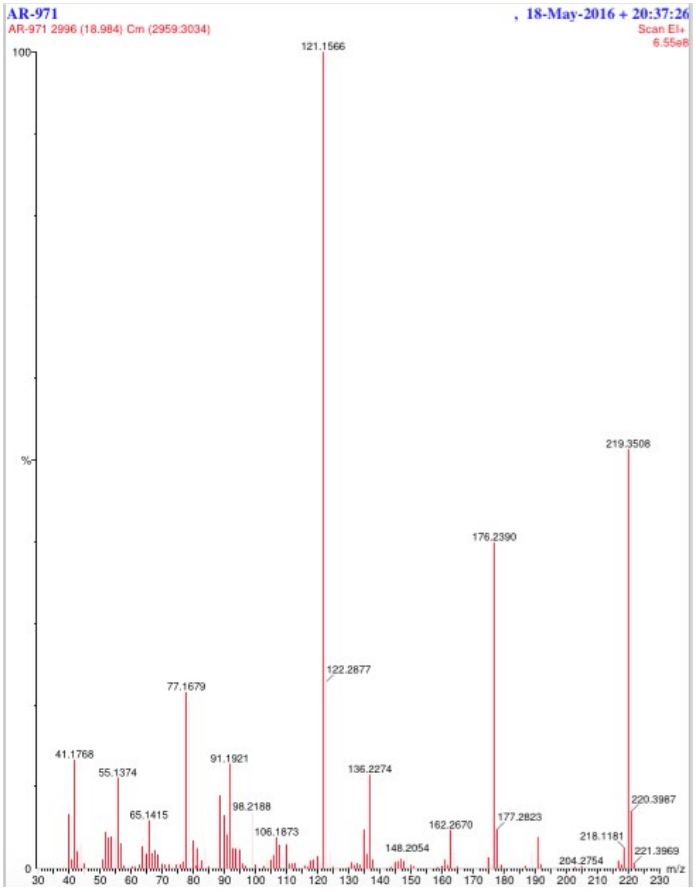

22e

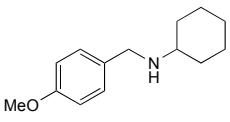

GC-MS chromatogram for **22e**.

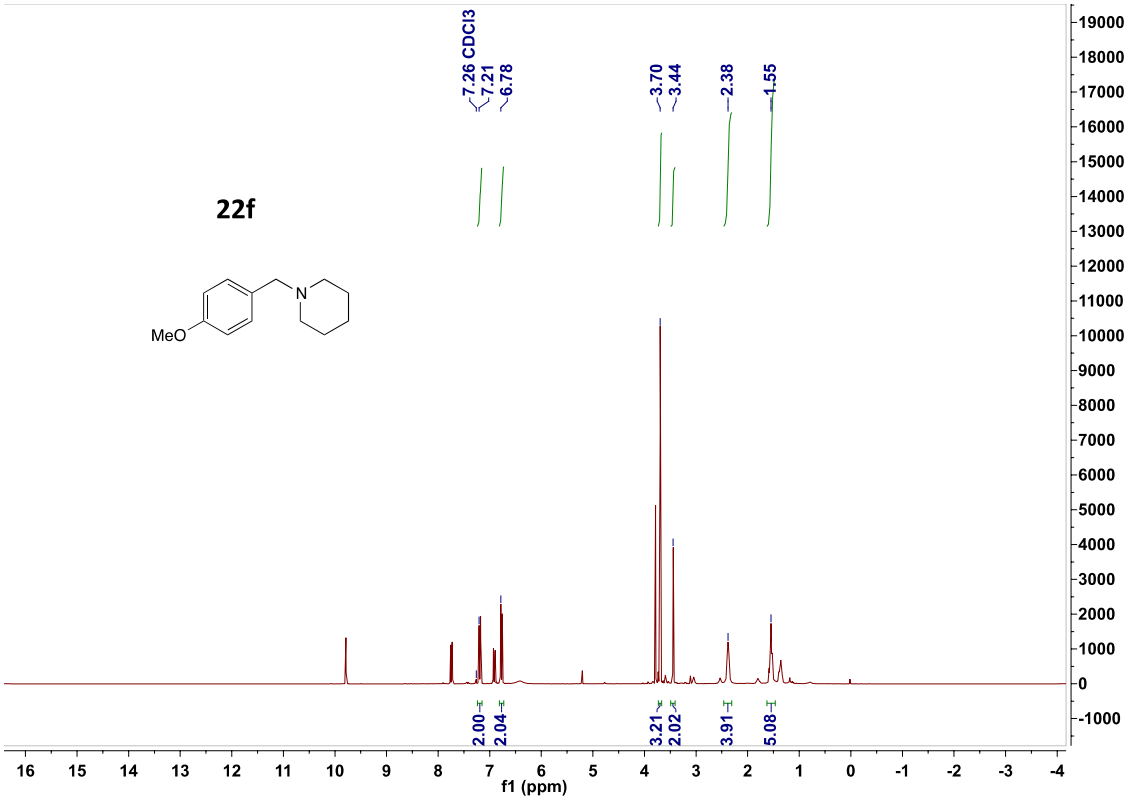

^{1}H NMR (300 MHz, 298 K) spectrum in $CDCl_3$ for **22f**.

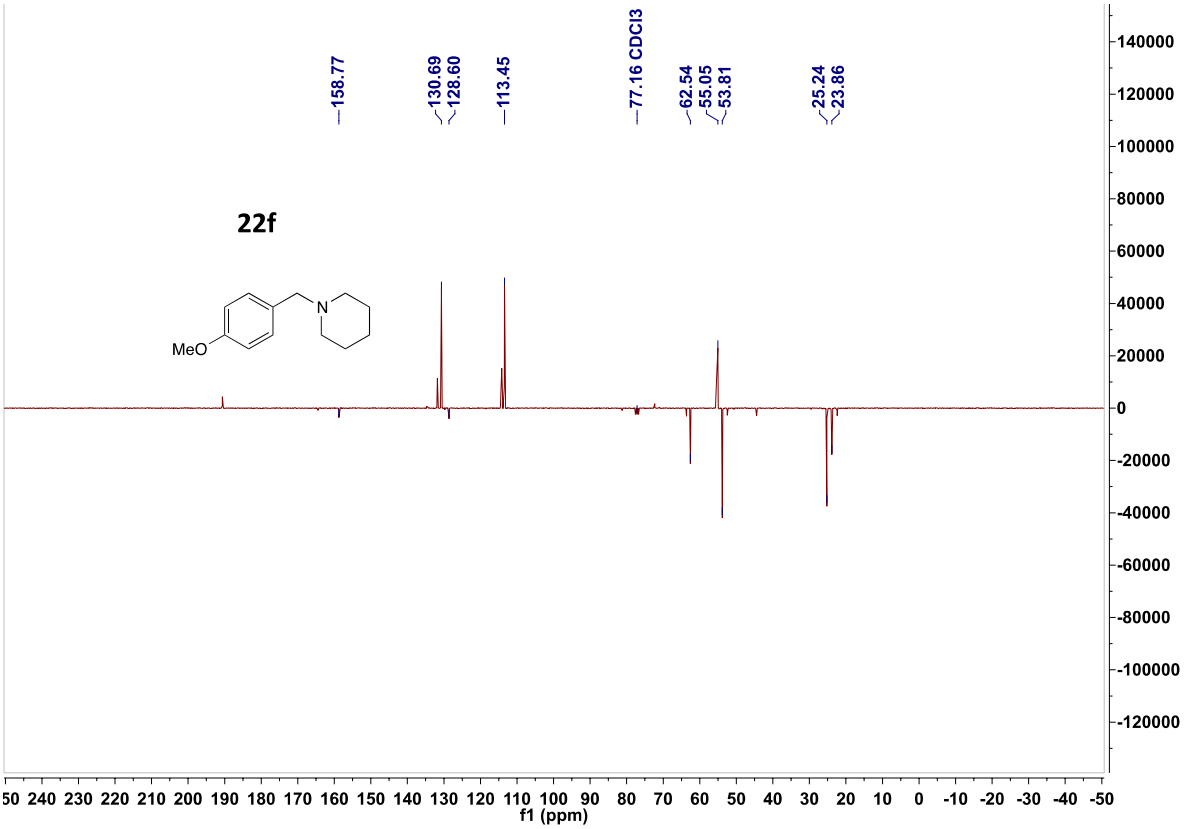

$^{13}C\{^{1}H\}$ Jmod NMR (75 MHz, 298 K) spectrum in $CDCl_3$ for **22f**.

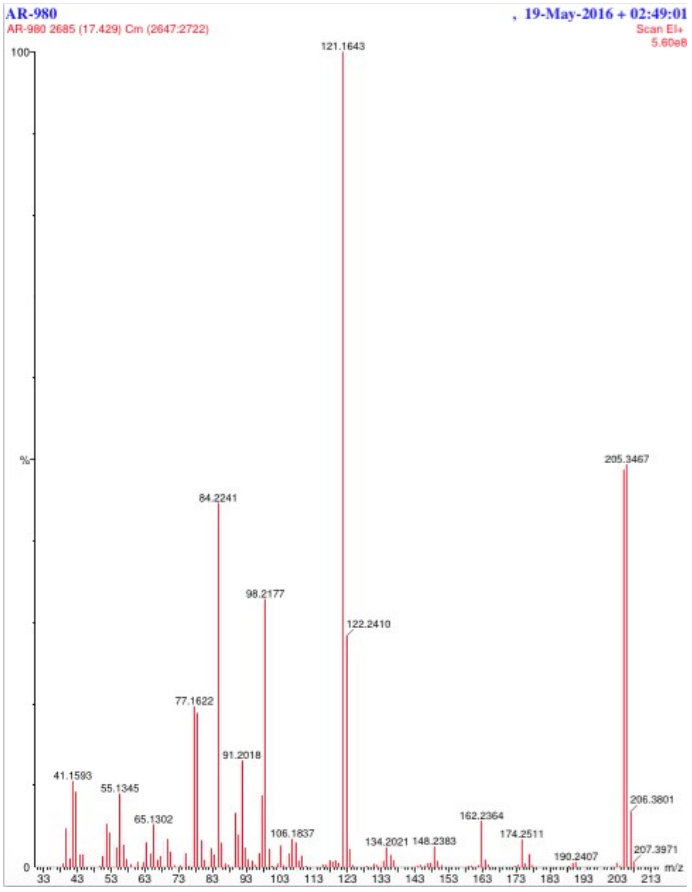

22f

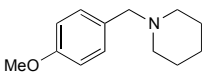

GC-MS chromatogram for **22f**.

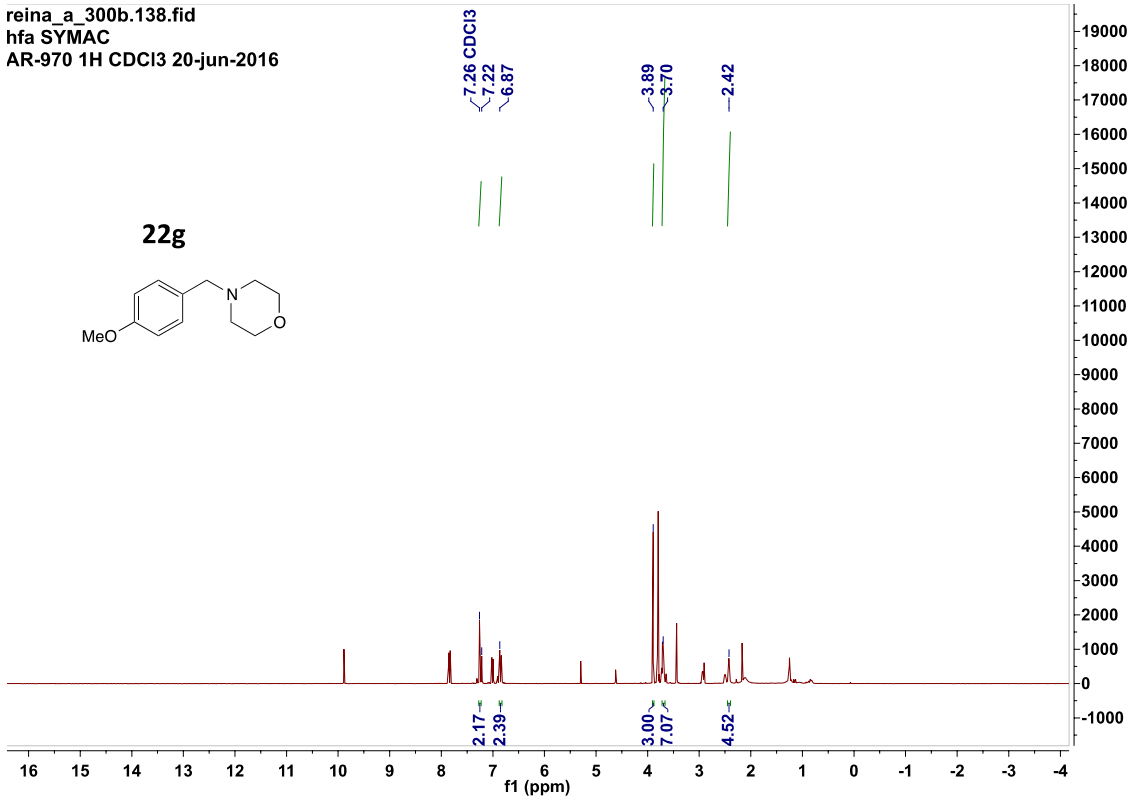

^{1}H NMR (300 MHz, 298 K) spectrum in $CDCl_3$ for **22g**.

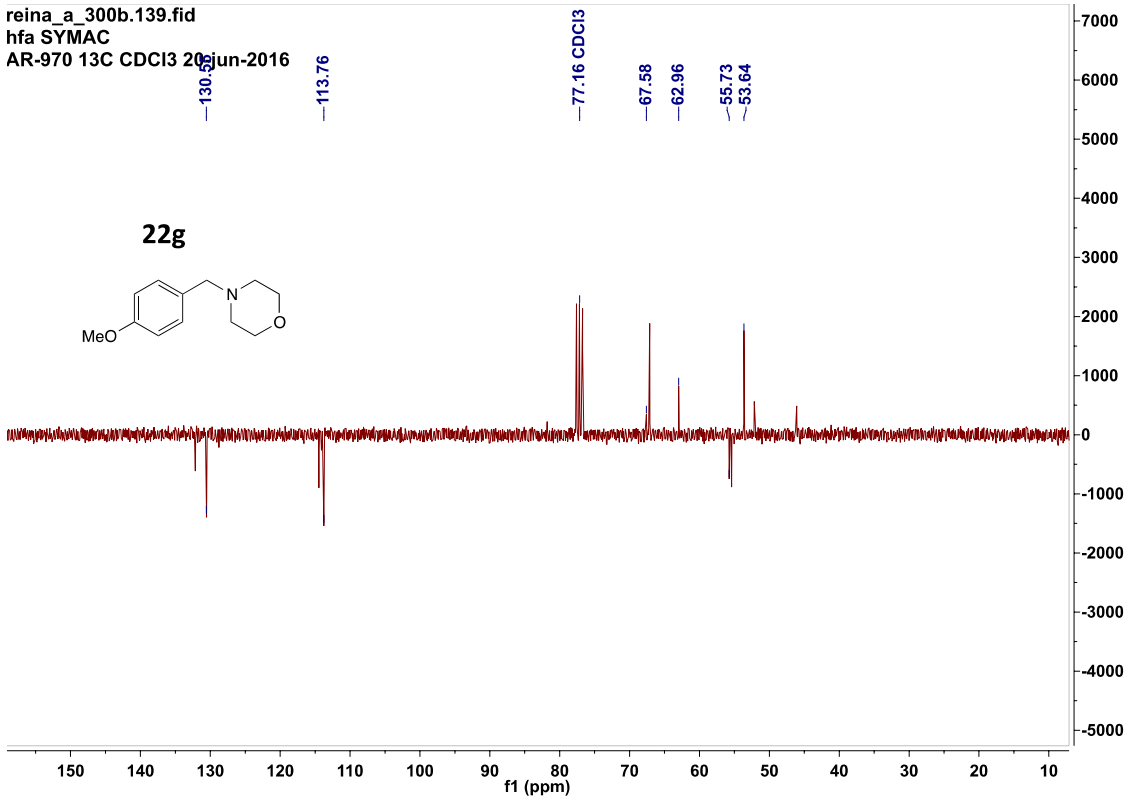

$^{13}C\{^{1}H\}$ Jmod NMR (75 MHz, 298 K) spectrum in $CDCl_3$ for **22g.**

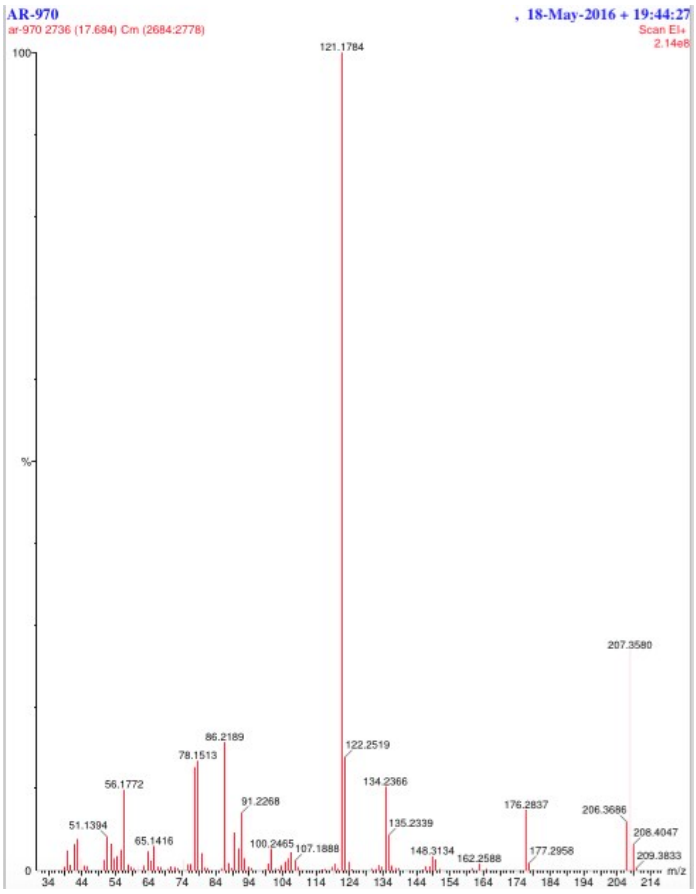

22g

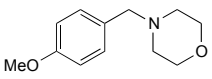

GC-MS chromatogram for **22g**.

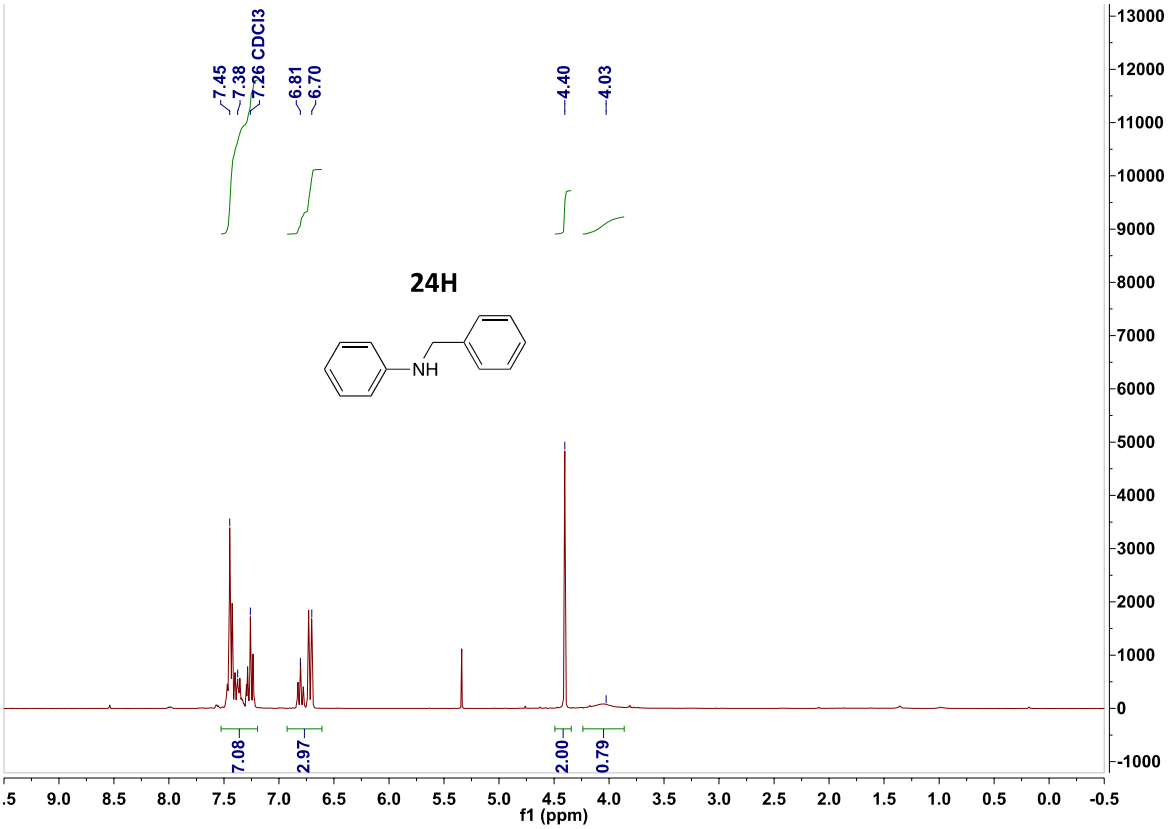

^{1}H NMR (300 MHz, 298 K) spectrum in $CDCl_3$ for **24H**.

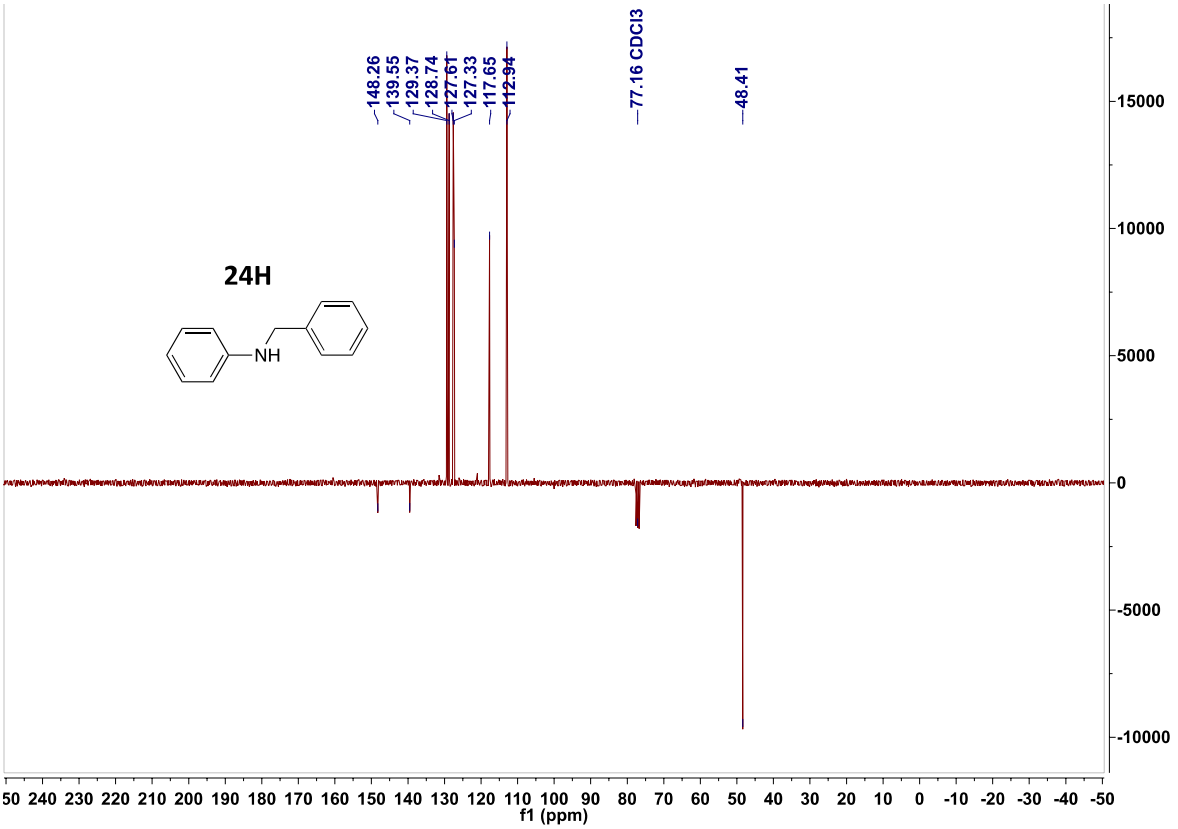

$^{13}C\{^{1}H\}$ Jmod NMR (75 MHz, 298 K) spectrum in $CDCl_3$ for **24H**.

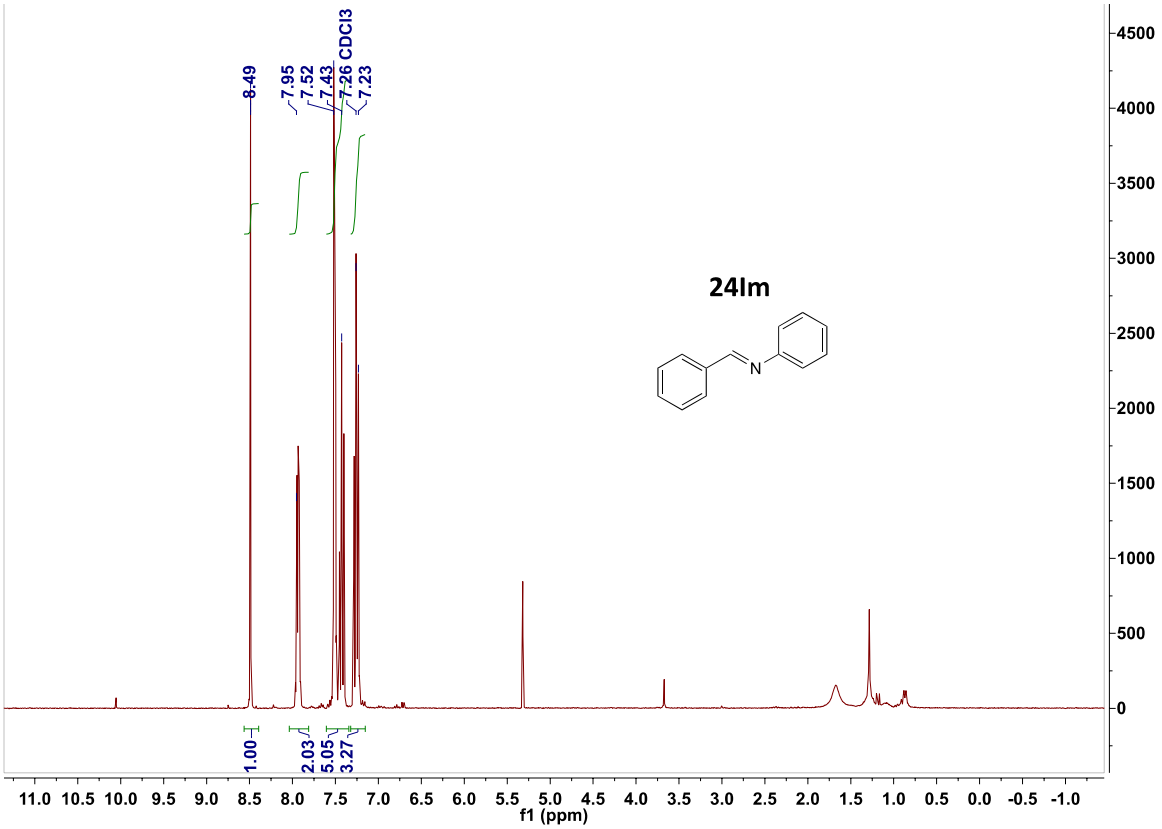

^{1}H NMR (300 MHz, 298 K) spectrum in $CDCl_3$ for **24Im**.

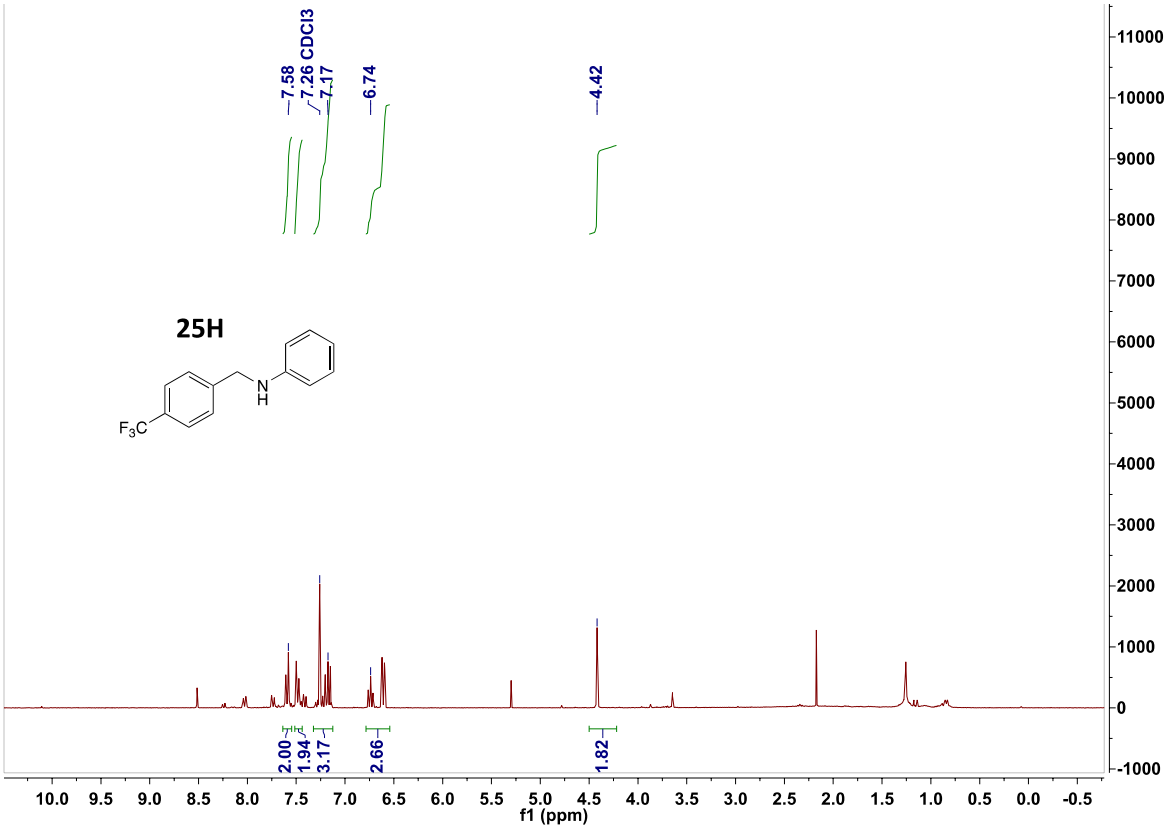

^{1}H NMR (300 MHz, 298 K) spectrum in $CDCl_3$ for **25H**.

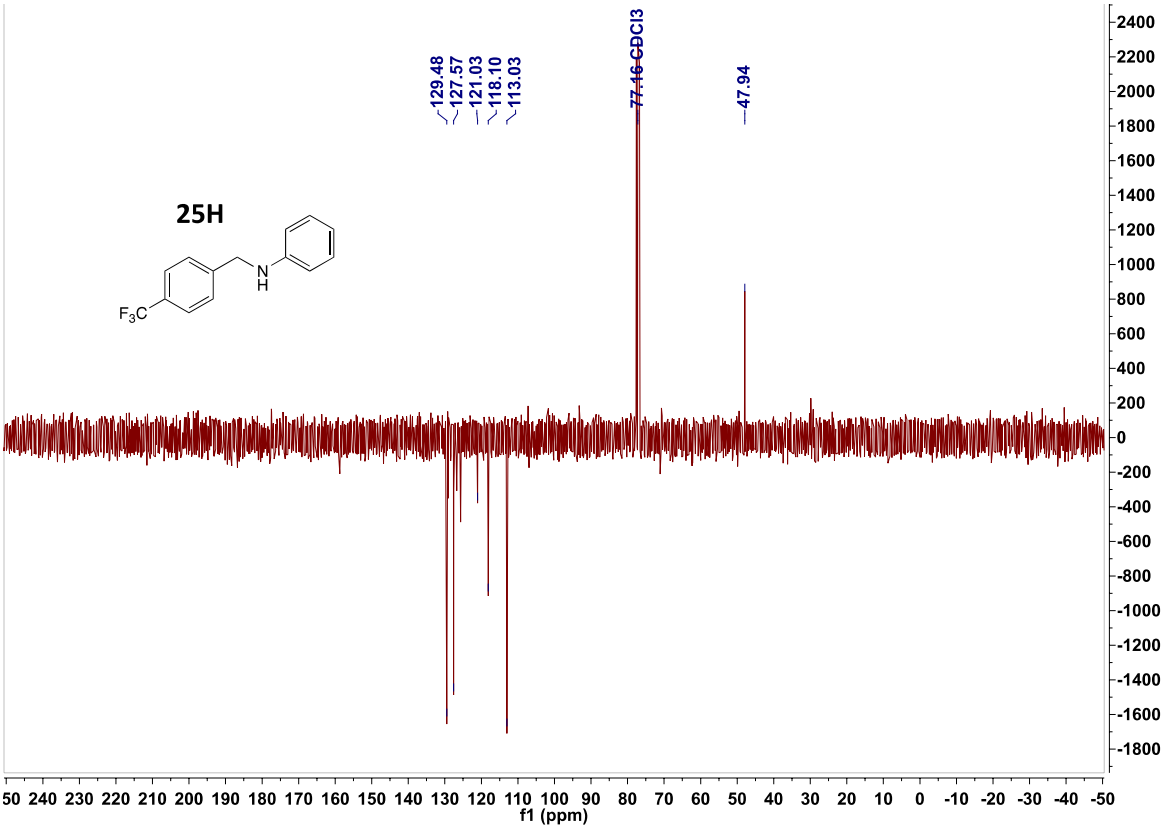

$^{13}C\{^{1}H\}$ Jmod NMR (75 MHz, 298 K) spectrum in $CDCl_3$ for **25H**.

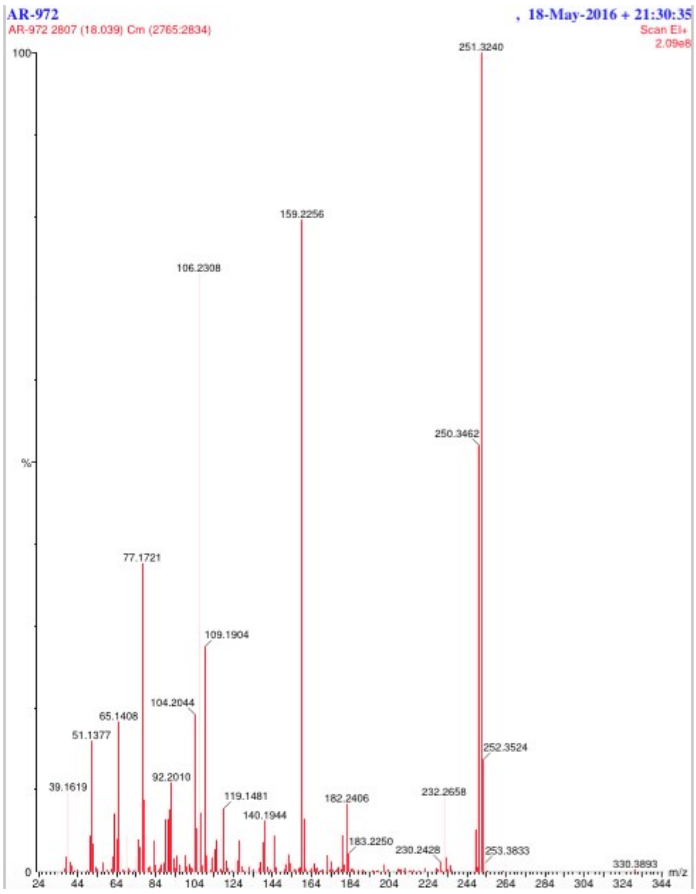

25H

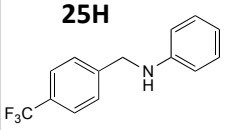

GC-MS chromatogram for **25H**.

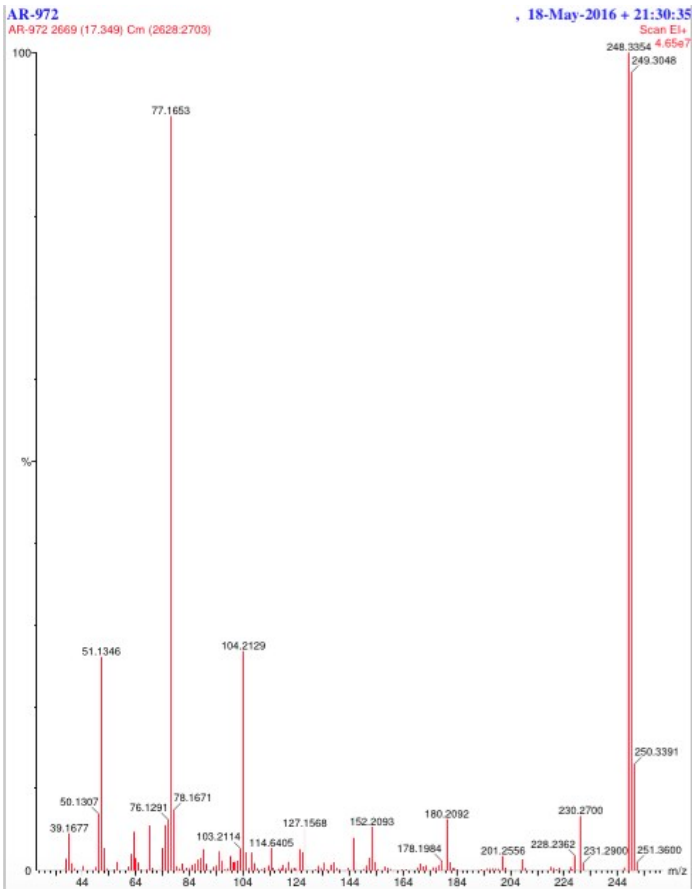

25Im

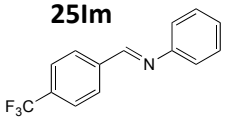

GC-MS chromatogram for **25Im**.

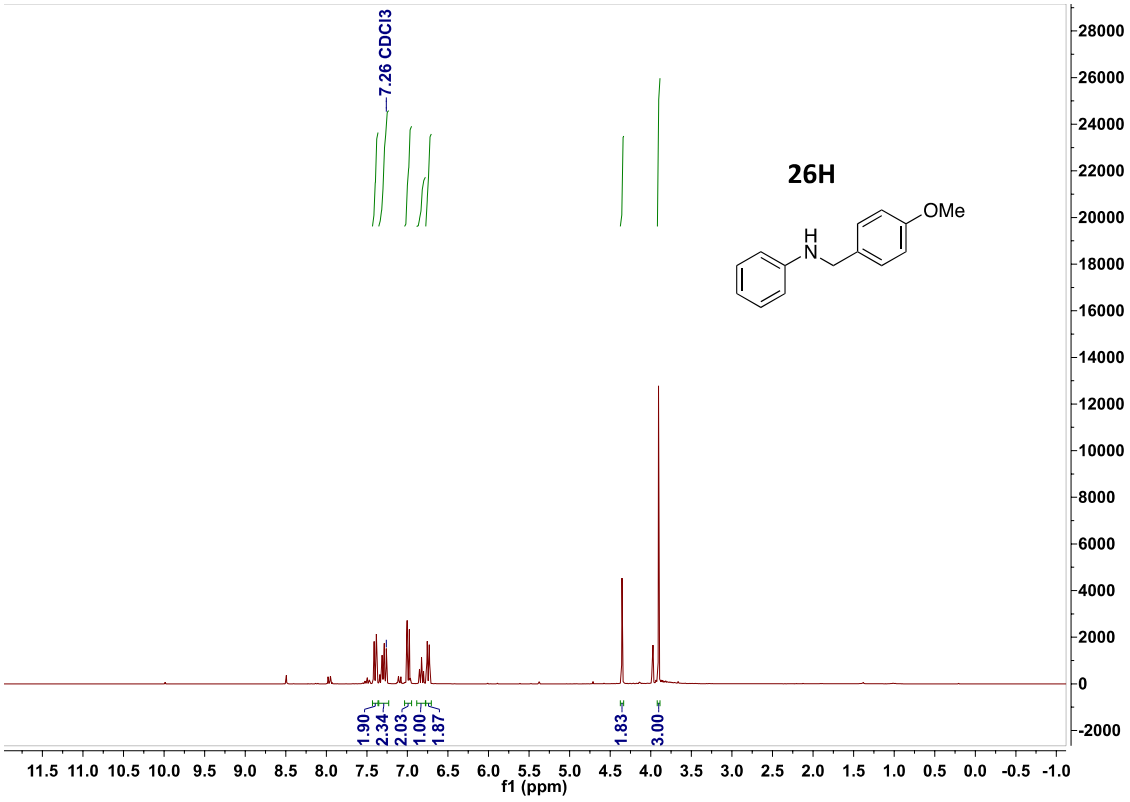

^{1}H NMR (300 MHz, 298 K) spectrum in $CDCl_3$ for **26H**.

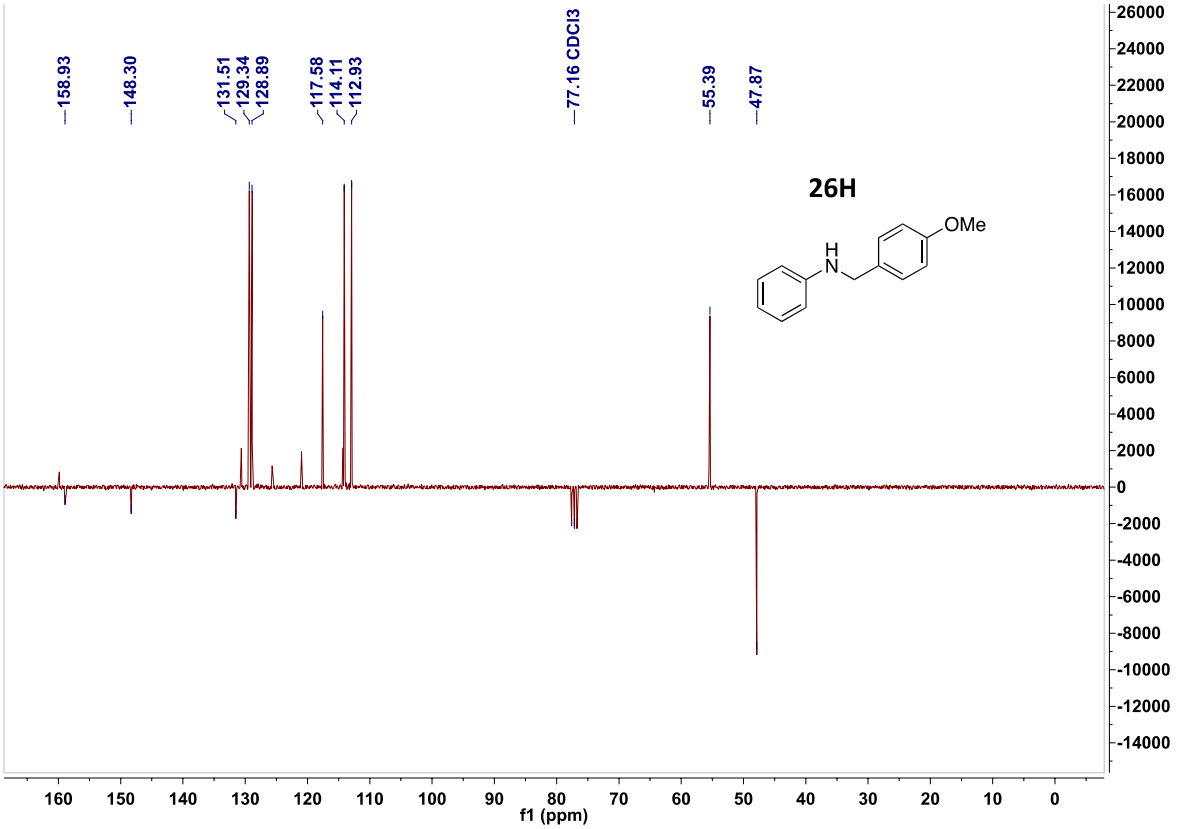

$^{13}C\{^{1}H\}$ Jmod NMR (75 MHz, 298 K) spectrum in $CDCl_3$ for **26H**.

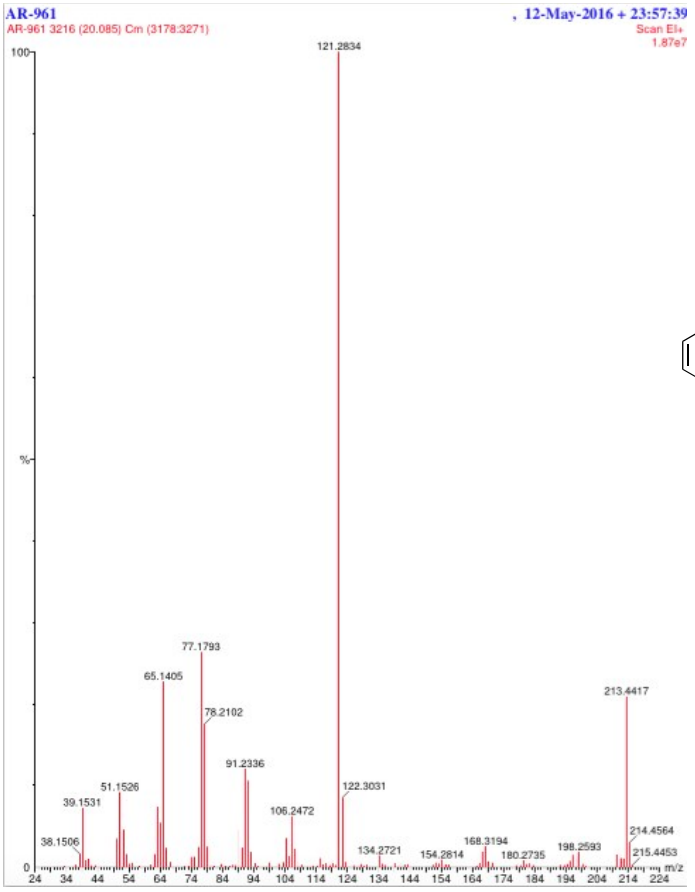

26H

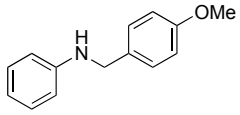

GC-MS chromatogram for **26H**.

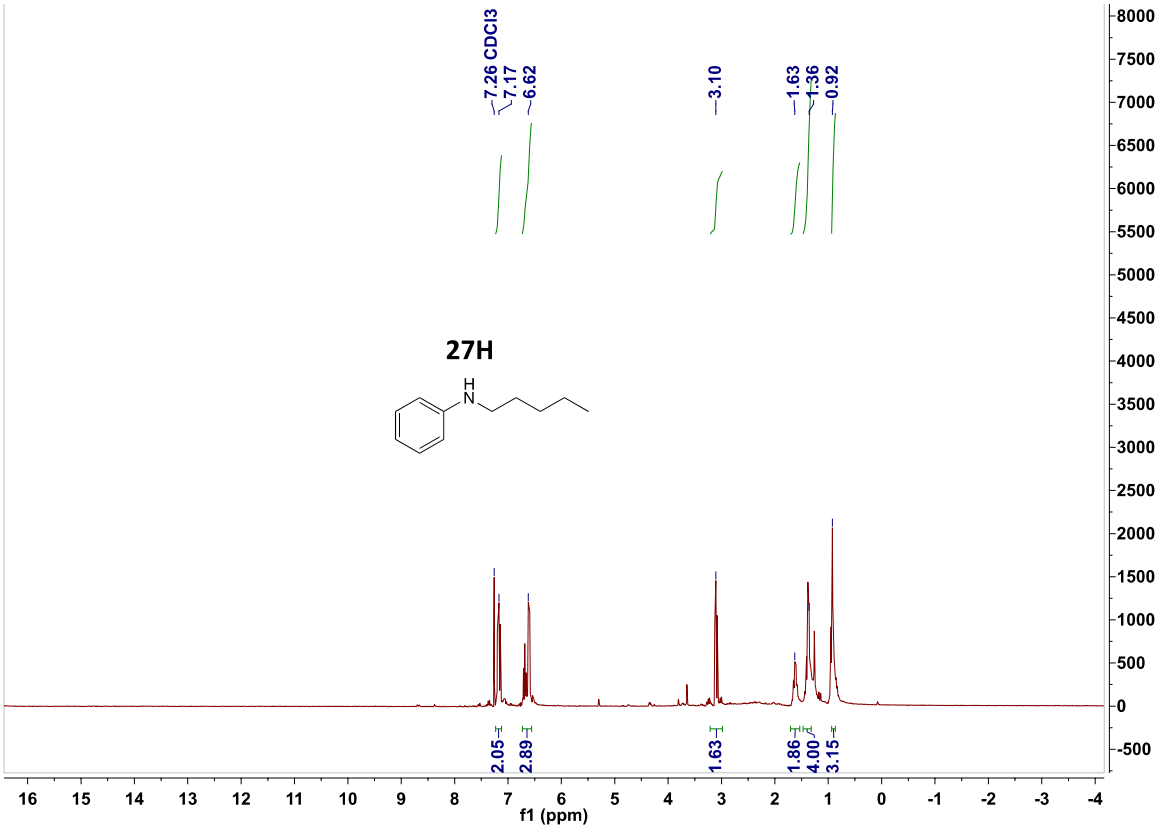

^{1}H NMR (300 MHz, 298 K) spectrum in $CDCl_3$ for **27H**.

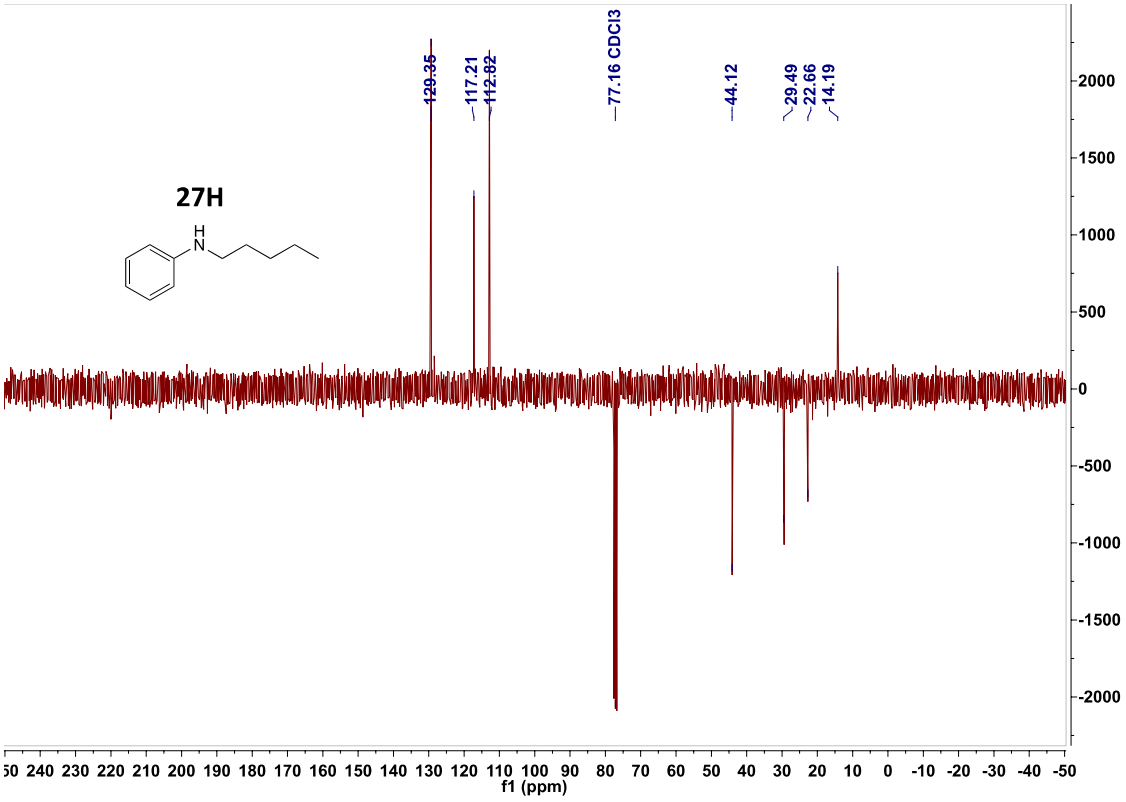

$^{13}C\{^{1}H\}$ Jmod NMR (75 MHz, 298 K) spectrum in $CDCl_3$ for **27H**.

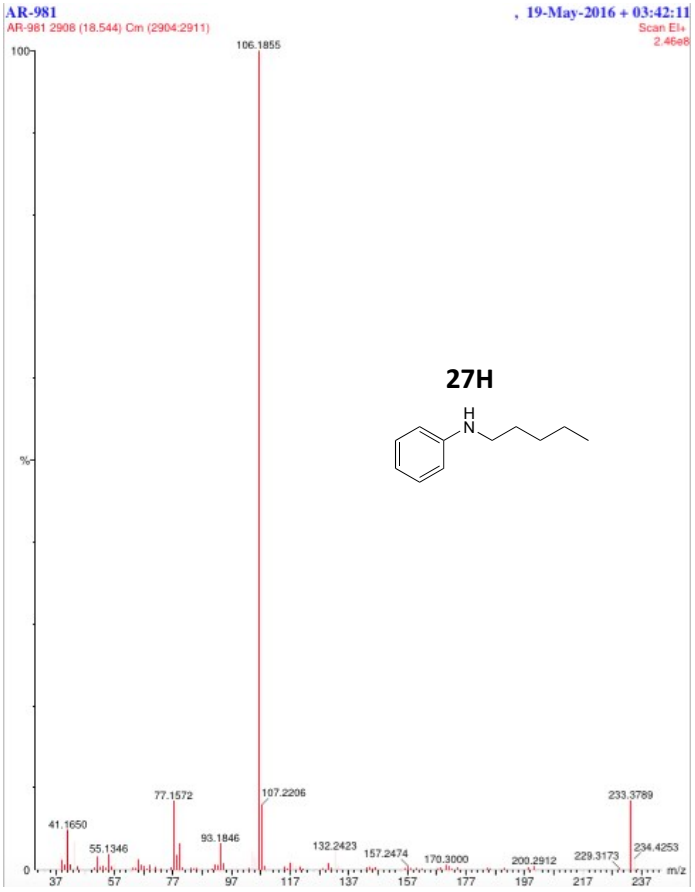

GC-MS chromatogram for **27H**.

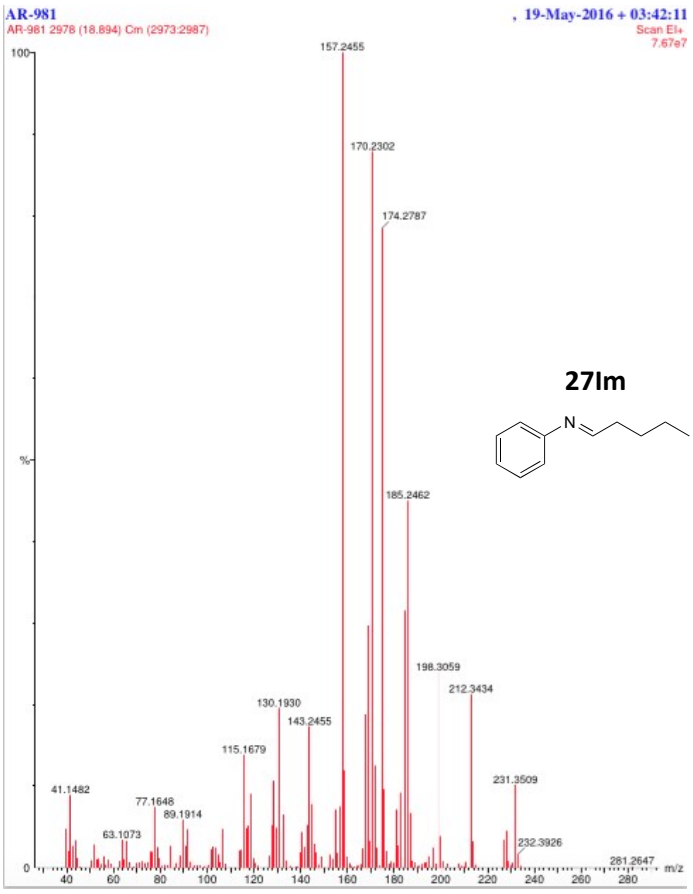

GC-MS chromatogram for **27Im**.

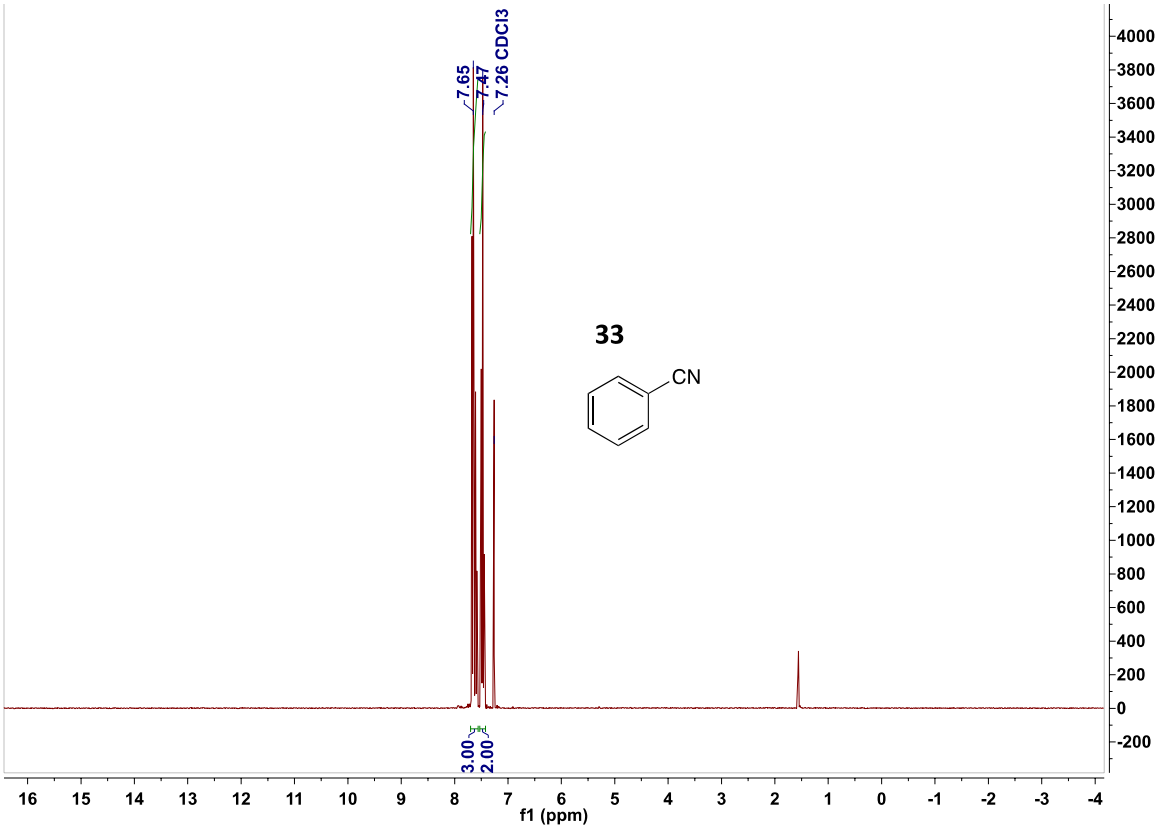

^{1}H NMR (300 MHz, 298 K) spectrum in $CDCl_3$ for **33**.

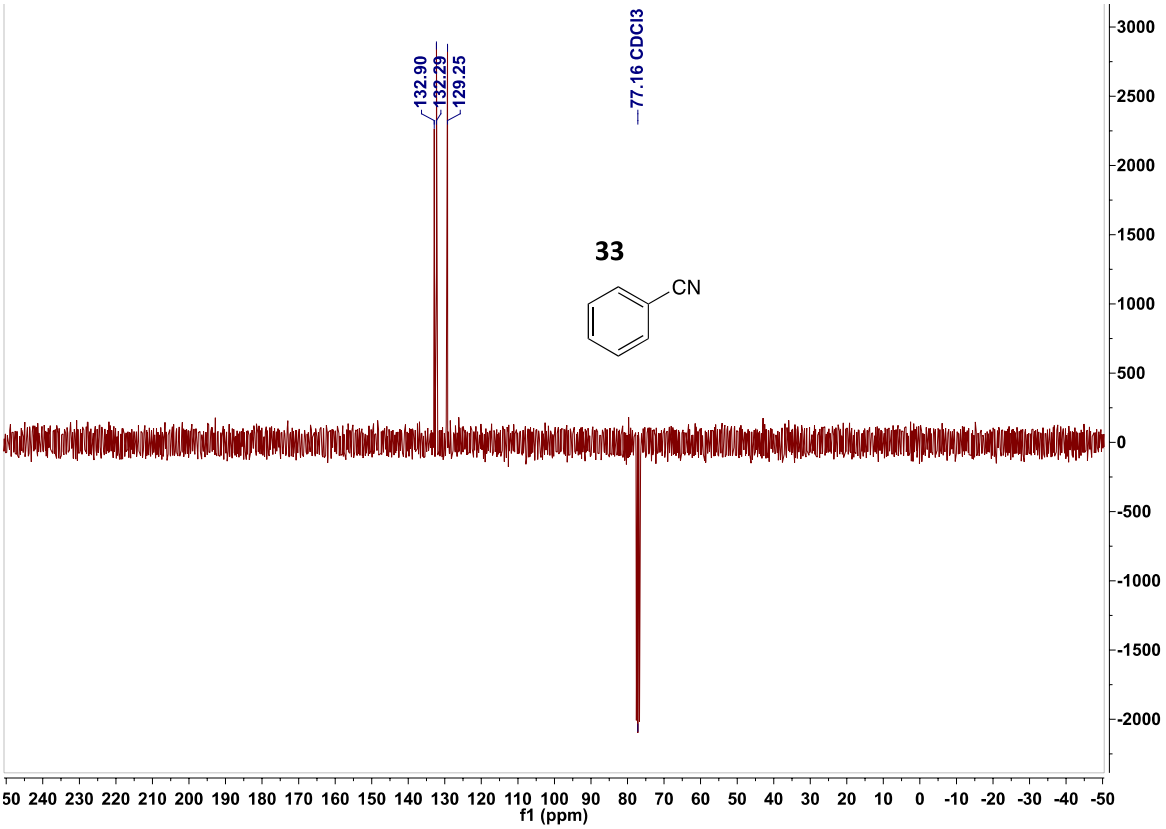

$^{13}C\{^{1}H\}$ Jmod NMR (75 MHz, 298 K) spectrum in $CDCl_3$ for **33**.

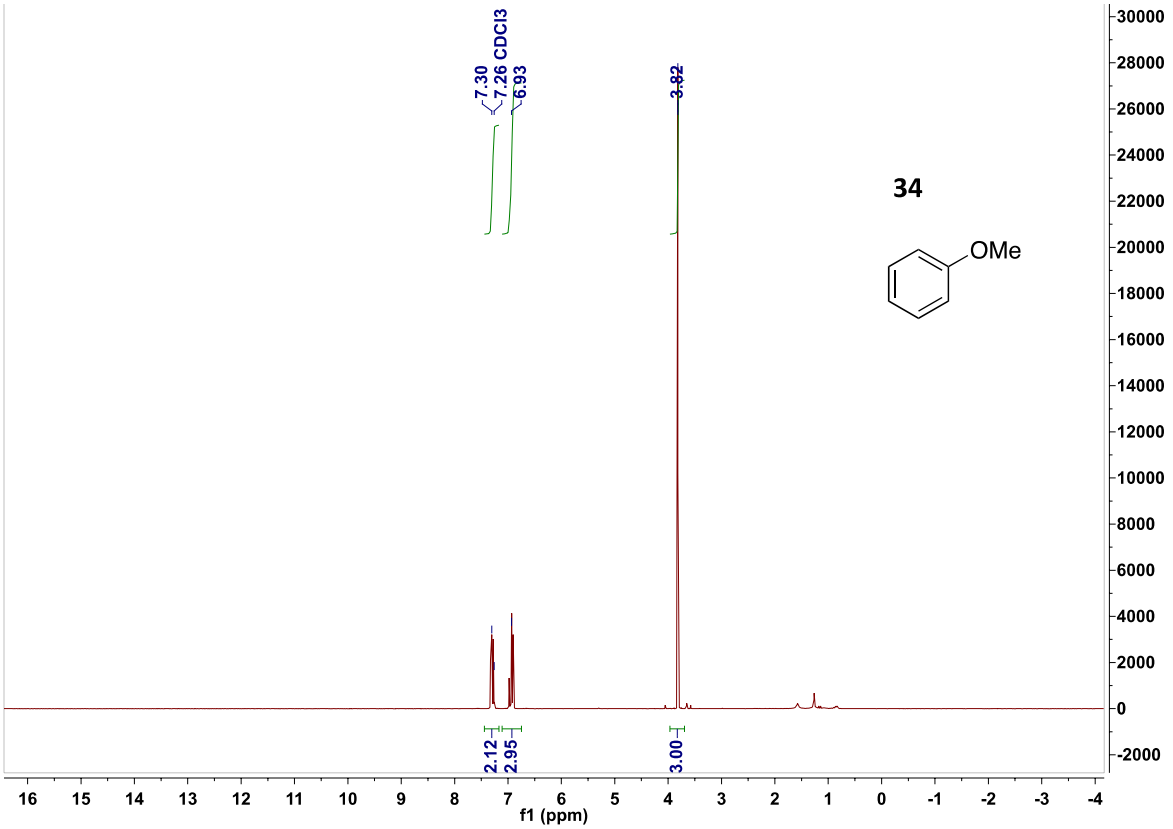

^{1}H NMR (300 MHz, 298 K) spectrum in $CDCl_3$ for **34**.

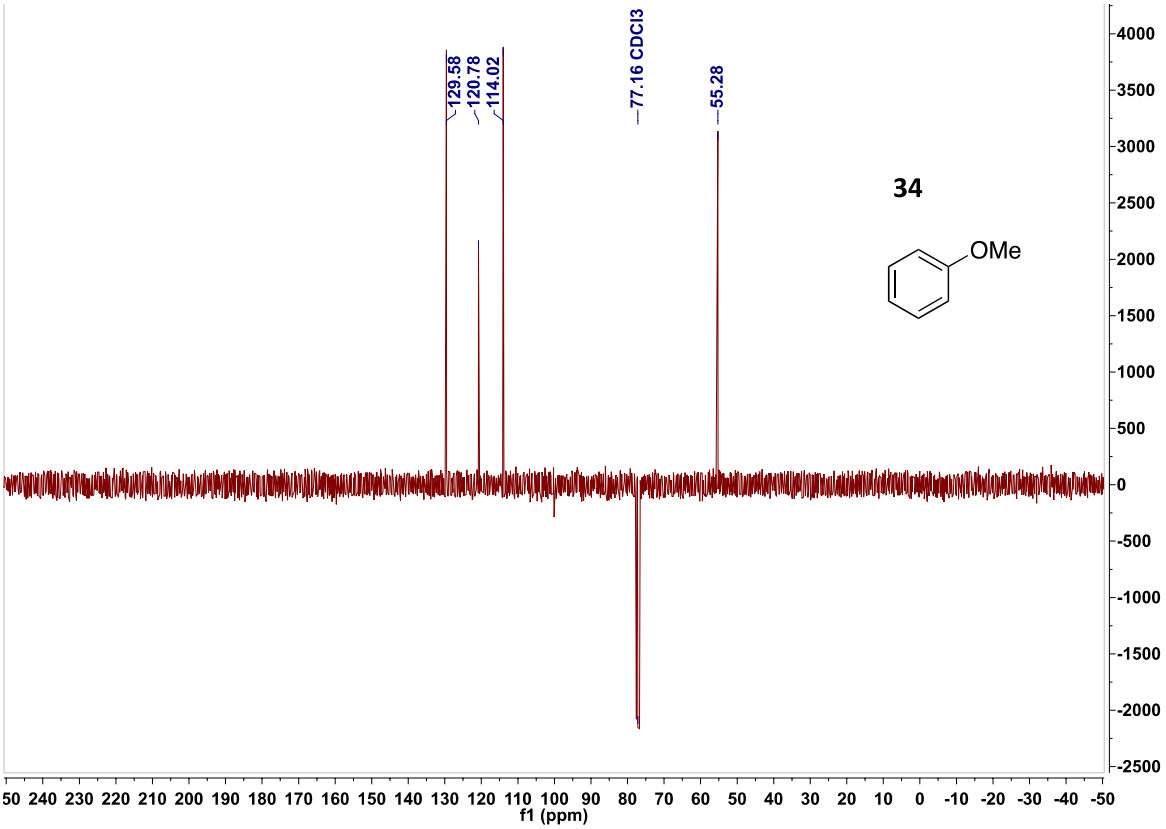

$^{13}C\{^{1}H\}$ Jmod NMR (75 MHz, 298 K) spectrum in $CDCl_3$ for **34**.

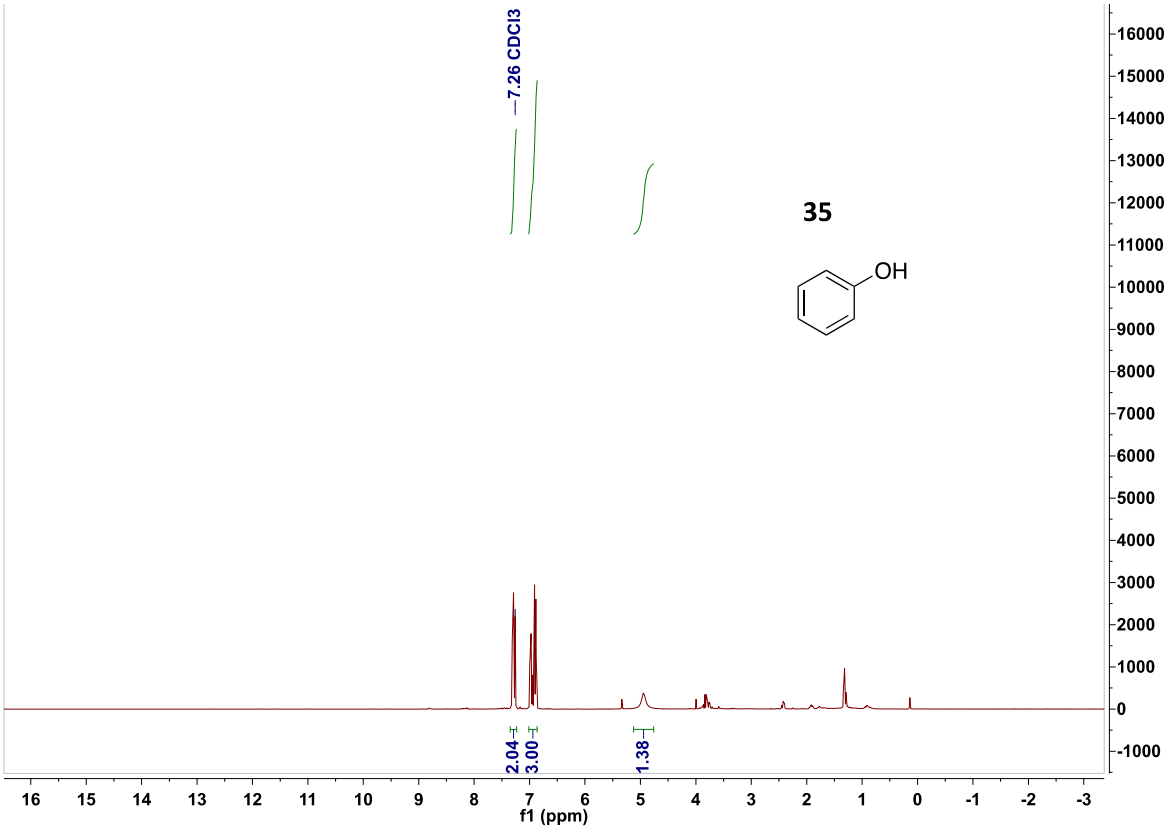

^{1}H NMR (300 MHz, 298 K) spectrum in $CDCl_3$ for **35**.

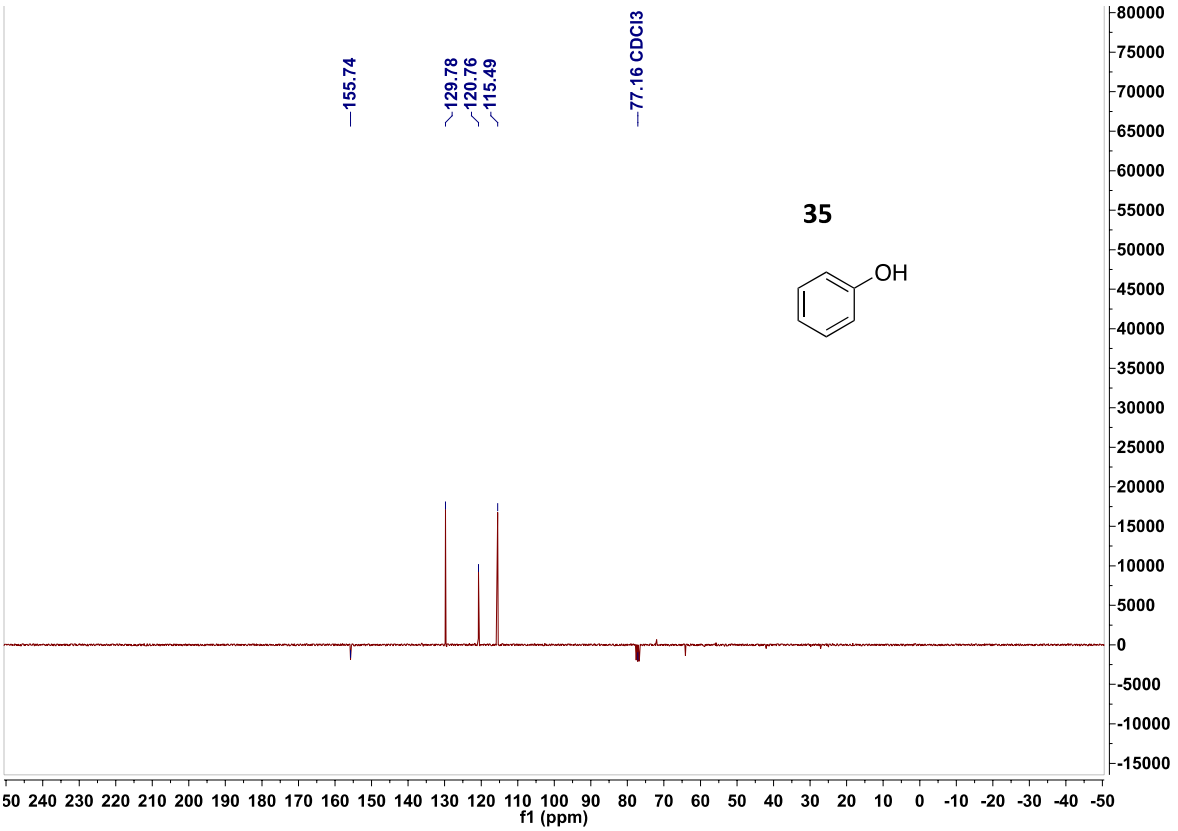

$^{13}C\{^{1}H\}$ Jmod NMR (75 MHz, 298 K) spectrum in $CDCl_3$ for **35**.

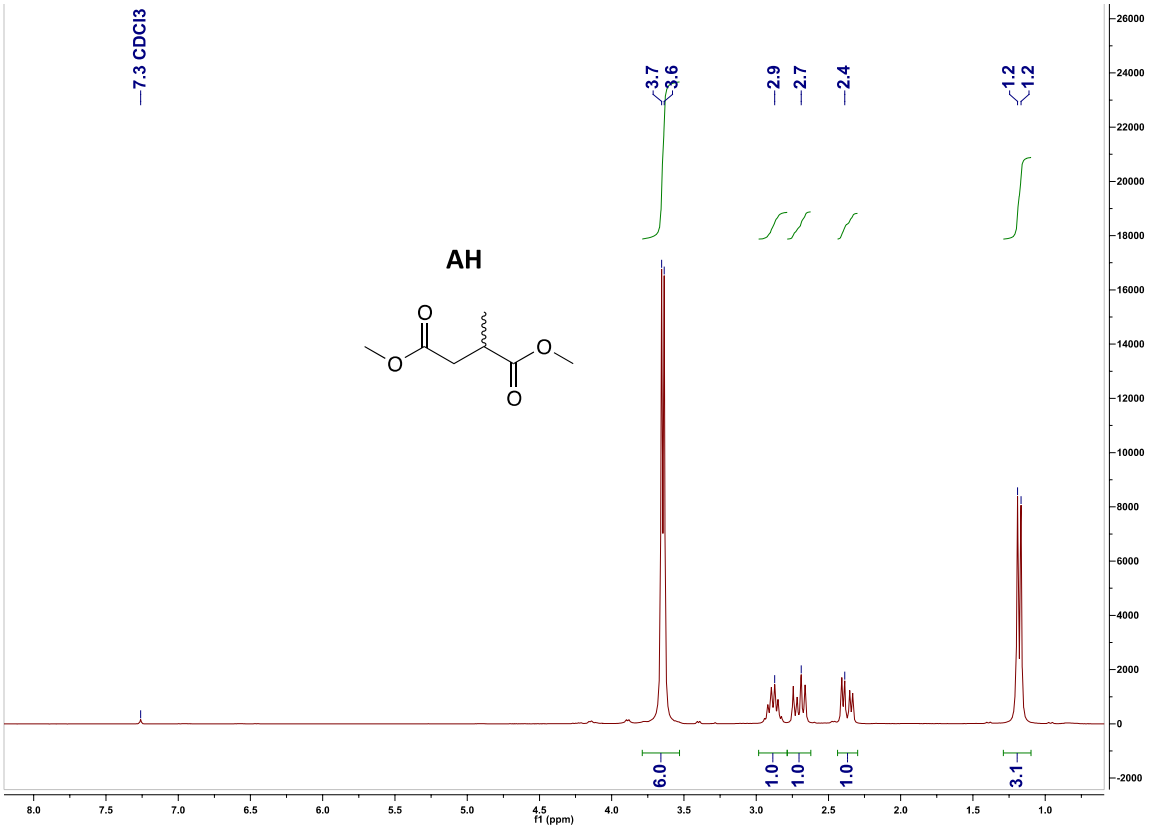

^{1}H NMR (300 MHz, 298 K) spectrum in $CDCl_3$ for **AH**.

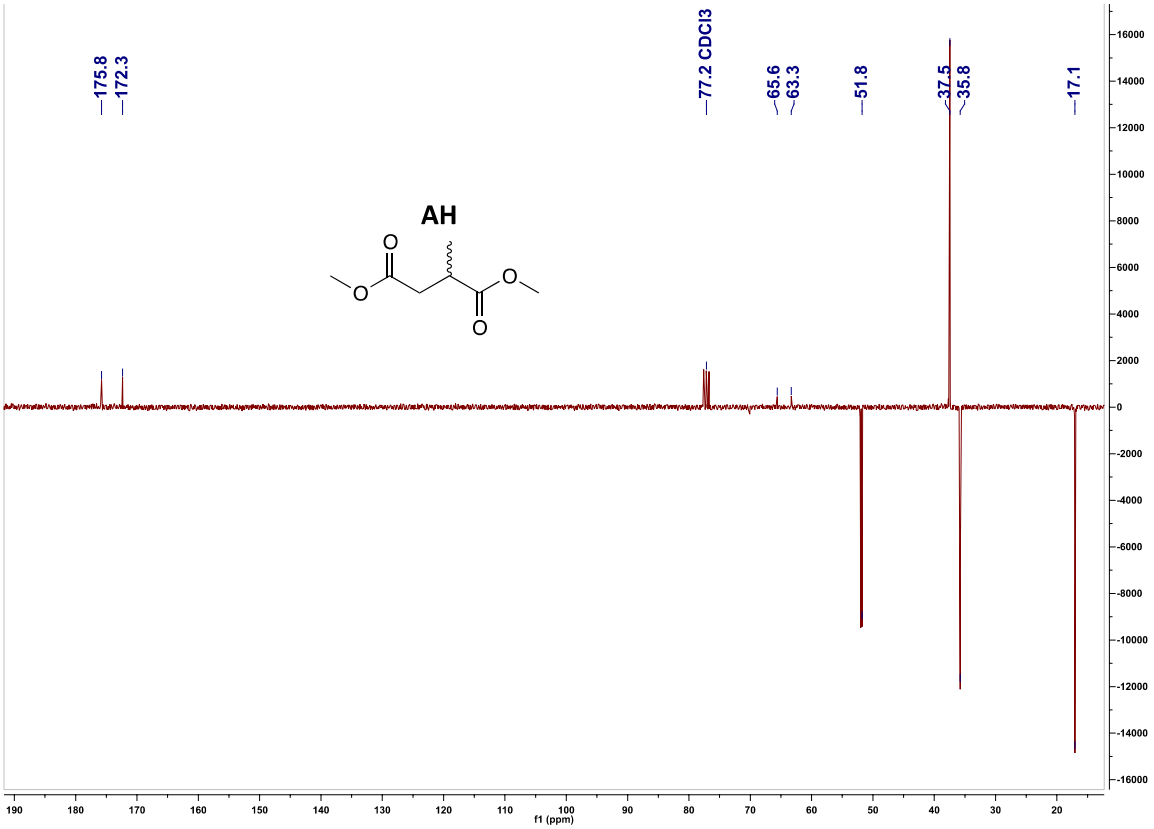

$^{13}C\{^{1}H\}$ Jmod NMR (75 MHz, 298 K) spectrum in $CDCl_3$ for **AH**.

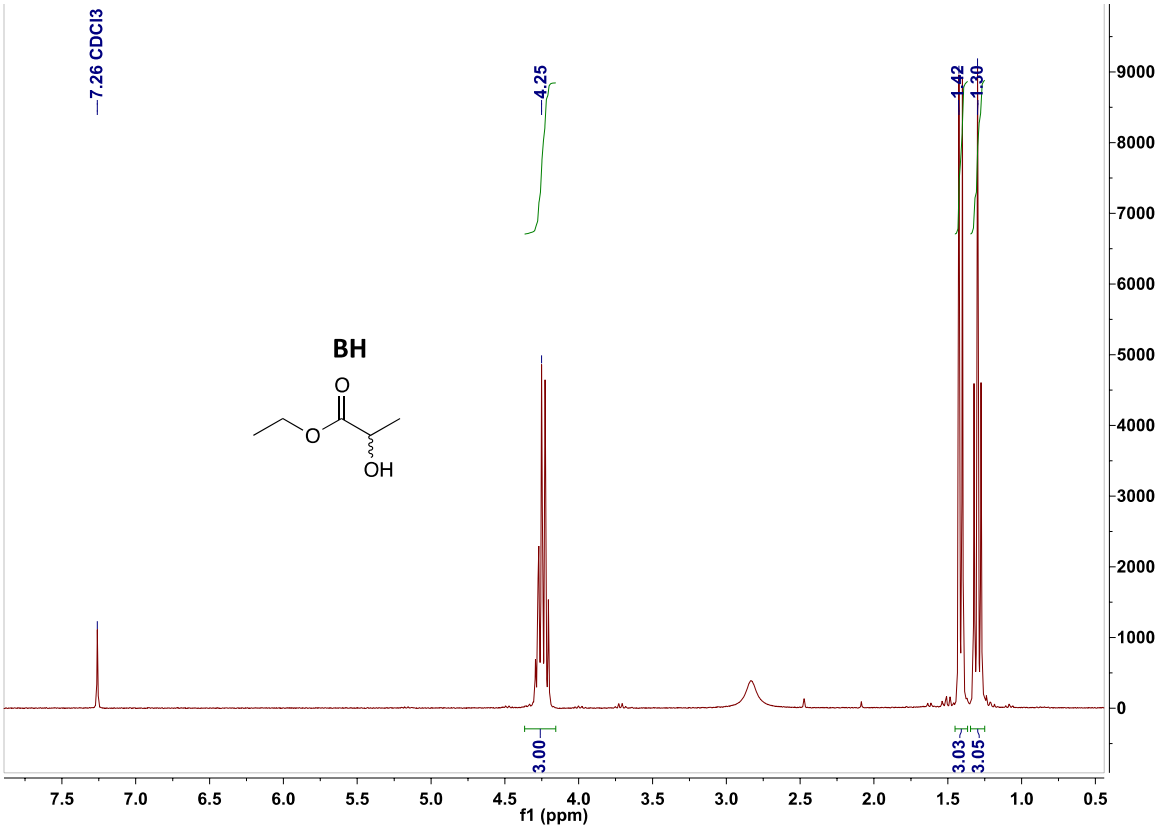

^{1}H NMR (300 MHz, 298 K) spectrum in $CDCl_3$ for **BH**.

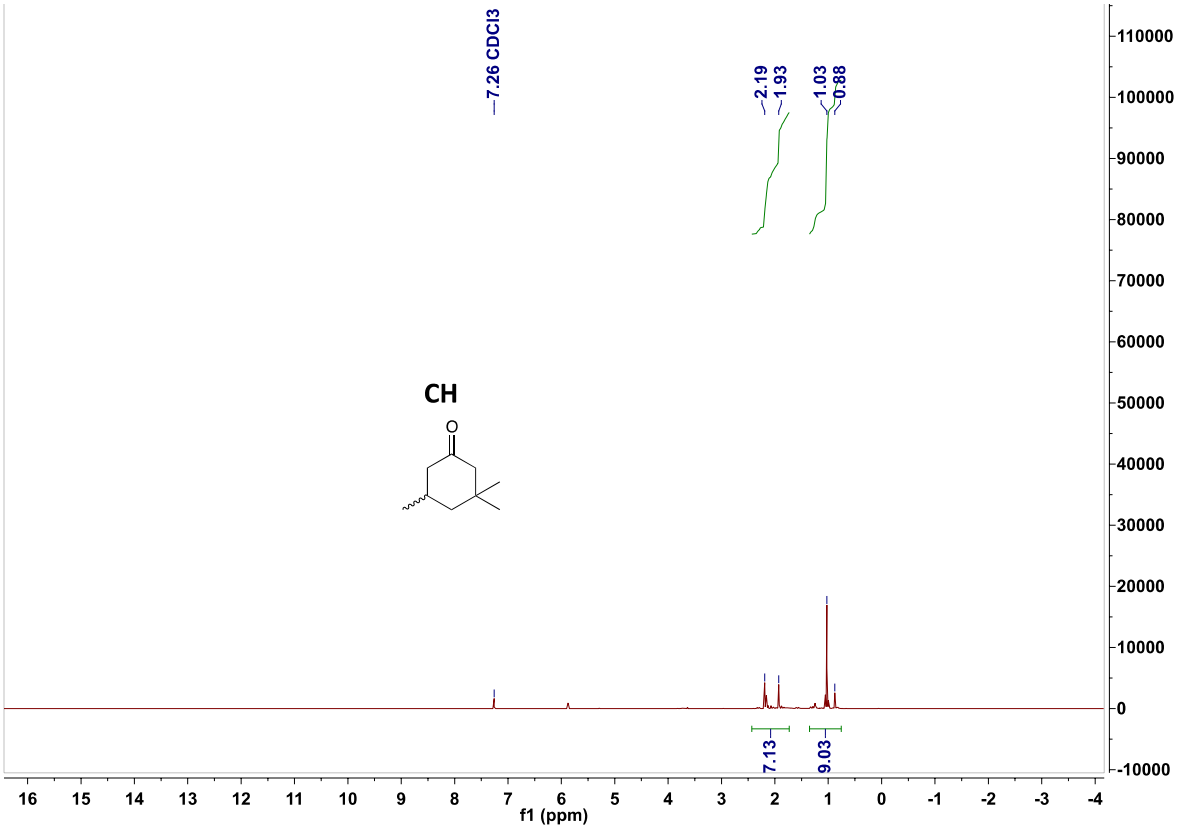

^{1}H NMR (300 MHz, 298 K) spectrum in $CDCl_3$ for **CH**.

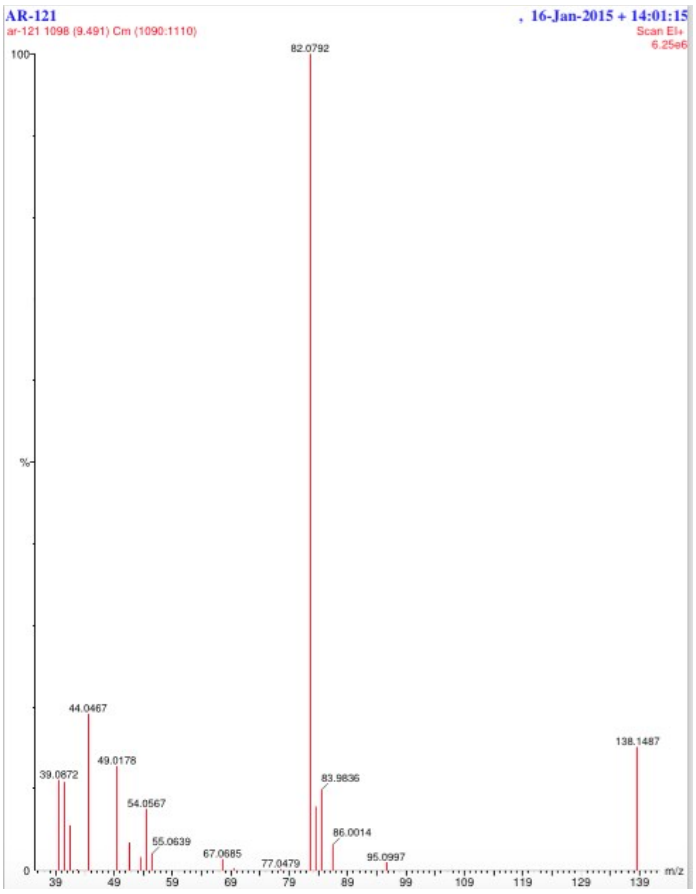

CH

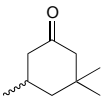

GC-MS chromatogram for **CH**.